

Review

Zeolites and Related Materials as Catalyst Supports for Hydrocarbon Oxidation Reactions

Angela Martins ^{1,2,*} , Nelson Nunes ^{1,2}, Ana P. Carvalho ^{2,3} and Luísa M. D. R. S. Martins ⁴ 

¹ DEQ, Instituto Superior de Engenharia de Lisboa IPL, Rua Conselheiro Emídio Navarro 1, 1959-007 Lisboa, Portugal; nnunes@deq.isel.ipl.pt

² Centro de Química Estrutural, Institute of Molecular Sciences, Faculdade de Ciências, Universidade de Lisboa, 1749-016 Lisboa, Portugal; apcarvalho@fc.ul.pt

³ Departamento de Química e Bioquímica, Faculdade de Ciências, Universidade de Lisboa, 1749-016 Lisboa, Portugal

⁴ Centro de Química Estrutural, Institute of Molecular Sciences, and Departamento de Engenharia Química, Instituto Superior Técnico, Universidade de Lisboa, Av. Rovisco Pais, 1049-001 Lisboa, Portugal; luisamargaridamartins@tecnico.ulisboa.pt

* Correspondence: amartins@deq.isel.ipl.pt; Tel.: +351-218-317-000

Abstract: Catalytic oxidation is a key technology for the conversion of petroleum-based feedstocks into useful chemicals (e.g., adipic acid, caprolactam, glycols, acrylates, and vinyl acetate) since this chemical transformation is always involved in synthesis processes. Millions of tons of these compounds are annually produced worldwide and find applications in all areas of chemical industries, ranging from pharmaceutical to large-scale commodities. The traditional industrial methods to produce large amounts of those compounds involve over-stoichiometric quantities of toxic inorganic reactants and homogeneous catalysts that operate at high temperature, originating large amounts of effluents, often leading to expensive downstream processes, along with nonrecovery of valuable catalysts that are lost within the reactant effluent. Due to the increasingly stringent environmental legislation nowadays, there is considerable pressure to replace these antiquated technologies, focusing on heterogeneous catalysts that can operate under mild reaction conditions, easily recovered, and reused. Parallely, recent advances in the synthesis and characterization of metal complexes and metal clusters on support surfaces have brought new insights to catalysis and highlight ways to systematic catalyst design. This review aims to provide a comprehensive bibliographic examination over the last 10 years on the development of heterogeneous catalysts, i.e., organometallic complexes or metal clusters immobilized in distinct inorganic supports such as zeolites, hierarchical zeolites, silicas, and clays. The methodologies used to prepare and/or modify the supports are critically reviewed, as well as the methods used for the immobilization of the active species. The applications of the heterogenized catalysts are presented, and some case-studies are discussed in detail.

Keywords: hydrocarbon oxidation reactions; zeolites; hierarchical zeolites; mesoporous silicas; immobilized catalyst; organometallic complexes; metal particles; alkanes; alkenes; aromatic substrates



Citation: Martins, A.; Nunes, N.; Carvalho, A.P.; Martins, L.M.D.R.S. Zeolites and Related Materials as Catalyst Supports for Hydrocarbon Oxidation Reactions. *Catalysts* **2022**, *12*, 154. <https://doi.org/10.3390/catal12020154>

Academic Editor: Roman Bulánek

Received: 29 December 2021

Accepted: 22 January 2022

Published: 26 January 2022

Publisher's Note: MDPI stays neutral with regard to jurisdictional claims in published maps and institutional affiliations.



Copyright: © 2022 by the authors. Licensee MDPI, Basel, Switzerland. This article is an open access article distributed under the terms and conditions of the Creative Commons Attribution (CC BY) license (<https://creativecommons.org/licenses/by/4.0/>).

1. Industrial Hydrocarbon Oxidation Reactions

Catalytic oxidation reactions are of high industrial relevance since many important commodities have synthesis paths involving oxidation. To understand their relevance, we can just refer to adipic acid, with a global production of over 4 million tons and expect to exceed a \$8 billion USD global market by 2025 [1].

If like some authors [2] we include ammoxidation (a process using ammonia and oxygen) and oxychlorination (a process using hydrogen chloride and oxygen) used, respectively, in the production of acrylonitrile and vinyl chloride monomers, the industrial importance of oxidation reactions is even higher.

Despite the focus of this manuscript being on hydrocarbon oxidation reactions, it is also worth mentioning the industrial importance of alcohols oxidation, namely methanol and ethanol to produce, correspondingly, formaldehyde (e.g., Formox process) and 1,3-butadiene [3].

When addressing hydrocarbon oxidation reactions, there are several significant industrial applications. The direct oxidation of alkanes is an attractive alternative to oxidation via olefins; however, only two industrial processes have been implemented, and other alkanes oxidations are only at the research or pilot plant status. One of these reactions is the production of maleic anhydride from *n*-butane (Figure 1).

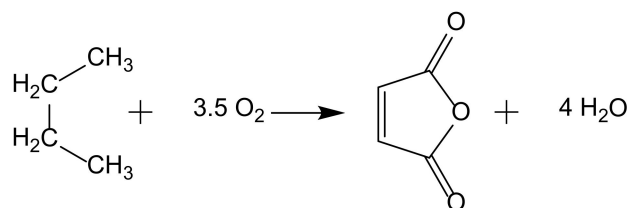


Figure 1. Maleic anhydride synthesis from *n*-butane oxidation.

This process uses supported (VO)₂P₂O₇ as heterogenous catalyst and achieves high weight yields (ca. 95%) replacing a previous method with benzene. In both methods, butane (or benzene) is fed into a stream of hot air, and the mixture passes through a catalyst bed at high temperature. Fixed, fluidized, and transport bed reactors technologies have been implemented in different industrial plants to address different technical difficulties [4].

Another example of alkane oxidation but in the liquid phase with homogeneous catalysis is the oxidation of cyclohexane into a mixture of cyclohexanol and cyclohexanone (also known as KA oil), which are intermediates in the manufacture of nylon-6 and nylon-6,6. KA oil is mainly obtained through the oxidation of cyclohexane using air or peroxide as the oxidant agent. In the present industrial conditions, liquid phase oxidation of cyclohexane is achieved at about 165 °C and O₂ pressures of 8–15 bar in the presence of manganese or cobalt naphthenates as catalysts (Figure 2). To avoid oxidative side reactions, a short retention time is used to assure 80–85% selectivity; thus, the conversion is limited to 10–11% per cycle, requiring separation and refeeding of the unconverted cyclohexane. Additionally, the currently used homogeneous catalysts are difficult to separate from the reaction media, leading to serious environmental pollution. [5]

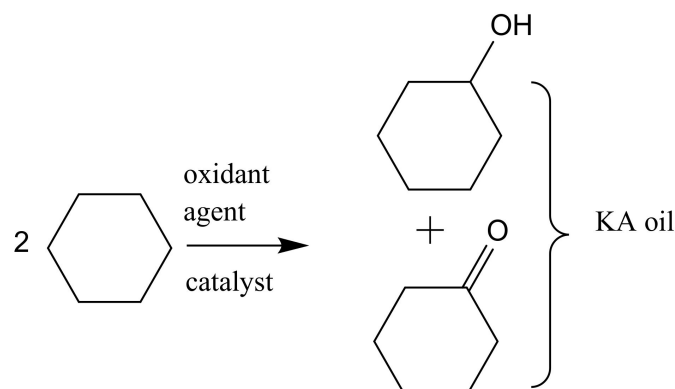
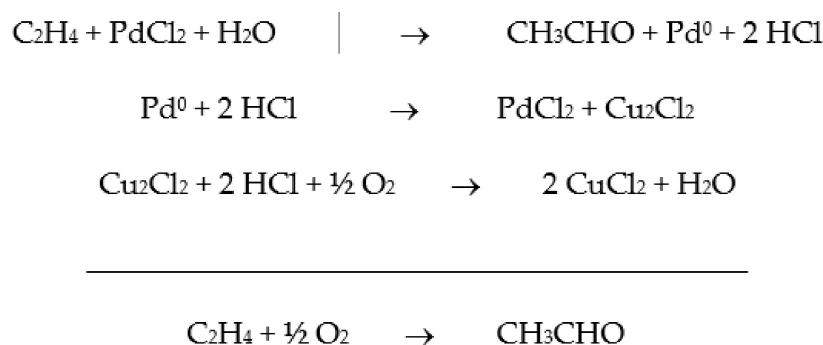


Figure 2. Oxidation of cyclohexane to cyclohexanol and cyclohexanone (KA oil).

There are several industrial alkenes oxidation processes, and two of the major products obtained by these methods are ethylene oxide and acetaldehyde. Both chemicals are produced from ethylene and are in turn raw materials to produce other compounds such as ethylene glycol, diethylene glycol, triethylene glycol (from ethylene oxide) and acetic acid, acetate esters, and pyridine derivatives (from acetaldehyde).

The current ethylene oxide production process was developed in the middle of the 20th century and uses finely dispersed metallic silver together with alkali and alkaline earth metals promoters, on ultrapure aluminum oxide, i.e., a low surface area support. There are two variations of this process: one uses air and the other oxygen, and both use fixed bed reactors which consist of large bundles of thousand tubes, each with a length of approximately 10 m and an internal diameter of 20–50 mm. The temperature and the pressure range between 200 and 300 °C and 15 and 25 bar, respectively.

The oxidation of ethylene to acetaldehyde, known as the Wacker process, was one of the first industrial homogeneous catalytic process (Scheme 1). The catalyst is a two-component aqueous solution consisting of PdCl₂ and CuCl₂, and from the proposed mechanism, O₂ is not directly involved.



Scheme 1. Proposed mechanism for the ethylene oxidation to acetaldehyde.

The process is a two-phase gas/liquid system, and there are variations in different industrial units, with some using a single-step process and others a two-step process. Each solution has different operational conditions and advantages.

As the final examples of substrates used in industrial hydrocarbon oxidation reactions, we can include the oxidation of aromatic hydrocarbons. Even though benzene oxidation is still not near industrial application, due to increasing ring activation with oxidation and further reactions, other molecules are already used.

The production of phthalic anhydride, a precursor of phthalate esters plasticizers, dyestuffs, and pharmaceuticals, is based on the oxidation reaction of naphthalene. Initially, the process was liquid phase based but was subsequently replaced by a cleaner gas phase process using mercury salt as a catalyst. A variation of this process uses *o*-xylene instead of naphthalene with further variations in the used catalysts (Figure 3).

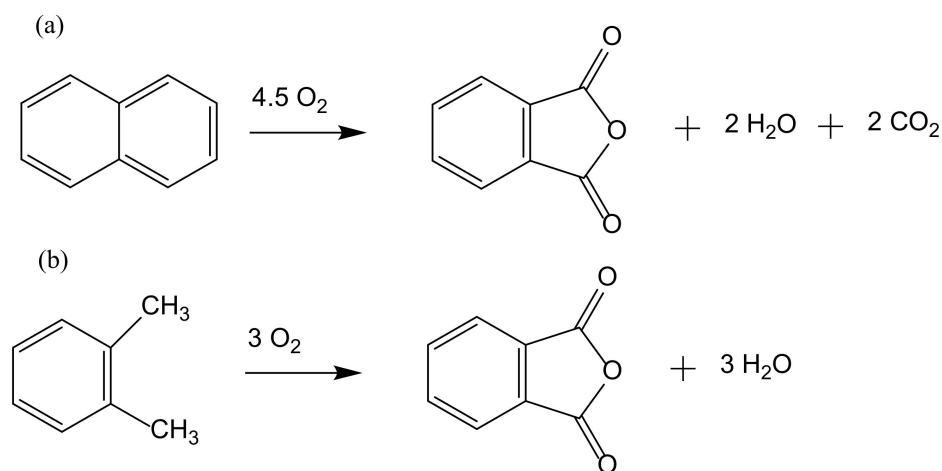


Figure 3. Oxidation of naphthalene (a) and *o*-xylene (b) to phthalic anhydride.

A xylene isomer is also used in one of the most important industrial oxidation reactions, the production of terephthalic acid from *p*-xylene (Figure 4). The relevance of terephthalic acid is based on being the precursor to polyethylene terephthalate (PET), the highest volume synthetic fiber. Since the 1960s, terephthalic acid has been mainly produced by the Amoco process; this homogeneous catalytic process uses soluble cobalt salt (acetate or naphthenate) simultaneously with manganese or bromide ions [3,4].

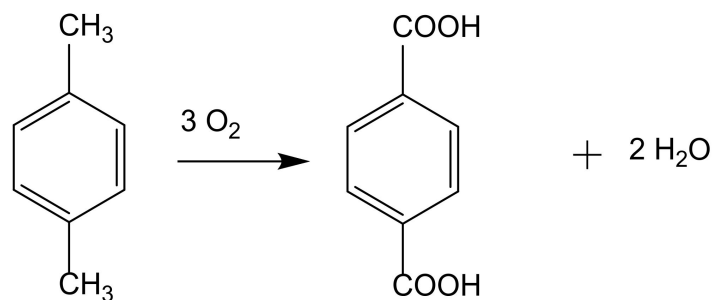


Figure 4. Terephthalic acid production from *p*-xylene oxidation.

2. From Homogeneous to Heterogenized Catalysts

The development of sustainable methods for the catalytic oxidation reactions of hydrocarbons-alkanes, alkenes, and aromatics is an important scientific challenge with significant technological potential. As mentioned previously, these reactions usually occur in the presence of traditional homogeneous catalysts, such as transition and neat metals or their salts, as well as mineral acids and complexes, due to their high activity and selectivity to the desired products. However, the intensive use of these catalysts is rather controversial due to the difficult separation and recovery of the catalyst from the reaction media. The immobilization of catalytic active species in solid supports is a possible strategy to overcome some of the disadvantages of homogeneous processes. Heterogenized catalysts are easily recovered from the reaction media, without expensive separation processes and large amounts of solvents involved, with the additional advantage of allowing the reuse of the catalyst in several cycles. These are, in fact, the main objectives that one expects to achieve through the immobilization of homogeneous catalysts, but some additional benefits may also be obtained, namely when porous supports are considered. In this case, the confinement effects may enhance the interaction of the substrate with the catalyst. However, the porosity of the support may also impose some diffusional constraints that, especially when voluminous substrates are considered, can result in an extensive loss of activity. In the case of complexes, the immobilization on solid supports has another additional benefit since it prevents dimerization phenomena that are some of the most common causes of homogeneous catalysts deactivation.

The advantages of immobilized catalyst have been attracting the attention of both industrial and academic researchers, as demonstrated by the number of publications focused on the heterogenization of metal or metal complexes, on zeolites and similar materials, in the last decade (Figures 5 and 6). In both cases, the number of publications presents a continuous growing, being more consistent in the case of metal-supported catalysts.

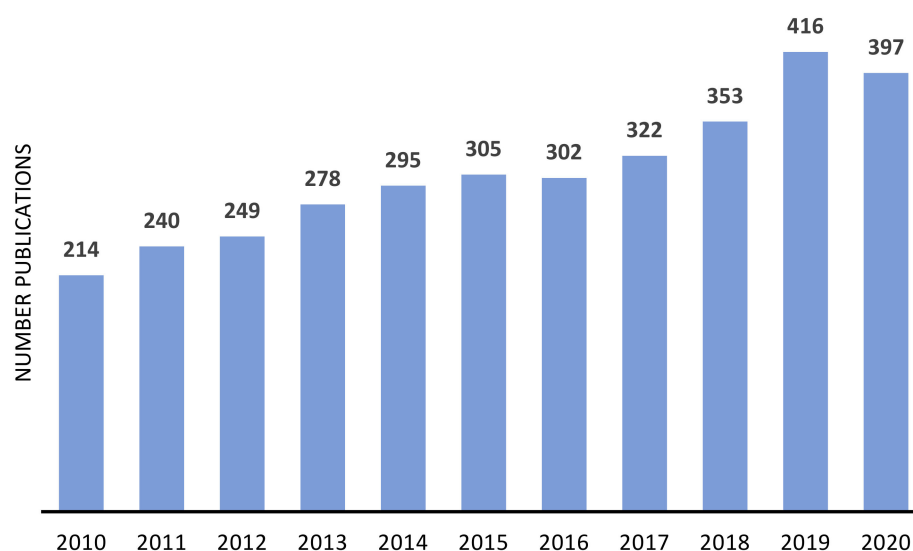


Figure 5. Approximate annual number of publications on immobilized metal complexes on zeolites and other similar materials since 2010. Source: ISI Web of Knowledge, 29 September 2021. Search terms: “immobilized metal complexes” OR “anchored metal complexes” OR “heterogenized metal complexes”.

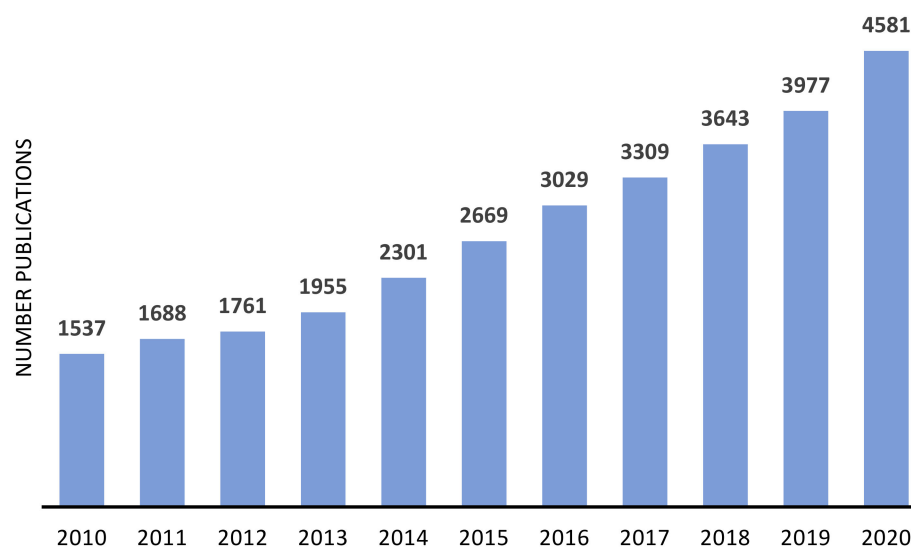


Figure 6. Approximate annual number of publications on metal supported on zeolites and other similar materials, since 2010. Source: ISI Web of Knowledge, 29 September 2021. Search terms: “metal-supported catalysts”.

3. Zeolites and Related Materials as Support for the Heterogenization of the Catalysts

Zeolites are microporous, crystalline aluminosilicate materials known since 1756 when the stilbite structure was identified by the Swedish mineralogist Crönstedt. This class of materials is composed of corner-sharing TO_4 tetrahedra, where T represents Si or Al. Adjacent SiO_4 and AlO_4^- tetrahedra are bridged by oxygen atoms that are arranged in a regular way, giving a three-dimensional system of cages and pores with dimensions comprised in the microporous range, i.e., between 3 and 20 Å, which is responsible by the “molecular sieving” property [6].

Zeolites were firstly considered as mineralogical curiosities and only became industrial important after the studies performed by Barrier and Milton in the 1940s [7,8], reporting the successful synthesis of numerous zeolite structures. Since then, zeolites have been widely used mainly as adsorbents, ion exchangers, and, especially, as heterogeneous catalysts or

as catalyst supports. Nowadays, according to the International Zeolite Association (IZA), which catalogues all zeolite structures, which can be consulted at Reference [9], there are more than 240 synthetic zeolites and 67 natural zeolites.

To maintain the electroneutrality of the zeolite framework, the presence of a compensation cation, such as Na^+ , is required, giving the ability to act as ion-exchange materials with a large application in detergents industry as water-softening agents. When the compensation cation is H^+ , the zeolite has a high content of Brönsted acid sites, allowing one to catalyze many reactions involving hydrocarbons. Allying a strong acidity with other unique properties, such as structural, thermal, mechanical, and chemical stability, makes zeolites ideal heterogeneous catalysts for gas-phase reactions that are typically conducted at temperatures higher than 300 °C. In fact, most of the current large-scale commercial processes in the petroleum refining and petrochemical industries use zeolite-based catalysts [10]. These processes involve cracking, isomerization, and transalkylation reactions. After several catalytic cycles, the catalysts may become deactivated due to the adsorption of products, byproducts, or the formation of coke, but in many cases, zeolites can easily be reactivated by performing thermal treatments. In addition, when they are exhausted and at the end of their regeneration cycles, they can be used as precursors for producing concrete [11], new adsorbent materials for the withdrawing of pollutants from the environment [12], or even new catalysts [13].

The catalysts can be classified according to the nature of their active sites as intrinsic, when the active sites are naturally present in the composition of the catalyst, for example Brönsted or Lewis acid sites in zeolites, or supported catalysts when the active sites are introduced on a solid support that has no catalytic activity on the targeted reaction [8]. As mentioned before, the immobilization of a catalysts/catalyst precursor is a common procedure, combining the advantages of both homogeneous and heterogeneous catalysts. The mechanical stability and high porosity of zeolite structures makes them very interesting supports with great advantages for certain immobilization methodologies and for recycling and reuse procedures. Most of the studies report the immobilization of metal complexes [14–18] and metal particles [19–21], which are the topics of the present review, but the immobilization of other species (out of the scope of this review) such as enzymes [22,23] has also been presented.

3.1. Hierarchical Zeolites

The strictly microporous nature of zeolite structures is responsible for the various types of shape selectivity that are fundamental to increasing the yield of a desired product. A classic example of shape selectivity is an important petrochemical reaction catalyzed by ZSM-5 zeolite (MFI structure): the transformation of *m*-xylene into *o*-xylene and, especially, *p*-xylene, which is the building block to produce polyethylene (PET)-based products. In this case, opposing the thermodynamic equilibrium where the more stable *m*-xylene is favored, the diffusional limitations for the molecular transport of *m*-xylene and *o*-xylene lead to the conversion of these two more voluminous isomers into the most valuable *p*-xylene [8,24]. Despite the importance of shape selectivity in several reactions catalyzed by zeolites, their native microporosity can also impose diffusion constraints that will limit the catalytic performance, especially in the presence of bulky molecules. Within the past two decades, intense attention has been devoted to the enhancement of accessibility of active sites in microporous zeolite frameworks. Although a large number of strategies have been proposed and demonstrated, the production of these hierarchical materials can be classified into two major categories: synthesis procedures, also called “bottom-up”, or postsynthesis procedures, also called “top-down” [25].

3.1.1. Bottom-Up Strategies

To introduce a supplementary pore system, usually mesopores, several strategies involve the addition of hard or soft templates to the synthesis gel, allowing the crystallization of the zeolites around those templates, giving intracrystalline mesoporosity. Alternatively,

the crystal can grow at the confined space between particles, originating small crystals where the mesopores appear as the consequence of the particle stacking (intracrystalline mesoporosity), as schematized in Figure 7. In both cases, after synthesis, the templates are removed by combustion, exposing the mesopores.

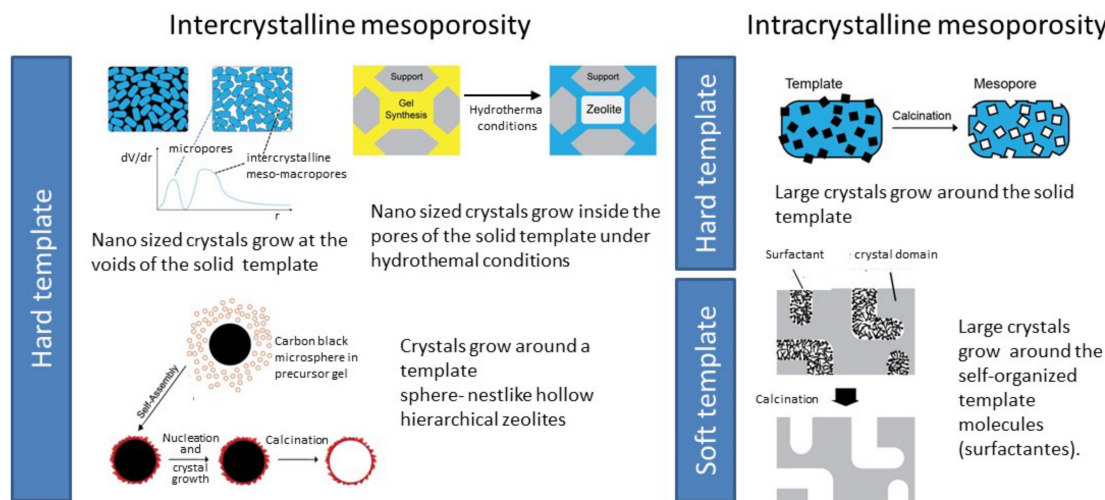


Figure 7. Overview of the various bottom-up synthesis methodologies to obtain hierarchical zeolites.

Table 2 resumes some representative examples regarding the application of hard and soft templating strategies for the synthesis of hierarchical zeolites. A few examples, related with the targeted reactions of this review, are briefly mentioned in the following section, and selected case-studies are discussed in detail ahead.

Table 1. Examples of recent studies on bottom-up processes used to synthesize hierarchical zeolite structures.

Zeolite Structure	Template	Observations	Ref.
Hard templating			
MFI	Carbon black	Nanosized crystals with intercrystalline mesoporosity.	[26]
MFI	Carbon black	Crystals with intracrystalline mesoporosity.	[27]
MEL	Carbon particles	Zeolite single crystals with intracrystalline mesopore volumes between 0.31 and 0.44 cm ³ g ⁻¹ were isolated.	[28]
MFI	Carbon black	Zeolite crystals with a large mesopore volume. Uniform and narrow mesopore size distribution centered at around 20 nm, due to the uniform size of the carbon black particles of about 18 nm.	[29]
AEL	Commercial carbon	Hierarchical SAPO-11 materials with both micro- and meso-pores were obtained with irregular cavities in shape and size.	[30]
MFI	Carbon fibers, carbon cloths, and monoliths	The combustion of zeolite/carbon composites produced, in the case of carbon fibers and carbon cloths, microtubes of pure zeolite.	[31]
RMMs	Carbon mesoporous molecular sieves	Aluminosilicate mesoporous materials with zeolite secondary building units were obtained The novel RMMs possess acidity and high hydrothermal, mechanical, and steam stability.	[32]

Table 1. Cont.

Zeolite Structure	Template	Observations	Ref.
MFI	Carbon aerogel	Meso-ZSM-5 monolith was synthesized with the crystalline form of ZSM-5 (micropores + mesopores).	[33]
MFI	Carbon nanotubes	The use of carbon nanotubes led to creating new mesopores in the ZSM-5 structure. However, increasing the carbon nanotubes content led to destruction of micropores along with some acidity decreasing.	[34]
MFI	Hydroxylated carbon nanotubes	Mesoporous structure with a size of about 10–35 nm, similar to the template diameter of was produced. Catalytic cracking of tri-isopropylbenzene was chosen as a probe reaction due to increased external surfaces.	[35]
FAU	Carbon aerogel	The pore size distribution obtained from N ₂ adsorption data shows the presence of meso and micropores with average pore widths are ca. 10 and 0.75 nm, respectively.	[36]
AFI	Cation exchange resin beads	Highly crystalline and mechanically stable AlPO-5 spheres were prepared. The presence of the micropores is due to the presence of AlPO-5, whereas the meso and macropores emanate from the resin removal.	[37]
MFI	Polystyrene beads	Silicates with bimodal pore structures of macropores (250 nm average diameter), surrounded by microporous silicalite walls were produced.	[38]
MFI	Nanosized CaCO ₃	Intracrystalline pores in the range of 50–100 nm were detected, which correspond to the morphology of nanosized CaCO ₃ .	[39]
MFI	Starch gel	Silicalite-starch gel monoliths and films, as well as sponge-like starch foams infiltrated with silicalite nanoparticles originated macroporous architectures of the zeolite silicalite with, at least, two levels of hierarchy in pore organization.	[40]
MFI	Wood cells	Seeded growth strategy was applied to fabricate self-standing zeolitic tissue that faithfully inherits the initial cellular structure of wood at various hierarchical levels.	[41]
BEA	Leaves and stems	BEA zeolite macrostructures with hierarchical porosity were prepared, retaining the morphological features of the vegetal template.	[42]
MFI	Silane-functionalized polyethylenimine polymer	Hierarchical MFI with small intracrystalline mesoporosity (average pore size 2.0–3.0 nm) and narrow pore size distributions (ca. 1.0–1.5 nm width at half maximum) was obtained.	[43]
LTA	Resorcinol-formaldehyde aerogels	The pore size shows a bimodal distribution with micropores and mesopores.	[44]
BEA, MEL	Polyvinyl butyral gel	The materials contained two levels of porosity: well-defined microporosity and irregular mesoporosity.	[45]
CHA	Coke containing spent MFI	Robust interzeolite transformation was reported to synthesize the hierarchical CHA with high crystallinity and well-developed mesoporosity (mesopore volume = 0.38 m ³ g ⁻¹).	[13]
Soft templating			
AFI	TPHAC	Direct hydrothermal assembly produced mesoporous aluminophosphates constructed with crystalline microporous frameworks.	[46]

Table 1. Cont.

Zeolite Structure	Template	Observations	Ref.
MFI	TEOS	Direct hydrothermal sylanization synthesis with molybdenum and titanium species encapsulated inside the zeolite crystals.	[47]
MFI	Gemini surfactant	Hierarchical ZSM-5 using Gemini surfactants as template that was directly added to the synthesis gel. Abundant intercrystalline mesoporosity was observed.	[48]
MFI	TPOAC, CTAB	The usage of different two mesogenous templates during the synthesis procedure resulted in the difference in the mesopore–micropore interconnectivity. Sample prepared with TPOAC presented excellent interconnectivity between micropores and mesopores and higher relative crystallinity.	[49]
MFI	CTAB	Hydrothermal crystallization using CTAB as a mesogenous template during synthesis, with crystal size and shape typical of MFI structure.	[50]
FAU	TPHAC	TPHAC surfactant was added prior to the hydrothermal step. Zeolite nanosheets with intracrystalline mesopores (around 7 nm) from which the zeolitic micropores can be accessed. This pore system is constructed of zeolitic nanosheets in a house-of-cards-like assembly with wide macroporous interstices between the nanosheet stacks.	[51]
MFI	CTAB	A nearly transparent zeolite seed solution allowed the direct self-assembly synthesis of the hierarchical zeolite using CTAB as the mesoporegen, and ethanol as a self-assembly modulator added prior to the hydrothermal step. Overaging the seed solution resulted in nanocrystals of about 100 nm in size and large aggregates.	[52]
MFI	CTAB	The crystal morphology was adjusted through a microemulsion-based hydrothermal synthesis. CTAB with cosurfactant butanol was used to form water-in-oil microemulsions. Small irregular rod-shaped nanoparticles were obtained, smaller, and more uniform than those synthesized without the microemulsion.	[53]
MFI	Igepal CO-520, CO-720, and CO-890,	The synthesis of silicalite-1 in nonionic microemulsions showed the ability to manipulate the shape and size of silicalite-1 materials, growing both as spheres and platelets. Large particles are robust aggregates of small submicron particles that were stable to calcination.	[54]
MFI	CTAB, TBAOH	Hierarchically macro-/meso-/micro-porous structured ZSM-5 with enhanced hydrothermal stability was synthesized by a simple route using CTAB and TBAOH as the meso- and micro-pore templates. Ethanol was used to generate macropores, probably via a proposed “ethanol-in-water” microemulsion mechanism.	[55]
MFI	Triton X-100	ZSM-5 with hexagonal cubic morphology was successfully synthesized using a nonionic surfactant as mesopore template, added prior to the hydrothermal step.	[56]
MFI	GPTMS	Hierarchical Fe-ZSM-5 zeolites with microspherical morphology was synthesized in the presence of GPTMS through a localized crystallization process.	[57]

Table 1. Cont.

Zeolite Structure	Template	Observations	Ref.
MFI	TPOAC	Hierarchical ZSM-5 was obtained through a two-step synthesis in the presence of organosilane TPOAC as the mesoporegen. The obtained materials are made up from very small microporous zeolite domains with sizes below 50 nm integrated into highly mesoporous particles.	[55]
MFI	C ₁₆₋₆₋₆ (Br) ₂ or C ₁₆₋₆₋₆ (OH) ₂	Hierarchical ZSM-5 zeolite was synthesized with a diquatery ammonium surfactant containing a hydrophobic tail. The materials consist of thin sheets limited in growth in the b-direction (along the straight channels of the MFI network.) The stacking of the zeolite sheets results in the formation of mesopores.	[58]

CTAB—cetyltrimethylammonium bromide; GPTMS—3-glycidoxypropyl-trimethoxysilane; RMMs—replication of mesoporous aluminosilicate molecular sieves; TEOS—tetraethyl orthosilicate; TPHAC—[3-(trimethoxysilyl)propyl] hexadecyldimethylammonium chloride; TPOAC—dimethyloctadecylammonium chloride; Triton X-100-Polyethylene glycol tert-octylphenyl ether.

Hard Templating

The first studies concerning bottom-up strategies reported the use of solid templates by Madsen and Jacobsen in 1999. The authors used carbon black particles to develop mesoporosity in MFI zeolite structure using different synthesis strategies and obtained nanosized zeolite crystals with intercrystalline mesoporosity [26] and, later, mesopore zeolite crystals with intracrystalline mesopores [27]. Following the same procedure, Koekkoek and coworkers [29] reported the use of uniform size carbon black particles (BP2000) to act as a solid template along with Fe(NO₃)₃·9H₂O for the synthesis of hierarchical Fe/ZSM-5 and obtained materials with uniform mesopore size distribution. The hierarchical catalysts exhibit superior catalytic performance, especially in terms of stability, in the selective oxidation of benzene to phenol. Soon, the same synthesis strategies were applied to a wide range of zeolite structures, as can be seen in Table 2. However, as some carbon black had a wide range of particle size, leading to randomly oriented or cavern-like mesopores, other carbon materials soon emerged as possible templates, such as, carbon nanotubes [34] or nanofibers [31], as well as the application of other materials such as polymers [43], or even more creative biological materials, such as starch [40], wood cells [41], or even leaves and stems of plants [42]. The use of these materials as templates brings the advantage of being abundant and relatively inexpensive, as well as offering a great diversity of shapes and sizes. A different, but also sustainable, approach was recently reported Li et al. [13] that used a wasted zeolite catalysts (coke-spent MFI zeolite) to produce hierarchical SSZ-13 zeolites (CHA structure), providing an efficient procedure to transform a waste zeolite catalyst into a new and valuable hierarchical zeolite.

Soft Templating

As an alternative to the use of solid materials as templates, the use of macromolecules has also been reported to produce hierarchical zeolites. The name “soft” comes from the fact that the extraporous system is generated by the presence of a macromolecule/surfactant that is added during the synthesis of the zeolite structure. Soft templating strategies can be categorized into primary or secondary methods. In the first case, all components including the soft template are introduced at the beginning of the synthesis, whereas in the second case the surfactant is added prior to the hydrothermal step [59]. The first methodology produced hierarchical zeolites with a high degree of mesoporosity. However, this strategy uses, frequently, surfactants that are not commercially available, as they prepared prior to zeolite synthesis, making this method expensive [25]. An example was recently reported by Li and coworkers [48] who prepared a series of Gemini surfactants to act as surfactants that were added directly to the synthesis gel to produce hierarchical ZSM-5 zeolite (see Figure 8). The obtained materials with abundant intercrystalline mesoporosity contained

a large amount of hydroxyl groups on the crystal surface that were used to immobilize a molybdenum compound and, later, used as supported catalysts for epoxidation of alkenes.

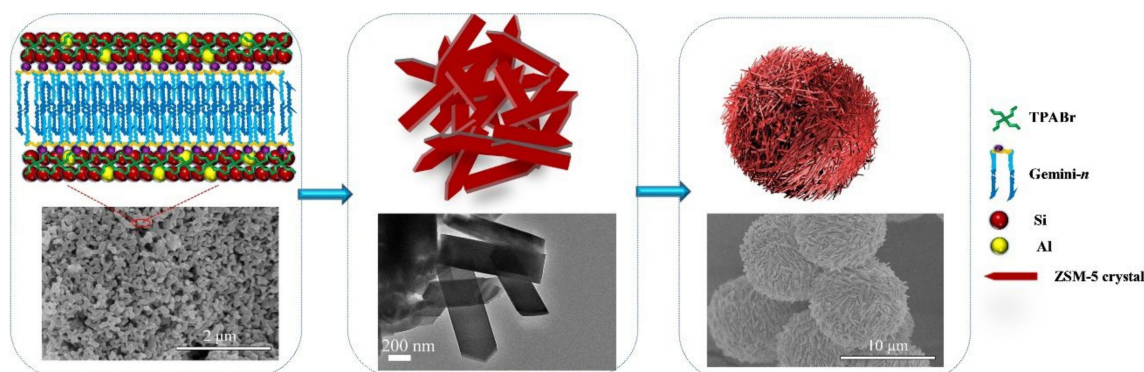


Figure 8. Proposed formation process for the synthesis of HZSM-5 using Gemini-n as a mesoporous structure directing agent. Reproduced with permission from Reference [48]. Copyright (2021), Wiley-VCH GmbH.

In secondary methods, a two-step synthesis procedure is carried out: on the first step, the zeolite synthesis gel is left to age in the absence of the surfactant at temperature around 100 °C for different periods of time to form seeds (subnanocrystals), and in the second step, a solution of the surfactant is added to direct the self-assembly of precrystalline zeolite units during the hydrothermal synthesis. This methodology was successfully used by Narayanan et al. [56] who added a nonionic surfactant (Triton-X, commercial designation of polyethylene glycol tert-octylphenyl ether) as mesoporegen template to the zeolite seeds, before the hydrothermal step. The textural analysis showed the presence of meso- and macro-pores without intensively destroying the microporosity, which allowed a significant higher conversion and reusability in the liquid phase oxidation of toluene. A variation of the secondary method consists of the creation of additional porosity in zeolites through the generation of biphasic emulsions. According to this methodology, a mixture containing the surfactant and an aqueous phase undergoes a phase-separations in order to obtain a stable biphasic emulsion [53,54]. A successful example of this procedure is described by Koekkoek et al. [55], where hierarchical MFI zeolite was prepared in the presence of TPOAC (dimethyloctadecylammonium chloride) surfactant in methanol (60% *w/w*), followed by the addition of an iron precursor solution. The Fe hierarchical ZSM-5 catalysts, made up from very small microporous zeolite domains with sizes below 50 nm integrated into highly mesoporous particles, were used in selective oxidation of benzene. As a final remark, it must be mentioned, in agreement with Schwieger et al. [25], that secondary methodologies are dual, since they can also be understood as Post-synthesis treatments, attending that the generation of the additional porosity occurs after the crystallization of the zeolite seeds.

Besides the approaches mentioned before, hierarchical zeolites can also be prepared using microwave radiation, which is a low-frequency form of electromagnetic energy that is commonly used to speed up slow reactions where high activation energies are required. The synthesis of hierarchical zeolites and zeotypes (i.e., crystalline structures based on the zeolite frameworks but with other elements than Al and Si, as is the case of SAPO, a silicoaluminium phosphate) using microwave radiation takes advantage of the reduced time needed to accomplish the crystallization step; thus, small crystals are obtained with intercrystalline porosity that results from crystal stacking. An extensive review concerning the synthesis of several zeolite structures and related materials using microwave radiation was presented by Tompsett et al. [60].

3.1.2. Top-Down Strategies

Postsynthesis or top-down strategies comprise the treatments performed on previously synthesized zeolites, aiming to modify its porosity through the creation of a secondary

pore system, generally mesopores. Some strategies are low cost since they involve cheap and common reactants to modify the zeolite porosity. On the other hand, the starting materials are generally commercial and robust structures with consolidated properties in adsorption and catalysis fields. The most common strategy to develop mesoporosity in a presynthesized zeolite is the demetallation, i.e., the removal of T atoms, either aluminum (dealumination), or silicon (desilication). Unfortunately, a common drawback of these procedures is that they may lead to significant mass losses that are reflected in significant impact on zeolite crystallinity and acidity. This is particularly important in more sensitive zeolite structures; thus, a careful choice of the experimental conditions, such as temperature, acid/base concentration, and duration of the treatment, is fundamental for obtaining hierarchical porosity, not disregarding other important properties such as crystallinity and acidity.

Table 2 displays some representative examples concerning strategies to attain demetallation in zeolite structures, that is, dealumination and desilication. Some examples are briefly mentioned in the following section, and selected case studies are analyzed in more detailed in the catalytic applications section.

Table 2. Examples of recent studies on dealumination and desilication processes used to prepare hierarchical zeolite structures.

Zeolite Structure	Treatment	Observations	Ref.
Dealumination			
FAU	Steaming + acid treatment	The treated zeolite samples were able to adsorb water-soluble organic molecules, thus improving their hydrophobicity.	[61]
FAU	Steaming, steaming twice + acid leaching	High mesoporous volume was obtained, comprising mainly interconnected cylindrical mesopores.	[62]
MOR	Steaming	Most of the framework Al species in the 12-membered ring channels of mordenite were removed while those in the 8-membered ring channels were retained. Strong reduction of acid sites located in the 12-membered ring channels.	[63]
BEA	Steaming	A significant reduction of acid sites as consequence of steaming dealumination hinders the occurrence of extensive cracking reactions and favors isomerization, as desired.	[64]
MWW	Steaming	The number of acid sites was decreased by hydrothermal treatment, but the acid strength was not modified. Aluminum debris located in the porosity reinforced the shape selectivity.	[65]
BEA	Acid treatment with HNO ₃	As-synthesized Al-BEA zeolite was submitted to acid treatment with HNO ₃ in a stainless-steel autoclave at 80 °C for 24 h to replace Al by Ti in the framework positions. Highly interconnected three-dimensional ordered mesopores were observed.	[66]
MFI	Steaming or acid treatment with oxalic acid and combination of steam+acid+alkali treatment	The steam treatment was performed in a quartz fixed bed tube at 700 °C for 3 h and 0.386 bar. For the acid treatment, 0.1 M oxalic acid for 2 h and 70 °C was used. For the alkaline treatment, 0.2 M NaOH at 80 °C for 2 h was employed. It was observed that the alkaline treatment heals the destructive parts of the zeolite that was produced by the steam and acid treatments.	[67]

Table 2. Cont.

Zeolite Structure	Treatment	Observations	Ref.
Desilication			
MFI	NaOH	Alkaline treatment with 0.2 M NaOH at 80 °C for 300 min. Development of mesopores whose size is almost uniform without destruction of microporous structure.	[61]
MFI	NaOH	Alkaline treatment with 0.2 M NaOH at 80 °C. Parent zeolite samples with distinct crystal size were submitted to the treatment: commercial sample with small crystallites and laboratory made large crystals. Desilication was proven to be highly efficient to alleviate diffusion limitations in small crystal commercial zeolites by producing hierarchical samples to an extent comparable to model large crystals produced in laboratory scale.	[68]
MFI	NaOH followed by acid washing with HCl	Desilication of ZSM-5 with Si/Al ranging from 10 to 1000 using 0.1–1.8 M NaOH. For Si/Al < 20, an additional acid treatment is essential for removing amorphous Al debris from alkaline treated samples, allowing the restoration of the zeolite acidity.	[69]
MOR	NaOH	Optimization of the desilication experimental parameters: base concentration, temperature, and time. The optimum desilication conditions (that is, allowing high crystallinity, acidity, and mesoporous volume) were obtained with the sample treated with 0.2 M NaOH, at 85 °C for 2 h.	[70]
BEA	TPAOH (tetrabutylammonium hydroxide)	“One-pot” desilication + ion exchange protocol using TPAOH was applied to zeolite BEA. The obtained material was highly mesoporous and acidic; showing that for specific zeolite structures, it is necessary to carefully search for the optimal base that stabilizes sensitive structures.	[71]
MWW	NaOH followed by acid treatment with HCl	Mesoporosity was attained using 0.05 M NaOH solution and practically no gain was observed when using 0.1 M NaOH. When desilicated sample with 0.1 M was submitted to acid washing with 0.1 M HCl the extraction of Al from the two internal porous systems promotes their interconnectivity, evolving from a 2-D to a 3-D structure.	[72]
BEA	NaOH followed by acid treatment with HCl	BEA zeolites with Si/Al ratio of 12.5 and 32 were submitted to alkaline treatment with 0.1 M NaOH solution followed by acid treatment with 0.1 M HCl. The Si/Al ratio has a determinant role on the properties of the final materials. For Si/Al = 12.5, the loss of acid sites during desilication is reversed upon acid treatment, whereas for Si/Al = 32, a continuous decrease in Brönsted acidity was observed simultaneously with a significant decrease in crystallinity.	[73]
BEA	NaOH followed by acid treatment with HCl	BEA (Si/Al = 12.5) was treated with 0.2 and 0.4 M NaOH, followed by acid treatment with 0.1 M HCl. Some decrease in microporous volume was observed, especially for the sample treated with 0.4 M NaOH. The development of mesoporosity also occurred with an uptake of 5–7% for the desilicated samples and an increase of 20–22% after the acid treatment.	[74]
MOR	NaOH	Desilication treatments with 0.2 M NaOH at 85 °C under conventional (0.5–10 h) and microwave (5–30 min, 300 W) heating. Both heating methods promoted the development of mesoporosity. However, microwave irradiation also results in the partial conversion of the zeolite pristine microporosity into larger micropores.	[75]

Dealumination

Dealumination is the oldest postsynthesis treatment that was originally developed to control the number and strength of acid sites in low-silica zeolites, through the increase in their Si/Al ratio. The procedure, firstly explored by Barrer and Makki in the 1960s [76], consists of the selective removal of Al atoms from the zeolite framework, leading to the creation of vacancies that constitute the additional porosity, mainly mesopores. Further, the hydrothermal stabilization of the zeolite structure is also achieved. There are several review papers that report dealumination procedures in several zeolite structures [25,77–80], being the larger number of publications dedicated to FAU structure due to the important industrial application of dealuminated Y zeolite in the fluid catalytic cracking (FCC) process [81].

The routes for extracting aluminum from a zeolite structure can be classified into two general groups: hydrothermal treatments and treatments employing chemical agents, mostly acids. Nevertheless, hydrothermal treatments, especially steaming are, by far, the most explored methodology, which is not surprising, considering that this method is used to produce ultrastable Y zeolite (USY), which is the base catalyst for the FCC process [81]. Acid treatments are also widely explored, as the main dealumination procedure or, more commonly, as a second step treatment to enable the removal of extra framework material formed during the hydrothermal process. Independently of the dealumination method used, the mesopores are created by the extraction of Al from the zeolite framework, which is responsible for the zeolite acidity. Accordingly, a decrease in the number of acid sites is always observed [77,82]. Still, an increase in the strength of the acid sites is also attained, until a certain level of dealumination is performed.

Desilication

Desilication is an alternative demetallation strategy that consists of the selective removal of Si atoms from the zeolite framework, generally using NaOH as a desilicating agent. This method was first mentioned in the literature with the purpose of modifying the Si/Al ratio of zeolites structures, without significant impact on the zeolite acidity, as opposed to dealumination procedures [83,84]. Nevertheless, the presence of mesoporosity was only mentioned in 2000 by Ogura et al. [85]. The authors submitted ZSM-5 to an alkaline treatment with NaOH solution and reported the presence of mesopores without significant damage of the original microporous structure. In spite of the great amount of research concerning the desilication method being dedicated to ZSM-5 (MFI structure), due to the expressive number of papers and reviews published by the Pérez-Ramirez group [68,69,86–89], an identical procedure has also been applied to a large number of zeolite structures (see Table 2). For example, MOR structure was subjected to an optimization of the desilication conditions by changing the temperature, base concentration, and duration of the treatment [90]. Figure 9 shows the corrosion of the crystals (lighter zones of the right TEM image) as a consequence of the treatment that leads to the development of mesoporosity.

The desilication procedures performed over several zeolite structures soon revealed that the experimental conditions used (e.g., NaOH concentration, temperature and duration of the treatment) had different impact, depending on the zeolite structure [70]. It was also found that the Si/Al ratio of the parent zeolite structure is an important parameter to account for desilication treatments. Verboekend and coworkers [69] deeply studied the effect of this parameter and found that for low Si/Al ratios an acid-washing subsequent to the desilication treatment is required, with the purpose of removing aluminum-rich debris to restore the occluded porosity. This effect was observed also in MWW (Si/Al = 13.8) [72] or BEA (Si/Al = 12.5) [73]. On the other hand, for high Si/Al ratios or even in the case of pure silica materials, such as silicalite-1, the addition of organic molecules, such as tetraalkylammonium cations with NaOH, was successfully reported [91,92]. These organic molecules act as “pore directing agents”, PDAs, which partially cover the outer surface of the zeolite crystals, allowing a controlled desilication of the zeolites, preserving their

properties, such as crystallinity and microporosity [69]. These organic molecules can also act as “softer desilication agents” when compared with NaOH, allowing one to perform desilication treatments over sensitive zeolites structures, namely BEA, as successfully reported by Holm et al. [71]. An additional advantage of using organic bases as desilicating agents is that the method allows one to combine desilication and ion exchange in only one procedure, whereas a second step of ion exchange is needed after desilication with NaOH to ensure that the final material is in the protonic form.

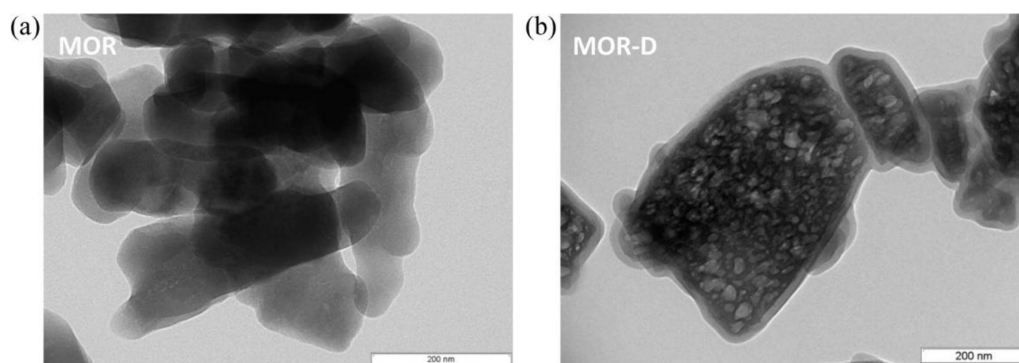


Figure 9. TEM images of (a) parent (MOR) and (b) desilicated MOR (MOR-D) zeolites. Reproduced with permission from Reference [90]. Copyright (2013) Elsevier B.V.

Desilication treatments in the presence of microwave radiations has also been reported as an effective postsynthesis method to modify the porosity of zeolites and zeotypes. The first study was firstly published in 2009 by Abelló and Pérez-Ramírez [93] where the desilication of ZSM-5 in the presence of NaOH was effectively performed in a few minutes irradiation time. The same methodology was later extended to other zeolite structures such as MOR [75] or MWW [72]. In all cases, hierarchical materials were obtained, and the time needed for the treatments was substantially shortened. However, in some cases, the textural modifications were distinct depending on the heat source: when conventional heating was used an increase in the mesoporous volume was observed whereas on the presence of microwave radiation an enlargement of the microporosity was verified [75].

Surfactant-Templated Zeolites

In spite of a high number of publications concerning the effective preparation of hierarchical zeolites through desilication methods, as well as the significant number of well-succeeded catalytic applications, it was also reported that one of the disadvantages of conventional desilication is the poor control of the mesoporosity, that is, the shape, size, connectivity and location of the mesopores, especially in the presence of strong bases such as NaOH [72]. Thus, current trends in the development of hierarchical materials are focused on controlling the mesoporosity through the combination of several methods to tune the hierarchical porosity and related properties of zeolites. An important contribution in this topic was given by Garcia-Martinez and coworkers [94–97] who proposed that hierarchical zeolites can be prepared by a postsynthesis treatment involving a base and a surfactant. Using optimized parameters of concentration, temperature, time, and pH, the silica dissolution takes place just locally, and the surfactant micelles lead to the rearrangement of the released zeolite subunits into an ordered meso structure, due to a local rearrangement mechanism. This effect was firstly described by Ivanova et al. [98] and, later, by Wang et al. [99], who described the treatment of MOR zeolite using solutions of cetyltrimethylammonium bromide (CTAB) and NaOH with different concentrations and observed that, for high base concentrations, the zeolite microporosity was completely removed and replaced by a mesoporous MCM-41 type material. On the other hand, when low base concentration was used, the zeolite recrystallizes, exhibiting both micro- and meso-pores; that is, a hierarchical MOR zeolite was developed. Garcia Martinez et al. [94] applied identical strategy and

made a clearer interpretation of the local crystal rearrangement phenomena. By performing a mild treatment to Y zeolite (FAU structure) using NH_4OH base solution and CTAB, followed by a hydrothermal treatment, under autogenous pressure. The resulting material presented, not only a higher mesoporosity, but its mesopore size distribution was more uniform, keeping the crystal size and morphology intact (see Figure 10).

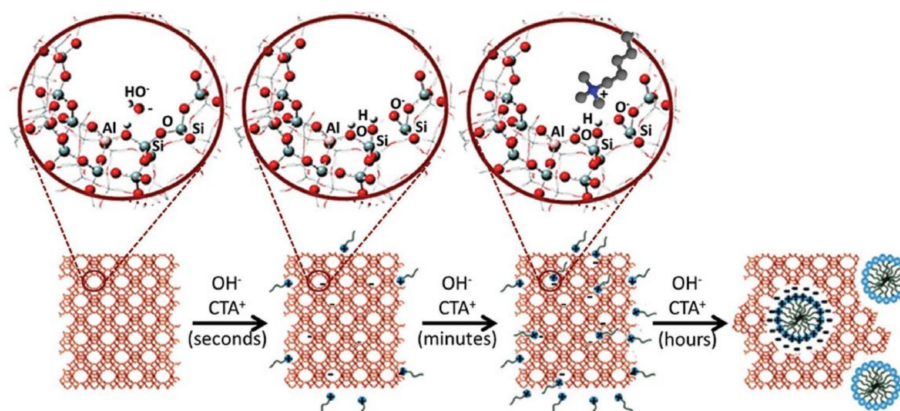


Figure 10. Schematic representation of the different steps involved in the surfactant-templating of zeolites: (i) the hydroxyl groups react with the zeolite network to generate negatively charged sites ($\text{Si-O-Si} + \text{OH}^- > \text{SiO}^- + \text{Si-OH}$); (ii) the cationic surfactant molecules are attracted inside the zeolite by electrostatic interaction; and (iii) the surfactant molecules self-assemble in micelles inside the zeolite crystals, forming the mesoporosity. Adapted with permission from Reference [97]. Copyright (2020) Wiley-VCH GmbH.

The same strategy has been applied to other zeolite structures, such as MOR [100], BEA, MFI, and LTA [101], as well as the exploration of other surfactants and bases [100,102,103]. Recently, Mendoza-Castro et al. [97] critically reviewed the surfactant-templated methodology, from the optimization of experimental parameters to the extension of this methodology to a large number of zeolite structures, focusing on their use for industrial purposes. In this scope, the most relevant application is the mesostructured Y zeolite as FCC catalysts that is already use on industrial scale by Rive Technology Inc. since 2006 [94,104], but other applications were recently reported, including the synthesis of pharmaceutical compounds through Friedel–Crafts alkylation reactions using surfactant-templated USY [105].

Mechanochemistry

Mechanochemistry is a versatile method to induce several types of transformations on zeolites and related materials, especially milling, which deals with high energy/speed processes. According to the review paper of Majano et al. [106], the precise control of the energy supplied to the materials by the mechanochemical method allows several types of transformations, by the interaction of the solid with the surrounding species. For example, ion exchange or catalysis is favored when low energies are applied. On the other hand, total amorphization or even recrystallization occur in the presence of high energies. The modification of textural properties through mechanochemistry generally occurs when medium energies are applied, leading to the fragmentation and partial destruction of crystal/crystal aggregates. The few examples available on the literature include the wet ball milling of Y zeolite reported by Akçay et al. [107], where the authors highlighted the importance of the operating parameters of the ball mill, such as ball size, milling speed, and time, as well as the presence/absence of solvent. For instance, it was observed that when faster milling speed was applied, smaller particles were obtained, with wider particle size distributions, but the crystallinity was hardly affected. On the other hand, using a small ball diameter, very small particles were obtained after a long milling time, with narrower pore size distribution. Finally, the presence of solvent resulted in high crystalline material when compared with dry ball milling performed under the same conditions.

Hernandez-Ramírez et al. [108] described the synthesis of hierarchical Y zeolite–carbon composites using a new seeding technique based on milling carbonized olive seeds and coconut fibers coupled with commercial Y zeolite. More recently, Ferreira et al. [109] modified SAPO-11 zeotype through ball milling aiming to modify their textural properties by optimizing the milling time. The authors found that after 60 min milling a partial destruction and disaggregation of the crystal aggregates is optimized leading to an increase in the external surface area but keeping the acidity properties. This allows one to improve the catalytic behavior of SAPO-11 based materials since the access of the reacting species to the pore openings of SAPO-11 structure is improved.

Delamination and Pillaring

Layered materials are made of a consecutive repetition of individual layers or sheets located in parallel spatial planes, bonded through electrostatic interactions (van der Waals or hydrogen bonds). These open structures, with high surface area, are constituted by crystalline ordered (pillared zeolites) or disordered (delaminated zeolites); however, it must be mentioned that the application of these methods is not restricted to zeolite and zeotypes but is also successfully applied to other types of materials, namely clay minerals.

The pillaring process is known for a long time due to its application in clays, hydrotalcites and other inorganic lamellar materials and consists of the permanent covalent-type intercalation of materials with organic inorganic or the combination of them into the interlayer space. The process allowed one to considerably increase the surface area of the pristine material due to the creation of a bidimensional pore system upon the intercalation of the pillaring species (e.g., Kegi type cation $[\text{Al}_{13}\text{O}_4(\text{OH})_{(24+x)}(\text{H}_2\text{O})_{(12-x)}]^{(7-x)+}$) followed by calcination to obtain stable pillars. Even though nowadays these materials continue to be explored, the greatest number of studies based on pillared-clays immobilized complexes dates from the beginning of this century [110,111]. More recently, some application for zeolites has been reported. Accordingly, the materials possess their native microporosity and additional porosity obtained by the expansion of the layers that can be customized depending on the size of the pillars. The first and most cited example of pillared zeolitic material is MCM-36, which is obtained from the intercalation of MCM-22 precursor [112]. The preparation of this material follows the classic protocol that includes an initial swelling step through cationic exchange with alkyl-ammonium species ($\text{C}_{16}\text{TMA}^+\text{OH}^-$), which are placed in the interlayer space. Secondly, the swollen precursor is pillared in an inert atmosphere using tetraethylorthosilicate (TEOS), which is finally hydrolyzed, and then, in a final step, the sample is calcined to decompose the surfactant and obtain stable pillars, that expand permanently, originating intercrystalline mesoporosity between the layers [113]. Following the same methodology, Liu et al. [114] synthesized Sn-MCM-56, obtained from delaminated Sn-MWW and found significant improvements to the diffusion of bulky molecules when compared in the presence of microporous zeolites. The use of this method to produce other pillared zeolite structures is rather scarce. An example using the MFI structure was reported by Na et al. [115] who reported the successful pillarization without the swelling step to obtain a 3-D ordered hierarchical MFI structure, where the diameter of the mesoporous formed can be easily controlled according to the surfactant tail length. In addition, concerning the pillarization of MFI structure, Zhang et al. [116] described a process of three-dimensional nanosheet assembly by the repetitive branching of orthogonally connected nanosheets of MFI. The house-of-cards type of rearrangement of the nanosheets creates a permanent network of mesopores with 2–7 nm, along with a high surface area with great potentialities for catalytic applications involving bulky molecules.

In opposition to pillared materials, delaminated zeolites are made of disordered layers. Thus, the mesoporosity is obtained from the random stacking of these layers. The delamination process involves the treatment of the zeolite precursor with an alkaline solution in the presence of surfactants to expand the interlayer distance. Then, the suspension is submitted to sonication to promote the complete separation of the layers and, finally, the delaminated material is calcined to remove the surfactant. Inside the family of delaminated zeolites,

ITQ-2 was the first and still the most cited delaminated material [117]. The preparation method comprises the swelling and exfoliation of MCM-22 precursor and individual layers of about 2.5 nm of thickness, with a high external surface area of more than $700 \text{ m}^2 \text{ g}^{-1}$ being obtained. Examples of other delaminated materials referred to in the literature are ITQ-6 [118] and ITQ-18 [119], obtained from FER and NU-6(2) precursors, respectively.

Despite delamination and pillaring being effective strategies to obtain hierarchical structures, with some proven catalytic applications, the scale-up production of these materials is still challenging due to the high costs of the surfactant used. In addition, the significant loss of material that occurs, especially during the delamination process, because of the high surfactant content and alkalinity used that leads to the dissolution of the zeolite structure, is also a drawback when compared to other strategies to produce hierarchical materials.

3.2. Mesoporous Silicas and Composite Hierarchical Materials

Mesoporous molecular sieves (MMS) are characterized by high surface area ($800\text{--}1400 \text{ m}^2 \text{ g}^{-1}$), large pore volumes, and tunable pore dimensions (2–50 nm). The arrival of the first member of the M41S family in 1991, designated as MCM-41 [120], carries great expectations for possible applications of these materials in catalysis and adsorption, overcoming the limitations of zeolites due to their intrinsic microporosity. Later, other related mesoporous silica materials, namely MCM-48, MCM-50, and SBA-15, were synthesized [121]. Recently, more robust mesoporous silica materials have been presented, such as, TUD-1 [122], FDU-12 [123], or KIT-6 [124]. However, despite MMS materials possessing large pores when compared to zeolites, which allows for improving molecular diffusion, and some improvement on the stability having been attained in the last years, their lack of acidity hinders the application of these materials to a wide range of catalytic reactions, when compared with traditional zeolites [121], limiting their use mainly as catalyst supports.

Composite materials are characterized by a mixture between a zeolite, which contributes to its characteristic microporosity, and another material that must be porous itself, or alternatively, contributes to the generation of intercrystalline porosity due to particle stacking. Schwieger et al. [25] reviewed several combinations of composite materials: the simplest approach is the shaped zeolitic bodies, comprising the mixture of a powder zeolite with a binder material, that, after compacting and shaping operations, originates pellets, beads, cylinder, etc., with interparticle macropores on the packed bed level, when used as reactor/column filling. More technological approaches include coating strategies where a support surface is functionalized with a zeolitic material, originating hierarchically organized materials with two or three levels of porosity. The preparation of these materials can be performed according to two strategies: *ex situ* coating where a layer of a presynthesized zeolite is deposited on a support such as alumina foams [125] or cordierite monoliths [126] and *in situ* coating comprising the direct hydrothermal synthesis of a zeolite on a support surface. In this later case, the supports can be classified as inert or reactive: in the first case, the crystallization of the zeolite takes place at the external surface of the support keeping it unchanged [127], but on the other hand, in the presence of reactive supports such as SiO_2 or Al_2O_3 , a fraction of the support is consumed with consequent incorporation and intergrowth between the zeolite layer and the residual support material [128,129]. Recently, the combination of a microporous zeolite with a mesoporous material has gained much attention, comprising a core–shell system where the core is made of zeolitic microporous material surrounded by a mesoporous shell. These composite materials combine two organized pore systems: a microporous zeolite containing the active sites enwrapped in a mesoporous material with large transport channels, leading to an improvement on both catalytic and adsorption behavior. Examples of core–shell materials can be found on the literature using several zeolite structures such as MFI [130,131] FAU [132], and MWW [133] enwrapped by mesoporous molecular sieves such as SBA-15 and MCM-41, bringing a new opportunity for the application of these mesoporous molecular sieves.

4. Immobilization Methodologies

4.1. Complexes

Several methodologies can be used to immobilize metal complexes on solid supports and a possible systematization can be made considering the type of complex–support interaction: (i) covalent bonding; (ii) physical adsorption or electrostatic interaction; and (iii) encapsulation.

When zeolite structures are used, encapsulation by flexible ligand method is a quite common synthesis methodology. This “ship-in-a-bottle” strategy is basically a two-step process that takes advantage of the ion exchange properties of zeolites and of their pore network characteristics, namely the presence of large cavities accessible through windows narrow enough to hinder complex leaching, which explains that FAU structures are specially suitable to prepare immobilized catalysts by this method and are in fact those selected for this purpose [14–16,18]. The scheme reproduced in Figure 11 was presented by N.C. Desai et al. [16] to illustrate the preparation of several metal complexes immobilized on Y zeolite by the flexible ligand method. Catalyst preparation starts with the ion exchange of the as-synthesized zeolite (Na-Y) with the metal salt, to obtain what is designated in scheme by M(IV)/(II)-Y, being M = Fe, Co, Ni, etc. The exchanged solid is then made to react with the ligand—in this study, a Schiff base, refluxing the mixture to promote the complex synthesis. The catalyst is then washed by Soxhlet extraction, back-exchanged with a NaCl solution to eliminate uncoordinated metal, and finally washed and dried. The complex formed inside the Y zeolite supercages is too bulky to spread out so it cannot leach into the liquid phase during the catalytic assay. On the other hand, the space available inside the 1.3 nm diameter large cavity of the Y zeolite is enough to accommodate the complex and to allow the diffusion of substrates and products no larger than 0.74 nm, i.e., the pore opening value. The catalysts prepared proved to be active for styrene oxidation and in the case of the best performing catalysts reuse tests shown that a short fall in the activity was observed only in the second cycle, attributed to the leaching of a small fraction of the immobilized complex, which was not observed in subsequent reuse cycles.

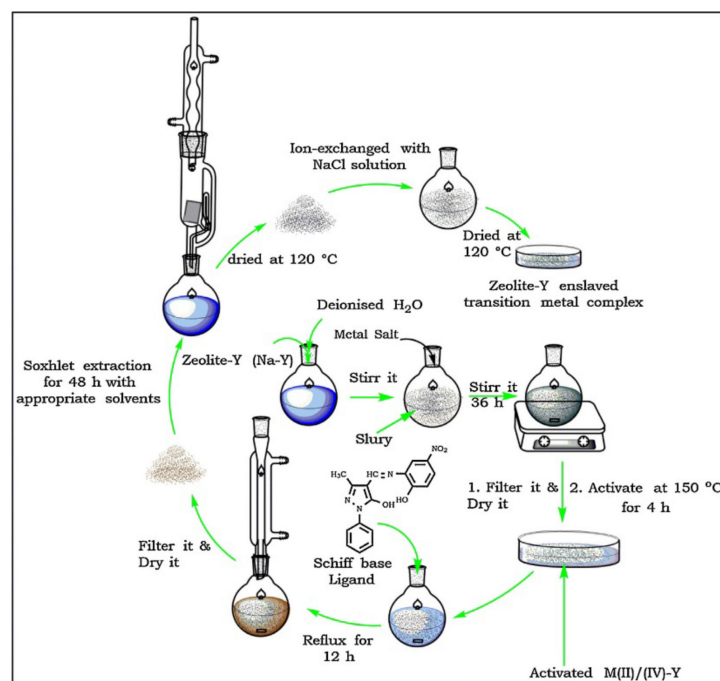


Figure 11. Scheme of the experimental procedure to encapsulate complexes on Y zeolite by flexible ligand method. Reproduced with permission from Reference [16] Copyright (2016) Elsevier B. V.

Other types of structures imply other synthesis approaches such as, for example, covalent bonding or electrostatic interaction that are widely used when large pore solid supports, such as mesopore silicas, are considered. To apply this synthesis methodology, it is necessary that the solid surface has functional groups that can react with the complex (either with the metal or with the ligands) during the immobilization, which is promoted by refluxing the mixture support-complex, typically overnight. The final steps are the usual washing and drying processes [74,100].

The catalysts obtained by this method have leaching as their main disadvantage, which can attain values as higher than about 50%, as reported in the study where Fe-scorpionates immobilized of NaOH treated MOR were tested for cyclohexane oxidation [90]. This result was interpreted as indicative of an electrostatic interaction of the complex with the support.

On the other hand, as consequence of the immobilization, the electronic structure of the homogeneous catalysts is modified, and consequently, its performance is not the same as that of the homogeneous counterpart. This is clearly shown by the results reported by Jarrais et al. [134] for $[\text{VO}(\text{acac})_2]$ immobilized on a ordered mesoporous silica (HMS). The catalysts were tested for geraniol epoxidation, and while the homogenous assays resulted in a total conversion of the substrate after 1h of contact time, when the catalyst obtained by direct immobilization (method A in Figure 12) was used, only 17% of substrate conversion was obtained after 48 h of reaction. To overcome this disadvantage, it is common to consider the use of a linker, that is, a molecule that has a moiety that forms a covalent bond with the support and a moiety that can coordinate with the complex (either with the metal or with the ligand), which is then immobilized. This approach was also followed by Jarrais et al. [134] to prepare catalyst B2 using APTES (3-aminopropyl-triethoxysilane) as a linker. In this case, there are more preparation steps, since the synthesis starts with the solid functionalization with the linker, after what the modified solid support is then refluxed with the solution containing the complex. The more elaborated synthesis process resulting in a much better catalytic performance than that of material A1, since after 48 h a total conversion of geraniol was attained not only with the fresh catalyst but also in the fifth reuse cycle.

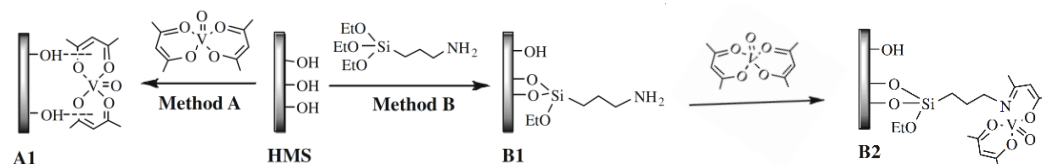


Figure 12. Methodologies for $[\text{VO}(\text{acac})_2]$ immobilization onto HMS materials. Adapted with permission from Reference. [134] Copyright (2009) Elsevier B. V.

Another example of how the abundance of Si-OH surface groups of HMS are used to immobilized organometallic complexes using a linker is provided by Pinto et al. [135]. These authors used ordered mesoporous silica SBA-15 and its correspondent chloropropyl-functionalized silica (SBA-15Cl) as supports for immobilization of different neutral and charged Mn porphyrins (MnP) (Figure 13). The resulting MnP-supported materials with MnP loadings of 0.3% *w/w* were obtained in these materials, and the heterogenized systems SBA-15/MnTM-X-PyPCL₅ and SBA-15Cl/MnT-X-PyPCL (X = 2, 3, 4) and nonimmobilized neutral MnP isomers were successfully evaluated as catalysts for cyclohexane oxidation using iodobenzene (PhIO) as oxygen donor, as is discussed in Section 5.

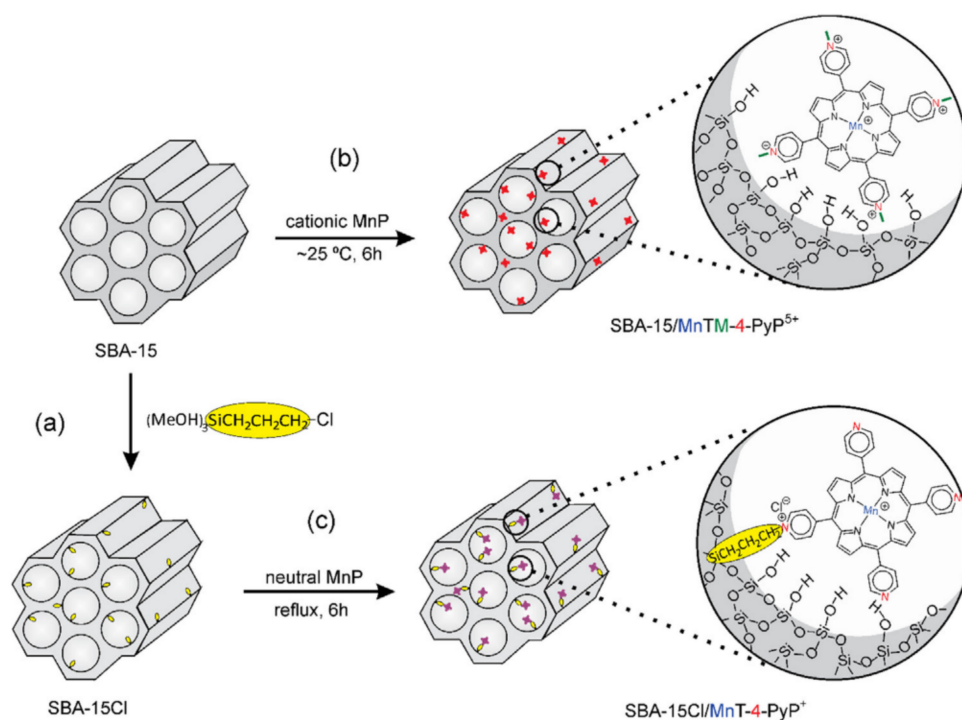


Figure 13. Schematic representation of the synthetic routes for (a) preparation of support SBA-15Cl by the silanization of SBA-15 with CPTS, (b) immobilization of MnTM-4-PyP⁵⁺ on SBA-15 by electrostatic interaction, and (c) anchorage of MnT-4-PyP on SBA-15Cl by covalent bonding. The two classes of heterogenized catalysts are illustrated with the para MnP isomers. Reproduced with permission from Reference [135]. Copyright (2016) Elsevier B.V.

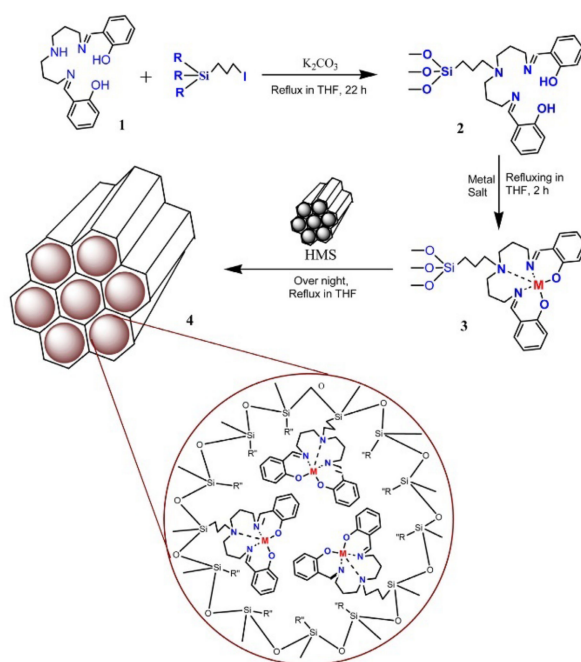
A different approach for the immobilization by covalent bonding with a linker is illustrated in the scheme in Figure 14, reproduced from the study by Machado and co-workers [136]. In this work the linker reacted with the ligand (step 1) that was further used in the complex synthesis (step 3). During the reflux of the complex solution with the mesopore silica HMS (step 4), the linker reacted with surface groups of the support leading to the immobilization of the complex. This procedure minimizes the changes in the electronic structure of the homogeneous catalysis and eventual constraints due to the solid surface proximity.

Even though in the literature, there are examples of immobilization by covalent bonding with a linker with various materials, namely carbon materials [137,138], inorganic solids like clays or clay-derived materials [134,139,140] and especially silicas are actually the most currently used supports when this immobilization process is envisaged due to the high amount of hydroxyl surface functionalities of these materials [111,135].

Lastly, it must be noted that the longer reaction time needed when immobilized catalysts in porous materials are used is a common result due to the presence of diffusion steps which are not present in homogeneous assays.

4.2. Metal Particles

The immobilization of metal particles in zeolites and other porous materials can be made by two distinct strategies: postsynthetic methods and confinement during synthesis. In the first case, the metals are introduced after the complete synthesis of the zeolite framework, whereas the second method deals with the co-crystallization of the zeolite and the metal precursors, followed by an in situ reduction to obtain the metal particles [19].



Where, R'' = other anchored units, M = Fe or Ni or Mn,
 HMS = hexagonal mesoporous silica support

Figure 14. Scheme of the experimental procedure to immobilize Fe, Ni, or Mn complexes on HMS–hexagonal mesoporous silica through covalent bonding. Reproduced with permission from Reference [136] Copyright (2013) Elsevier B.V.

The postsynthesis immobilization is simple and widely used. It deals with contacting the support with a solution containing the soluble metal precursor and can be made by two methods [141]: (i) using an excess of solution (ion exchange) [142,143] or (ii) using the minimum amount of solution needed to fill the porosity of the material (incipient wetness impregnation) [144,145]. Upon these procedures, the material is dried and submitted to a thermal treatment in the presence of hydrogen to promote the reduction of the metal precursors into its active state, where special care should be taken during this procedure to avoid metal sintering. To avoid this step, an alternative method comprising the contact between two solids can be performed. In this case, the zeolite and the inert support containing the dispersed metal are put in contact through mechanic mixing using a simple mortar or, more sophisticatedly, a ball mill to allow an improved contact between the two solids [30,109,146].

In pure microporous zeolites, the dimension of the confined metal particles is restricted to a few nanometers, that is, limited by the dimension of the pores [147]. In the presence of small size metal particles, their diffusion is allowed inside the pores; even so, this is only facilitated in the presence of large pore zeolite structures such as BEA, MOR, or FAU, where the metal particles can be encapsulated inside the pores. For larger particles or in the presence of medium to small pore zeolites, a large amount of metal is restricted to be fixed to the external surface of the zeolite crystals.

To overcome this limitation, the use of supports with hierarchical porosity has been revealing promising results. For instance, Wang et al. [148] reported what they called a “fish in the hole” strategy to trap Pd nanoparticles in FAU, BEA, and MFI zeolite structures. The authors performed a thermal treatment at 700 °C for a slight dealumination to create “traps” with diameter of 20–30 nm. Upon mixing the Pd precursors with the “trap”, rich zeolite and further heat treatment, the metal particles became confined at the “traps”, preventing the metal aggregation, even under harsh thermal conditions. In another study, hierarchical MOR was prepared through alkaline treatments followed by acid treatment, originating an effective support for the introduction of Pt nanoparticles [149]. The Pt loaded on hierarchical MOR showed superior metal dispersion when compared with the pristine

microporous MOR, giving superior catalytic performance for toluene combustion and long-term stability (60 °C) making this material a promising catalyst for real application in volatile organic compounds (VOCs) control.

Metal sites can also be introduced inside zeolite crystals during synthesis. In this case, as-synthesized metal particles or soluble metal precursors are mixed with the zeolite synthesis gel. Upon the crystallization step, the material is calcined to remove organic species and reduced under hydrogen atmosphere to form the metal sites [55,57].

An important issue to successfully confine metal particles during the synthesis is to accomplish an adequate balance between the simultaneous crystallization of both the zeolite and the metal clusters to obtain a homogeneous dispersion and size of inside the zeolite crystals. To achieve this goal, a judicious choice of the experimental conditions of the synthesis (e.g., alkalinity, silica source), as well as the type of metal or metallic precursor, is mandatory [19].

5. Catalytic Applications

This section presents the catalytic applications of coordination compounds or metals particles immobilized at inorganic supports whose synthesis/modification was described in Section 3.

Among commercial zeolites, FAU structure is the most cited material used as catalyst support. This can be explained by the presence of large supercavities in its structure that can accommodate large species. The introduction of mesoporosity in zeolites, leading to the so-called hierarchical materials (see Section 3.1), as well as the use of purely mesoporous materials (see Section 3.2) allowed one to overcome the accessibility limitation of commercial zeolite and triggered the applications of these porous materials as catalytic supports. Representative examples are summarized in Tables 3–5, and relevant examples follow.

Table 3. Catalytic applications of commercial/hierarchical zeolites and other related materials as catalysts support for oxidation of alkanes.

Support	Catalyst	Reaction Type	Observations	Reference
FAU	[M(salophen)] and [M(H ₄ salophen)], (M = Mn(II), Co(II), Ni(II) and Cu(II); salophen = <i>N,N</i> -bis-(salicylidene)-1,2-phenylenediamine; H ₂ [H ₄ salophen] = 2-((2-[(2-hydroxybenzyl)amino]anilino)methyl)phenol	oxidation of cyclohexane with H ₂ O ₂	Catalysts encapsulated in the pores of NaY by exchanging the Na by the transition metal M(II), followed by reaction of metal-exchanged Y zeolite (M(II)-NaY) with H ₂ salophen and H ₂ [H ₄ salophen] in the molten state. The encapsulated catalysts systems [M(H ₄ salophen)]-NaY were more active than the corresponding complexes [M(H ₄ salophen)].	[150]
FAU	[M(SFCH)·xH ₂ O]-Y [M = Mn, Fe, Co, Ni (x = 3) and Cu (x = 1)]; H ₂ SFCH = (<i>E</i>)- <i>N'</i> -(2-hydroxybenzylidene) furan-2-carbohydrazide]	oxidation of cyclohexane with H ₂ O ₂	Complexes entrapped in the cages of Y zeolite (suitable in size for the zeolite channels shown by DFT calculations). The initial run showed a conversion of 45.1% which was only slightly reduced after the 2nd reuse of the supported catalysts.	[151]
FAU	[M(L)] [M = Co(II) or Cu(II)]; (L = Schiff bases)	oxidation of cyclohexane with H ₂ O ₂	Immobilization of the complex inside the zeolite pores using the flexible ligand method. The immobilized complexes afforded a maximum yield of 75.2% and could be recovered and reused without loss of catalytic activity. In addition, active in oxidation of cyclooctane (76.8% yield).	[17]

Table 3. Cont.

Support	Catalyst	Reaction Type	Observations	Reference
Hierarchical FAU	[FeCl ₂ {κ ³ -HC(pz) ₃ }] (pz = pyrazol-1-yl)	oxidation of cyclohexane with H ₂ O ₂	Y zeolite was modified through alkaline treatments (NH ₄ OH, NaOH or TPAOH) assisted by CTAB surfactant. Iron complex was immobilized at the support by incipient wetness impregnation method. The reuse of the sample in the catalytic oxidation reaction led only to a small decrease in Fe content, after the 3rd catalytic cycle.	[100]
Hierarchical MOR	[VO ₂ {HB(κ ³ -3,5-Me ₂ pz) ₃ }] (pz = pyrazol-1-yl)	oxidation of cyclohexane with <i>t</i> -BuOOH	Hierarchical MOR zeolite prepared through alkaline treatments (NaOH or TPAOH) assisted by CTAB surfactant. The vanadium complex was immobilized at the support by the incipient wetness impregnation method. Reuse up to four consecutive catalytic cycles with no appreciable leaching	[103]
Hierarchical MOR	[FeCl ₂ {κ ³ -HC(pz) ₃ }] (pz = pyrazol-1-yl)	oxidation of cyclohexane with H ₂ O ₂	Hierarchical MOR prepared through desilication using 0.5 M NaOH. Iron complex immobilized at the support by incipient wetness impregnation method. Much higher TON, high yield values, and lower loading of oxidant for the heterogeneous than for the homogeneous one. However, a considerable (46%) loss of activity, mainly due to lixiviation was observed.	[90]
Hierarchical MFI	Cu(I)/Cu(II) dispersed in the zeolite framework	oxidation of cyclohexane with H ₂ O ₂	Copper species incorporated in one-pot hydrothermal synthesis of hierarchical ZSM-5 zeolite. The excellent catalytic activity was ascribed to the hierarchical porous structure, allowing a fast diffusion of molecules and the highly dispersed framework copper ions (Cu ⁺ /Cu ²⁺) as catalytic active sites	[152]
SBA-15	Mn(III) <i>N</i> -methylpyridiniumporphyrins (MnTM-X-PyPCL ₅ , X = 2, 3,4)	oxidation of cyclohexane with PhIO	Immobilization of the catalysts by electrostatic interactions or covalent bonding. A low-leaching of manganese porphyrins from the supports was observed in both cases due to strong interaction with SBA-15.	[135]
SBA-15	[Mn(saldien)(N ₃)] (saldien = <i>N,N'</i> -dibis(salicylidene)diethylenetriamine)	oxidation of cyclohexane with H ₂ O ₂	[Mn(saldien)(N ₃)] was anchored on mesoporous SBA-15. The immobilized complex is stable and recyclable and gives comparable or even higher cyclohexane conversion than homogeneous system. In the oxidation of cyclohexane, products were formed in up to 355 turnovers.	[153]
MFI	Manganese Mn(IV)	oxidation of cyclohexane with H ₂ O ₂	ZSM-5 zeolite functionalized in situ with Mn was obtained via a one-pot hydrothermal approach. Mn-ZSM-5 materials, especially the 2% Mn ⁴⁺ doped ZSM-5, shows a high catalytic activity and selectivity.	[154]
HMS	[M(Sal)(PMeOSi)DPTA] (M = Fe, Ni, Mn; Sal = salicylaldehyde; DPTA = bis(2,4-pentanedionato)cobalt, bis(aminopropyl)amine)	oxidation of cyclohexane with O ₂	Complexes covalently anchored into HMS (2–10 nm pore size) via condensation process. The supported catalysts were stable under the applied temperature (200 °C) and could be recycled.	[136]

Table 3. Cont.

Support	Catalyst	Reaction Type	Observations	Reference
MCM-48	Ce(III) and Ce(IV)	oxidation of cyclohexane with O ₂	Cerium-doped MCM-48 was prepared hydrothermally, and its surface was modified with organic groups or fluorine. Postfunctionalized Ce-MCM-48 exhibited the higher conversion and selectivity. The F-modified catalyst showed excellent reusability, and its catalytic performance has no deterioration upon 5 reuse cycles.	[155]
KIT-6	(VO) ₂ P ₂ O ₇	oxidation of cyclohexane with H ₂ O ₂	Vanadium catalysts postsynthesis incorporated at KIT-6. The catalyst was reused several times, and no leaching/soluble vanadium phosphate species could be detected in the filtrate.	[156]
SBA-15, KIT-6 and FDU-12	CoMoO ₄	oxidation of cyclohexane with O ₂	The supports were soaked with the catalyst's precursors for 3–4 h, dried at 70 °C, and calcined changing the temperature from 350 to 550 °C. The calcination temperature influenced the catalyst activity, being the lowest temperature the most favorable. All suffer deactivation but activity could be restored on recalcination. Catalysts were used in multiple cycles of regeneration and reaction with no decrease in the performance.	[157]
TUD-1	Co(II) and a metal oxide (Cr, Cu, Ti, Mn, Bi, V or Sr)	oxidation of cyclohexane with <i>t</i> -BuOOH	One step synthesis of dual function M-Co on mesoporous TUD-1. The dual-function catalysts exhibited higher activity than either Co-TUD-1 or other M-TUD-1. Mn-Co-TUD-1 and Ti-Co-TUD-1 exhibited an excellent stability during the reaction, and Mn-Co-TUD-1 was successfully recycled up to 4 runs.	[158]

Table 4. Catalytic applications of commercial/hierarchical zeolites and other related materials as catalyst supports for oxidation of alkenes.

Support	Catalyst	Reaction Type	Observations	Reference
FAU	Mn(II) complex with a Schiff base ligand derived from L-tyrosine plus salicylaldehyde	oxidation of cyclohexene with H ₂ O ₂	Manganese(II) complex encapsulated in the supercages of Y zeolite by the flexible ligand method. The heterogeneous catalyst exhibited higher activity and selectivity than the homogeneous system. Catalytic activity of heterogenized system almost unchanged up to 5 cycles.	[159]
FAU	VO(IV), Mn(II), Fe(II), Co(II), Ni(II), Cu(II), and HNIMMPP Schiff base ligands	oxidation of styrene with <i>t</i> -BuOOH	Flexible ligand method used to synthesize Y zeolite imprisoned transition metal complexes. [VO(HNIMMPP)(H ₂ O)]-Y afforded the highest conversion of styrene and selectivity of benzaldehyde.	[16]
FAU	VO(IV) complexes of 7-amino-5-aza-4-methyl-hept-3-en-2-one and 4,4-(ethane-1,2-diyl)dinitrilo)dipentan-2-one	oxidation of phenol, benzene, styrene, cyclohexene with H ₂ O ₂	Complexes immobilized inside the cages of Y zeolite using the flexible ligand method. The homogeneous complexes were found to be more active than the corresponding encapsulated VO(IV) complexes, but the heterogenized complexes showed higher turnover frequency values (TOF) and better selectivity than the corresponding homogeneous catalysts.	[160]

Table 4. Cont.

Support	Catalyst	Reaction Type	Observations	Reference
FAU	V(IV)O, Mn(II), Co(II) complexes of a Schiff base ligand derived from 2,4-dihydroxyacetophenone and 1,2-diaminocyclohexane	oxidation of cyclooctene, cyclohexene, styrene, α -methyl styrene with <i>t</i> -BuOOH	Complexes encapsulated in the cavities of Y zeolite by the flexible ligand method. The catalytic activity decreased in the order CuL-Y > VOL-Y > MnL-Y. 100% selectivity for epoxide formation was obtained in the case of cyclooctene.	[161]
FAU	Binuclear complexes of V(IV)O and Fe(II)	oxidation of cyclohexene, limonene, α -pinene with H ₂ O ₂	Complexes encapsulated in the cavities of Y zeolite by the flexible ligand method. The formation of olefinic oxidation products follows the sequence α -pinene < limonene < cyclohexene due to steric hindrance. The heterogeneous catalyst kept the catalytic activity upon two consecutive runs.	[15]
FAU	[VO(sal ₂ bz)] ₂ and [Fe(sal ₂ bz)(H ₂ O)] ₂ ·2H ₂ O H ₂ sal ₂ bz = (Z)-3-methyl-1-phenyl-4-(2,2,2-trifluoro-1-(2-hydroxyphenyl)imino)ethyl)-1H-pyrazol-5-ol	oxidation of limonene, cyclohexene, styrene, and α -pinene with H ₂ O ₂	Complexes entrapped in the supercages of Y zeolite by the flexible ligand method. The effect of solvents, mole ratio of substrate and oxidant, amount of catalyst, and reaction time was tested. [VO(L)·H ₂ O]-Y exhibits exceptional activity by providing superior conversion (>80%) of limonene.	[162]
FAU	[CuL ¹ (NO ₃) _n] and [CuL ² Cl] (HL ¹ = 1-[(3-dimethylaminopropyl-imino)methyl]-naphthalen-2-ol and HL ² = 3-[(3-dimethylamino-2,2-dimethyl-propylimino)methyl]-naphthalen-2-ol)	oxidation of styrene and cyclohexene with H ₂ O ₂	Complexes entrapped in the supercages of NaY in the solvent phase through two-stage process (i) ion exchange of the selected Cu(II)-salt; (ii) encapsulation of Schiff-base ligands (HL ¹ /HL ²) in Cu(II) exchanged zeolite. The heterogeneous catalyst can be reused for several cycles without decay of activity as confirmed by PXRD, cyclic voltammetry, SEM, and FTIR studies.	[14]
FAU	Triazenido Cr complexes recovered from biosorption studies	oxidation of cyclohexene with <i>t</i> -BuOOH	Chromium containing FAU zeolite, in sodium form (NaY) and in proton form (HY), was recovered from biosorption studies and reused as a support for the preparation of heterogeneous catalysts by the flexible ligand method, using 1,3-diphenyltriazene derivatives. Cr-FAU supports lost some of the Cr into the reaction medium, whereas immobilization of Cr-complexes reduced the referred leaching.	[111]
Hierarchical MFI	Native active sites of the zeolite with Si/Al ratio modified during synthesis.	oxidation of styrene with <i>t</i> -BuOOH	Hierarchical ZSM-5 samples were prepared with Si/Al = 20, 60 and 100 using TPAOH as structure directing agent. Sample with Si/Al = 60 showed significantly higher yield of benzaldehyde. The catalyst was recovered and recycled three times without a significant loss in activity and selectivity.	[163]
MFI	Co ₃ O ₄	oxidation of styrene with H ₂ O ₂	The precursor Co ₃ O ₄ /SiO ₂ with 10 wt.% Co loading was prepared via impregnating the SiO ₂ support with an aqueous solution containing the required amount of Co(NO ₃) ₂ ·6H ₂ O. Under the optimized reaction condition, the yield of benzaldehyde can achieve 78.9% with 96.8% styrene conversion and 81.5% benzaldehyde selectivity. Such an excellent catalytic performance can be attributed to the synergistic effect between the Co ₃ O ₄ encapsulated zeolite structure with a confined reaction environment and the acidity.	[144]

Table 4. Cont.

Support	Catalyst	Reaction Type	Observations	Reference
Hydrotalcites	Cu(II)	oxidation of styrene with <i>t</i> -BuOOH or H ₂ O ₂	Substitution of Mg ²⁺ by Cu ²⁺ in the brucite sheets. The selectivity to products (80–90%) was dependent on the copper ions in the catalysts and on the nature of the oxidant.	[164]
CMK-3	Cu(II), Co(II), Fe(III) or V(II)O Schiff base complexes	oxidation of styrene with air	CMK-3 support was prepared using as solid template SBA-15 and sucrose as carbon precursor. High conversion of styrene (94.1%) and selectivity to styrene oxide (73.9%) can be achieved over the heterogeneous Co(II) catalyst with isobutyraldehyde as co-reductant. Functionalized CMK-3 catalyst was quite stable and could be recycled at least three times.	[165]
Mesoporous MFI	Cr and W-Cr	oxidation of styrene in the presence of H ₂ O ₂	Mesoporous ZSM-5 was produced by adding CTAB soft template during synthesis. Chromium and tungsten were introduced in the zeolite through incipient impregnation method. W-Cr-ZSM-5 sample showed higher catalytic activity than that of Cr-ZSM-5.	[50]
MEL	Co	oxidation of styrene in the presence of H ₂ O ₂	Microwave-assisted introduction of cobalt in the zeolite by ionic exchange. Co-ZSM-11 catalyst presented a reaction rate about 30% higher than the found in the literature and a higher benzaldehyde selectivity (ca. 80%) under optimal reaction conditions.	[142]
Hierarchical MFI	Mo and Ti	oxidation of 1-octene and cyclohexene with H ₂ O ₂ or <i>t</i> -BuOOH	Molybdenum confined hierarchical materials prepared via a silanization procedure. Most of Mo and titanium are encapsulated inside the zeolite pores giving high stability to the catalysts.	[47]
Hollownest-structured zeolite (Ti-HSZ)	Ti	oxidation of cyclooctene, cyclopentene with <i>t</i> -BuOOH	Seed-assisted synthesis of Ti-containing hollownest-structured zeolite (Ti-HSZ). About 85% cyclopentene and 87% cyclooctene can be converted into corresponding epoxides (selectivity for epoxides of nearly 100%). The hierarchical porous structure increases the diffusion and mass transfer of various reaction molecules (alkene, oxidant, and solvent).	[166]
Hierarchical Ti-BEA	Ti	oxidation of cyclohexene and cyclooctene with H ₂ O ₂	Hierarchical titanasilicate beta zeolite was produced through successive postsynthetic dealumination and titanation. The highly interconnected intracrystalline meso-/micro-porosity enhanced diffusion and improved the accessibility of active sites to the bulky substrates. The catalyst exhibited not only a superior stability but also a facile recyclability by simple calcination.	[66]
Hierarchical MFI	Mo	cyclooctene, cyclohexene, norbornene, and styrene with <i>t</i> -BuOOH	Gemini surfactants were synthesized to act as templates for the synthesis of hierarchical ZSM-5, with high intercrystalline mesoporosity and OH rich surface, used to immobilize molybdenum compound by the stable Mo-O bond. The supported catalysts exhibited high yield and selectivity for the epoxidation of several alkenes and the ability to be reused more than 5 cycles.	[48]

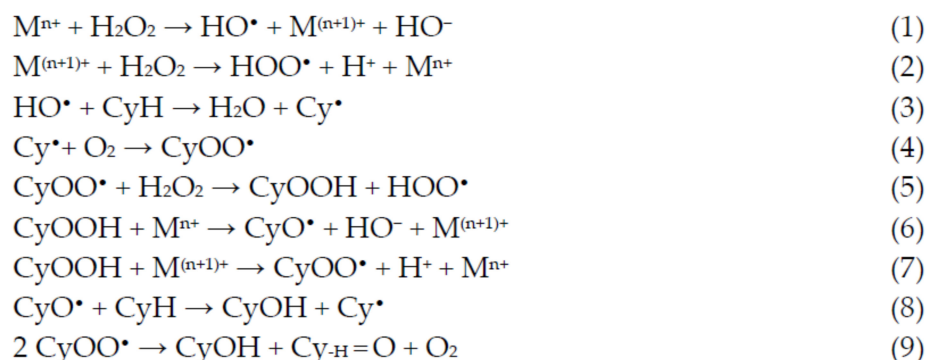
5.1. Oxidation of Alkanes

Reports on the oxidation of alkanes are scarce due to the low reactivity of this class of hydrocarbons. The most relevant reactions are the synthesis of maleic anhydride from *n*-butane and, by far, the oxidation of cyclohexane to cyclohexanol and cyclohexanone. The homogeneous oxidation of cyclohexane is highly important due to the industrial relevance of its products. In fact, as explained in detail in Section 1, the mixture of cyclohexanol and cyclohexanone is an intermediate in the synthesis of nylon-6 and nylon-6,6. However, the current industrial catalysts lead to very low cyclohexane conversions to achieve moderate selectivities. Thus, the large number of papers concerning metal catalysts immobilized in several supports devoted to this reaction is not surprising (see Table 3). Selected examples are discussed in more detail ahead.

An alternative to the industrial process that has been explored in the last years is the room temperature oxidation, using peroxides instead of dioxygen (for example, using its formally equivalent, hydrogen peroxide). This oxidation occurs through the formation of cyclohexyl hydroperoxide (CyOOH) as the primary product, which further evolves into the mixture of cyclohexanol and cyclohexanone (see Figure 2, Section 1). Several experiments and theoretic calculations revealed that the reaction should proceed through free-radical pathways, where the catalyst does not interact directly with the substrate but instead with the oxidant (reactions 1 and 2, Scheme 2), forming radicals such as the hydroxyl which, in turn, abstracts one hydrogen atom from the cyclohexane (reaction 3, Scheme 2), starting the propagation chain that leads to the desired products, cyclohexanol and cyclohexanone (reactions 8 and 9, Scheme 2).

In a significant number of publications, Y zeolite (FAU structure) is used as support, as its characteristic supercages allow the immobilization of bulky active species (mainly complexes). For example, Chetan and coworkers [151] described the successful synthesis of Y zeolite entrapped transition metal complexes of general formula $[M(\text{SFCH}) \cdot x\text{H}_2\text{O}] \cdot \text{Y}$ [$M = \text{Mn, Fe, Co, Ni}$ ($x = 3$) or Cu ($x = 1$); $\text{H}_2\text{SFCH} = (E)\text{-}N'$ -(2-hydroxybenzylidene)furan-2-carbohydrazide] by flexible ligand method as evidenced by several characterization techniques including inductively coupled plasma/ optical emission spectrometry (ICP-OES), elemental analyses, (FT-IR, electronic and X-ray diffraction) spectroscopic studies, low-temperature N_2 adsorption, and SEM. Density functional theory (DFT) calculations were also performed to address the relaxed geometry, bond angle and length, dihedral angle, highest occupied molecular orbital (HOMO)–lowest unoccupied molecular orbital (LUMO) energy gap, and electronic density of states of H_2SFCH ligand and its neat transition metal complexes. It was concluded that complexes $[M(\text{SFCH}) \cdot x\text{H}_2\text{O}]$ are suitable in size for the zeolite channels, which confined the complex and restricted it from coming out of the supercages of Y zeolite. The catalytic activity of $[M(\text{SFCH}) \cdot x\text{H}_2\text{O}] \cdot \text{Y}$ for the liquid-phase oxidation of cyclohexane by hydrogen peroxide was evaluated. Among the tried metals, $[\text{Cu}(\text{SFCH}) \cdot \text{H}_2\text{O}] \cdot \text{Y}$ catalyst exhibited the highest conversion (45.1%) and selectivity (84.5%), which agrees with the calculated HOMO–LUMO gap and Fermi energy (higher for the copper complexes). The effect of encapsulation on the stability of $[\text{Cu}(\text{SFCH}) \cdot \text{H}_2\text{O}]$ was assessed through recycling experiments of $[\text{Cu}(\text{SFCH}) \cdot \text{H}_2\text{O}] \cdot \text{Y}$. The conversion of cyclohexane to cyclohexanol and cyclohexanone on first (43.6%) and second (42.3%) reuses of the catalyst was marginally reduced compared with the obtained in first cycle (45.1%), which may be due to some blockage of the zeolite channels during the first cycle.

The use of hierarchical supports has been reported in recent years, where the mesoporosity created through several strategies is considered a positive effect to improve the anchorage of catalytic active bulky species and prevent their leaching during consecutive cycles.



Scheme 2. Radical mechanism accepted for the catalytic oxidation of cyclohexane to cyclohexanol and cyclohexanone.

An illustrative example is the anchorage of the C-scorpionate iron(II) complex $[\text{FeCl}_2\{\kappa^3\text{-HC}(\text{pz})_3\}]$ (pz = pyrazol-1-yl) on a commercial (MOR) or desilicated (MOR-D) mordenite zeolite modified through a classic alkaline treatment with NaOH, reported by Martins et al. [90]. The catalytic behavior of the immobilized iron(II) complex for the oxidation of cyclohexane by hydrogen peroxide (30% aqueous solution) in a slightly acidic medium was evaluated. The metal content, quantified by ICP, of the immobilized $[\text{FeCl}_2\{\kappa^3\text{-HC}(\text{pz})_3\}]$ at the desilicated support ($[\text{FeCl}_2\{\kappa^3\text{-HC}(\text{pz})_3\}]\text{@MOR-D}$) was 0.28%, whereas in the case of the commercial zeolite, ($[\text{FeCl}_2\{\kappa^3\text{-HC}(\text{pz})_3\}]\text{@MOR}$) was 0.40%. Thus, it appears that, under the experimental conditions used for the desilication of MOR support, some of the surface active sites were lost, affecting the interaction of the iron(II) complex with the zeolite. However, the desilication treatment promoted a significant development of mesoporosity along with a small reduction of the microporous volume. This indicates that the mesoporosity results mainly from the corrosion of the external surface of the crystals, leading to the development of intercrystalline mesoporosity, along with some decrease in the microporous volume. Complex immobilization led to an important decrease in all the textural parameters of the zeolitic supports, indicating that the voluminous complex is mainly immobilized at the intercrystalline mesoporosity created during the desilication procedure.

The hybrid material $[\text{FeCl}_2\{\kappa^3\text{-HC}(\text{pz})_3\}]\text{@MOR-D}$ provided a noticeable catalytic activity ($\text{TON}_{\text{max}} = 2.90 \times 10^3$) for the selective oxidation of cyclohexane leading to an overall (cyclohexanol and cyclohexanone) yield of 38% after 10 h reaction at room temperature. Thus, the desilicated support allowed the existence of the Fe(II) complex in the intercrystalline mesoporosity of the modified zeolite and originated a significant enhancement of the accessibility of the reactants, leading to a superior catalytic activity. Moreover, $[\text{FeCl}_2\{\kappa^3\text{-HC}(\text{pz})_3\}]\text{@MOR-D}$ was easily recovered from the reaction medium and reused. However, only 54% of its initial catalytic activity was preserved after the first reuse run, indicating the occurrence of leaching during the catalytic reaction or the catalyst recovery process and a weak type of electrostatic interaction between the complex and the support.

A more sophisticated postsynthesis treatment to obtain hierarchical zeolites with an accurate control of the size and shape of mesopores is the surfactant templated methodology, where the zeolite is submitted to an alkaline treatment in the presence of a surfactant, under autogenous pressure, as discussed in detail above (see Section 3.1.2). Van-Dúnem et al. [100] applied this postsynthesis methodology to Y zeolite using several alkaline agents (NaOH, NH_4OH and TPAOH) in the presence of CTAB surfactant. The obtained materials present a hierarchical structure with enlarged micropores (supermicropores, especially when TPAOH and NH_4OH were used) and mesopores, preserving most of the original microporosity.

The anchorage of the C-scorpionate iron(II) complex $[\text{FeCl}_2\{\kappa^3\text{-HC}(\text{pz})_3\}]$ at the above hierarchical materials ($[\text{FeCl}_2\{\kappa^3\text{-HC}(\text{pz})_3\}]\text{@Y}$, $[\text{FeCl}_2\{\kappa^3\text{-HC}(\text{pz})_3\}]\text{@Y_NaOH}$, $[\text{FeCl}_2\{\kappa^3\text{-HC}(\text{pz})_3\}]\text{@Y_NH}_4\text{OH}$, and $[\text{FeCl}_2\{\kappa^3\text{-HC}(\text{pz})_3\}]\text{@Y_TPAOH}$) led, in all the cases, to a slight reduction of the characteristic microporosity of the zeolitic structure. The authors observed that the effect of the immobilization on larger porosity (supermicropores) for samples

$[\text{FeCl}_2\{\kappa^3\text{-HC}(\text{pz})_3\}]\text{@Y}$ and $[\text{FeCl}_2\{\kappa^3\text{-HC}(\text{pz})_3\}]\text{@Y_NaOH}$ was minimal (porosity values identical to the exhibited by the zeolitic supports), indicating that $[\text{FeCl}_2\{\kappa^3\text{-HC}(\text{pz})_3\}]$ should be dispersed on the outer surface of the crystals. However, for the supported catalysts $[\text{FeCl}_2\{\kappa^3\text{-HC}(\text{pz})_3\}]\text{@Y_NH}_4\text{OH}$ and $[\text{FeCl}_2\{\kappa^3\text{-HC}(\text{pz})_3\}]\text{@Y_TPAOH}$ at least a fraction of the iron(II) complex should be located inside the supermicropores and narrow mesopores. The catalytic performance of the prepared hybrid materials was tested toward the oxidation of cyclohexane by hydrogen peroxide at room temperature for 24 h. Yields of cyclohexanol and cyclohexanone up to 34% were attained with concomitant turnover numbers (TONs) up to 271. The hybrid catalysts were easily recovered from the reaction medium and reused in three consecutive catalytic cycles (Figure 15). Their performance appeared to be related with the porosity differences observed in the hierarchical materials. When the complex anchorage occurred mainly at the outer surface of the support ($[\text{FeCl}_2\{\kappa^3\text{-HC}(\text{pz})_3\}]\text{@Y}$ and $[\text{FeCl}_2\{\kappa^3\text{-HC}(\text{pz})_3\}]\text{@Y_NaOH}$), high leaching after the first catalytic cycle was observed. The location of a fraction of the iron(II) complex inside the zeolite supermicropores and narrow mesopores favored catalysts recyclability, especially in the case of $[\text{FeCl}_2\{\kappa^3\text{-HC}(\text{pz})_3\}]\text{@Y_NH}_4\text{OH}$. The predominance of the Fe(II) oxidation state on the recycled catalysts was detected by XPS, in agreement with the regeneration of the initial oxidation state of the catalysts in the proposed mechanism of cyclohexane oxidation (see Scheme 2).

More recently, another work addressing this topic was reported by Ottaviani et al. [103], where MOR zeolite was modified by using NaOH and TPAOH in the presence of CTAB surfactant. The hierarchical zeolite support was used to immobilize the B-scorpionate dioxido-vanadium(V) complex $[\text{VO}_2\{\kappa^3\text{-HB}(3,5\text{-Me}_2\text{pz})_3\}]$ (pz = pyrazol-1-yl), affording three hybrid catalysts: $[\text{VO}_2\{\kappa^3\text{-HB}(3,5\text{-Me}_2\text{pz})_3\}]\text{@MOR}$, $[\text{VO}_2\{\kappa^3\text{-HB}(3,5\text{-Me}_2\text{pz})_3\}]\text{@MOR_NaOH}$, and $[\text{VO}_2\{\kappa^3\text{-HB}(3,5\text{-Me}_2\text{pz})_3\}]\text{@MOR_TPAOH}$. As expected, the alkaline-surfactant treatment provided a mesopore network, along with a significant change in the textural characteristics of the materials, especially when the strongest base NaOH was used. The vanadium-loaded zeolitic material $[\text{VO}_2\{\kappa^3\text{-HB}(3,5\text{-Me}_2\text{pz})_3\}]\text{@MOR_NaOH}$ performed as an efficient catalyst for the oxidation of cyclohexane to cyclohexanol and cyclohexanone using TBHP (70% aq. solution), at room temperature, in a slightly acidic medium. A maximum overall yield of 52% was achieved with concomitant TON values up to 6.2×10^2 . The attained yield in the presence of $[\text{VO}_2\{\kappa^3\text{-HB}(3,5\text{-Me}_2\text{pz})_3\}]\text{@MOR_NaOH}$ is considerably higher than the achieved (38%) by the above hybrid C-scorpionate catalyst $[\text{FeCl}_2\{\kappa^3\text{-HC}(\text{pz})_3\}]\text{@MOR-D}$ [100]. Moreover, $[\text{VO}_2\{\kappa^3\text{-HB}(3,5\text{-Me}_2\text{pz})_3\}]\text{@MOR_NaOH}$ was easily recovered and reused in up to four consecutive cycles, where the first decrease (18%) in the oxidation yield is observed but without significant leaching of $[\text{VO}_2\{\kappa^3\text{-HB}(3,5\text{-Me}_2\text{pz})_3\}]$. The authors assign the catalytic activity decrease to some adsorption phenomena that may cause diffusional constraints and restrict the access the complex immobilized at the mesoporosity of the zeolitic material.

The results obtained in the above independent studies [100,103] show that the careful choice of the basic agents used during the treatments assisted by CTAB surfactant play a key role on the effective anchorage of the metal complex and, consequently, on the number of catalytic cycles that can be effectively performed by the supported catalyst.

Mesoporous silicas are of great interest as catalyst supports due to their large surface area and uniform mesopore size distribution which facilitates the anchorage of voluminous species and accelerates mass transfer. Moreover, as it was already mentioned, the abundance of Si-OH groups on the surface of some materials surface makes them excellent materials for surface modification. An illustrative example of the role of mesoporous silicas as supports for metal complexes is provided by Pinto et al. [135]. The application of ordered mesoporous silica SBA-15 and its derived chloropropyl-functionalized silica SBA-15Cl as supports for anchorage of different neutral and charged manganese porphyrins was investigated (see Figure 13). Here, 0.3% *w/w* complex loadings were obtained for the hybrid materials evaluated as catalysts for cyclohexane oxidation using iodosylbenzene (PhIO) as oxidant. The performance of the SBA-15Cl/MnT-X-PyPcI ($X = 2, 3, 4$) catalysts was as

good as the observed for homogeneous systems, pointing out that catalyst deactivation did not occur upon the anchorage process. However, a change in selectivity (relative to the homogeneous reaction) was observed, as an increase of ca. 10% of cyclohexanol yield was reported by the heterogenization of the catalyst. These results indicate an effective participation of the inorganic matrix, even though, the authors state some difficulty in rationalizing the influence of the support. Nevertheless, as SBA-15Cl exhibits a lipophilic character (due to the hydrophobic nature of the pendant carbon chain), cyclohexane approach should be favored, whereas the one of cyclohexanol product (more polar) may be prevented, thus justifying the increase in the alcohol production and the decrease in cyclohexanone yield, when compared with the homogeneous system. The strong interaction between the manganese porphyrin complexes and the mesoporous silica systems (SBA-15 and SBA-15Cl) was confirmed by their low leaching from the supports even after extensive washings. Moreover, the heterogenized catalysts exhibited high resistance against oxidative decomposition as no considerable changes in their efficiency was detected by reuse in consecutive catalytic cycles.

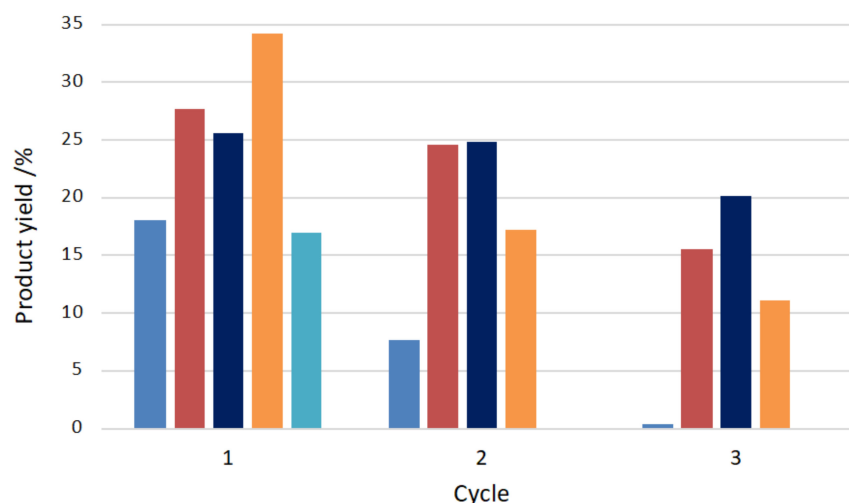


Figure 15. Effect on the products yield of cyclohexane oxidation of the anchorage of the C-scorpionate iron(II) complex $[\text{FeCl}_2\{\kappa^3\text{-HC}(\text{pz})_3\}]$ at the Y zeolite hierarchical materials: ■— $[\text{FeCl}_2\{\kappa^3\text{-HC}(\text{pz})_3\}]@Y$, ■— $[\text{FeCl}_2\{\kappa^3\text{-HC}(\text{pz})_3\}]@Y_{\text{TPAOH}}$, ■— $[\text{FeCl}_2\{\kappa^3\text{-HC}(\text{pz})_3\}]@Y_{\text{NH}_4\text{OH}}$, ■— $[\text{FeCl}_2\{\kappa^3\text{-HC}(\text{pz})_3\}]@Y_{\text{NaOH}}$, and ■— $[\text{FeCl}_2\{\kappa^3\text{-HC}(\text{pz})_3\}] [100]$.

Mesoporous silicas can also be used as effective supports for metal oxide catalysts. The potentialities of several materials were studied. For example, Unnarkat et al. [157] compared the performance of three mesoporous silicas as supports—SBA-15, KIT-6, and FDU-12 for immobilizing the cobalt-molybdenum oxide CoMoO_4 and their use in the liquid phase oxidation of cyclohexane by molecular oxygen. The catalysts were characterized by several techniques, including TEM, where the good dispersion of the active species (not uniform) in the mesopores of the support is clearly observed, as well as the typical channel structure of SBA-15, the cubical pore structure for KIT-6, and the hexagonal pore structure for FDU-12 (Figure 16).

The catalyst performance as function of catalyst loading, pore size, or calcination temperature was studied for each support at 150 °C, 1.0 MPa O_2 pressure and 800 rpm stirring. Among the supported catalysts, 20%CoMo/FDU-12 showed the highest activity (up to 8% conversion) for a selectivity of 85% for the cyclohexanone and cyclohexanol mixture. The silica-supported oxide exhibited deactivation, apparently due to adsorption of reaction products. However, a deactivated catalyst could be successfully regenerated by recalcination, which prompted its reuse in a further (up to four) cycle, retaining activity and selectivity over consecutive cycles (Figure 17).

Mesoporous silica KIT-6 presents a unique structure with 3D interpenetrating bi-continuous networks of channels, offering a huge number of active sites as well as high resistance to form clusters, thus attracting a significant interest to act as catalyst support. Rezaei et al. [156] immobilized vanadium phosphate (mainly $\text{VOHPO}_{40} \cdot 5\text{H}_2\text{O}$ phases) at KIT-6 [$(\text{VO})_2\text{P}_2\text{O}_7$ phase after calcination] and applied it for the oxidation of cyclohexane by hydrogen peroxide. The characterization of the supported catalysts by N_2 adsorption isotherms revealed a considerable decrease in the surface area and pore volume upon vanadium phosphate loading, suggesting their location inside KIT-6 pores, which agrees with the observed increase in pores diameter.

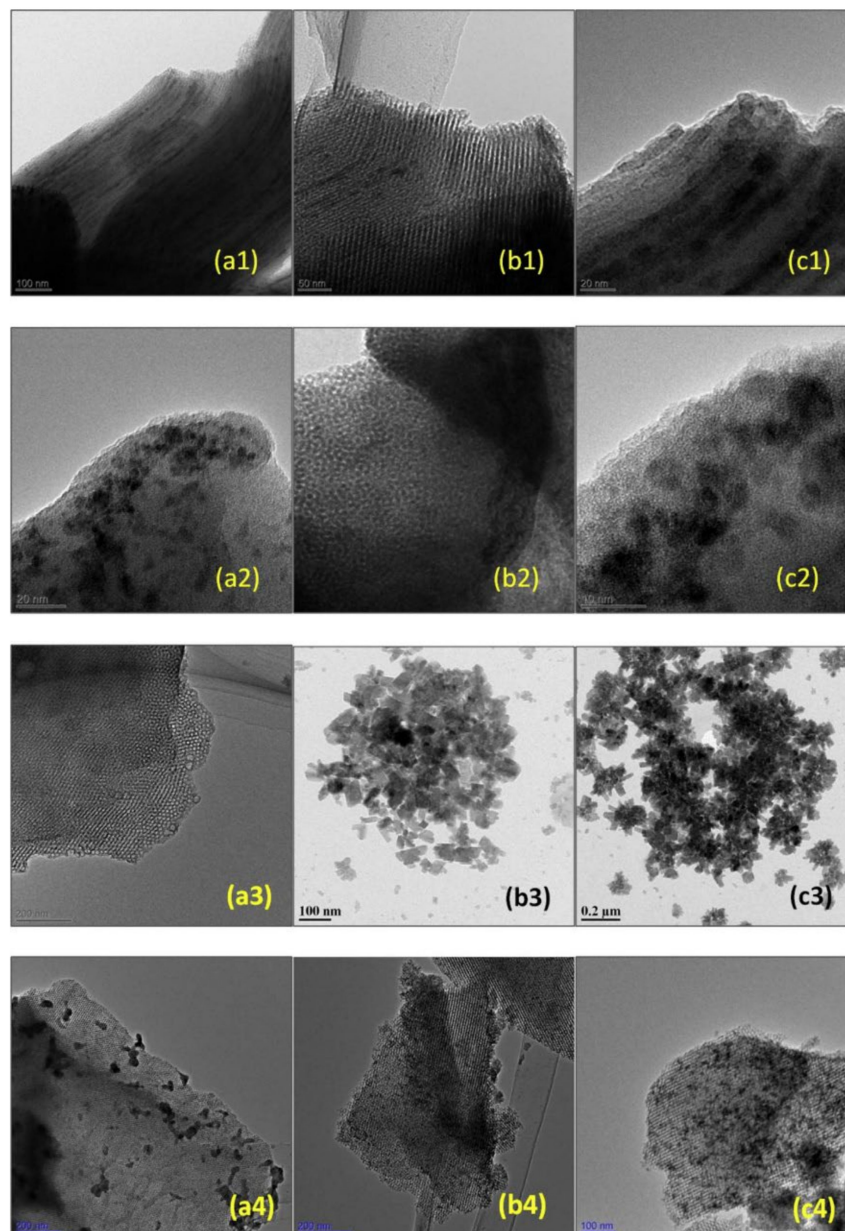


Figure 16. TEM images (a1,b1,c1) 20%CoMo/SBA-15; (a2,b2,c2) 20%CoMo/KIT-6; (a3) FDU-12; (b3,c3) 20%CoMo/FDU-12; (a4) 5%CoMo/KIT-6; (b4) 10%CoMo/KIT-6; (c4) 20%CoMo/KIT-6. Reproduction with permission from Reference [157]. Copyright (2017) Elsevier B.V.

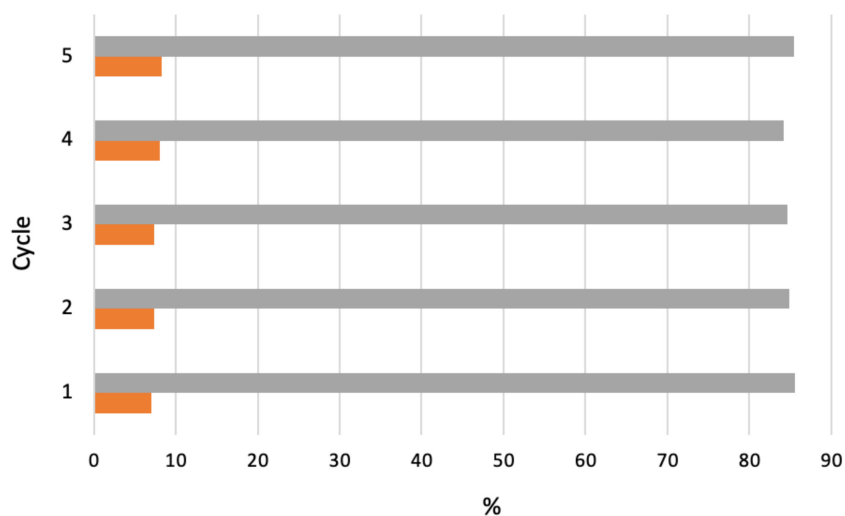


Figure 17. Effect of four cycles of recalcination–reuse of 20%CoMo/FDU-12 catalyst on cyclohexane conversion (■) and selectivity (■) to cyclohexanol and cyclohexanone [157].

The authors report a cyclohexane conversion and selectivity toward cyclohexanol and cyclohexanone of 19.3% and 69.9%, respectively, after 4 h reaction with 1:4 cyclohexane: H_2O_2 molar ratio at 65°C and using 27 wt.% catalyst vanadium loading. The corresponding proposed reaction mechanism is depicted in Figure 18. No significant change in activity or selectivity was found in the first three consecutive catalytic cycles. Then, a lower conversion of cyclohexane (without selectivity loss) was detected. The stability of the VPK-6 immobilized catalyst appears to be due to the high dispersion of vanadium phosphate in the support, as shown by SEM. Moreover, the nature of the textural characteristics for the catalyst after being reused five times remains unchanged, although the surface area and pore volume values present a decrease, most likely due to some blockage of the support pores.

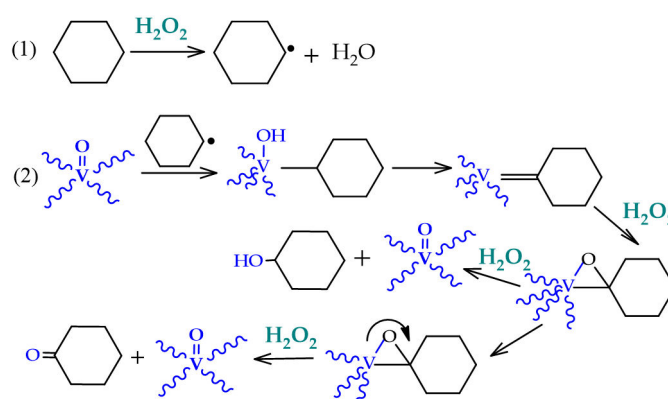


Figure 18. Proposed reaction mechanism for the oxidation of cyclohexane catalyzed by vanadium phosphate immobilized at KIT-6. Reproduction with permission from Reference [156]. Copyright (2017) Elsevier B.V.

5.2. Oxidation of Alkenes

Alkenes are more reactive molecules than alkanes. Therefore, their range of oxidation reactions is also wider. Representative examples of reactions that occur in the presence of metal or metal complexes supported on zeolites and related materials are presented in Table 4. Selected examples are discussed in more detail ahead. It is worth mentioning that styrene oxidation is also considered in this topic because the transformation occurs in the double bond of the vinyl group.

Following the same trend as for reactions involving alkanes, the most used native microporous zeolite as catalytic support is FAU structure (see Table 4), taking advantage of the presence of the supercages that can effectively anchor voluminous catalysts through the flexible ligand method. For example, Modi and co-workers [162] applied Y zeolite entrapped VO^{2+} or Co(II) pyrazalone complexes bearing the Schiff base ligand L, $[\text{VO}(\text{L})\cdot\text{H}_2\text{O}]$ and $[\text{Co}(\text{L})\cdot\text{H}_2\text{O}]\cdot\text{H}_2\text{O}$ ($\text{H}_2\text{L} = (\text{Z})$ -3-methyl-1-phenyl-4-(2,2,2-trifluoro-1-(2-hydroxyphenyl)imino)ethyl)-1H-pyrazol-5-ol) (Figure 19 a-c) as catalysts for the oxidation of styrene by H_2O_2 . The metal complexes were entrapped in the supercages of the Y zeolite by the flexible ligand procedure, leading to $[\text{VO}(\text{L})\cdot\text{H}_2\text{O}]\text{-Y}$ and $[\text{Co}(\text{L})\cdot\text{H}_2\text{O}]\text{-Y}$ materials (Figure 19 e-f). The catalytic ability of the hybrid materials $[\text{VO}(\text{L})\cdot\text{H}_2\text{O}]\text{-Y}$ and $[\text{Co}(\text{L})\cdot\text{H}_2\text{O}]\text{-Y}$ was evaluated under the effect of different experimental variables (amount of catalyst, substrate and oxidant mole ratios, solvents, and reaction time) and compared with the homogeneous systems. $[\text{VO}(\text{L})\cdot\text{H}_2\text{O}]\text{-Y}$ was found to be the best catalyst, achieving 82% conversion of styrene and high benzaldehyde selectivity (54.9%) along with expected minor amounts of styrene glycol, styrene oxide, and phenyl acetic acid (35.9, 6.7 and 2.4%, respectively). The superior catalytic activity of $[\text{VO}(\text{L})\cdot\text{H}_2\text{O}]\text{-Y}$ was studied by DFT, highlighting that vanadium-based complex is molecularly more stable and chemically more reactive, led to higher catalytic activity compared to the cobalt analogous. Moreover, $[\text{VO}(\text{L})\cdot\text{H}_2\text{O}]\text{-Y}$ was recyclable five times with no significant loss of activity.

Following the same strategy for the immobilization of the active species at the microporous Y zeolite support, Godhani et al. [17], besides testing the catalytic oxidation of cyclohexane (Table 3), also performed the oxidation of cyclohexene by H_2O_2 , in acetonitrile at 80 °C for 18 h) using the prepared catalysts $[\text{M}(\text{L})]\text{-Y}$ ($\text{M} = \text{Co}(\text{II})$ or $\text{Cu}(\text{II})$; $\text{L} =$ Schiff bases). The immobilized metal complexes (within the Y zeolite nanovoids) extensively catalyzed the cyclohexene oxidation to 2-cyclohexen-1-one and 2-cyclohexen-1-ol and were easily recovered and reused without loss of activity and the selectivity for the allylic products. Moreover, the heterogenized catalysts were found highly selective for oxidation of benzene, styrene, limonene, and α -pinene with a moderate conversion.

When the immobilized active species are small, as in the case of metal oxides, the application of other zeolite structures as catalytic supports was explored. Medium pore size zeolites are the most employed structures, especially the ones with tridimensional pore structure (e.g., ZSM-11 or ZSM-5) since this feature allows an efficient catalyst distribution while avoiding possible deactivation during the catalytic reactions. An illustrative example is the work by Jury and coworkers [142] on the synthesis of an effective Co-ZSM-11 catalyst for the microwave-assisted selective oxidation (by H_2O_2) of styrene to benzaldehyde at 60 °C and 350 rpm. ZSM-11 zeolite was synthesized through a classic hydrothermal process and further doped with Co through a simple ionic exchange procedure [167] to afford Co-ZSM-11 zeolite. At optimized reaction conditions Co-ZSM-11 exhibited a reaction rate about 30% higher than the previous literature systems concomitant with a higher selectivity towards benzaldehyde (ca. 80%).

Another example, yet more sophisticated, was reported by Liu and coworkers [144] that developed a tailor-made cobalt oxide encapsulated at ZSM-5 zeolite during the synthesis of the zeolitic support. The $\text{Co}_3\text{O}_4@\text{HZSM-5}$ catalyst, obtained by the hydrothermal method from $\text{Co}_3\text{O}_4/\text{SiO}_2$, exhibited a well-organized structure with encapsulated Co_3O_4 particles within the zeolite crystals. Its catalytic performance was evaluated toward the oxidation of styrene to benzaldehyde by H_2O_2 : a much higher styrene conversion to benzaldehyde was achieved in the presence of $\text{Co}_3\text{O}_4@\text{HZSM-5}$ than with $\text{Co}_3\text{O}_4/\text{SiO}_2$. In fact, under optimized reaction conditions, 79% of benzaldehyde was selectively (82%) attained (Figure 20). The remarkable catalytic activity of $\text{Co}_3\text{O}_4@\text{HZSM-5}$ was assigned by the authors to the synergy achieved between the unique Co_3O_4 encapsulated zeolite structure (in a confined reaction ambient) and its acidic character.

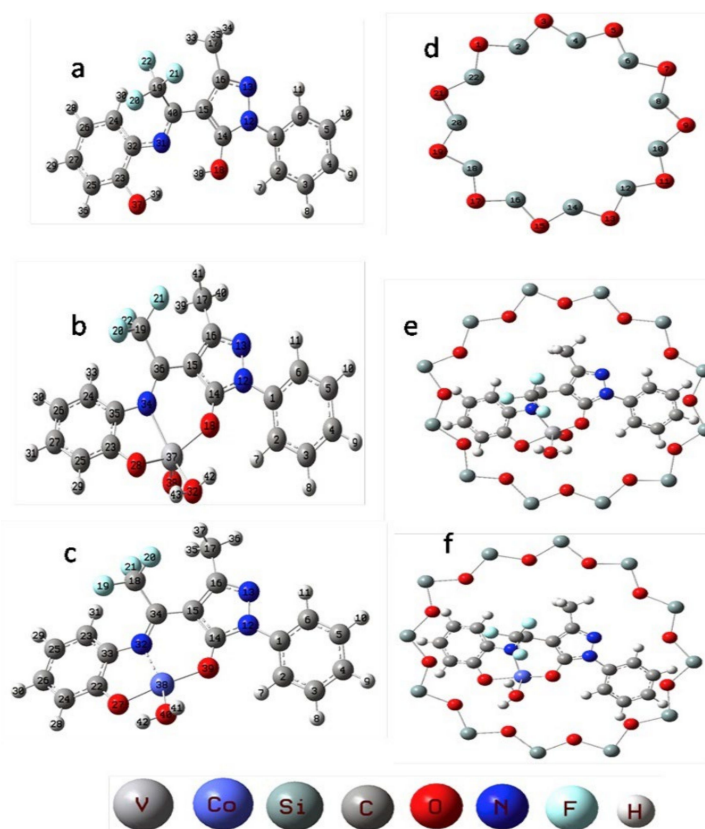


Figure 19. Structures for (a) Schiff base H_2L ; (b) $[VO(L)\cdot H_2O]$; (c) $[Co(L)\cdot H_2O]\cdot H_2O$; (d) Y zeolite pore opening; (e) $[VO(L)\cdot H_2O]-Y$ and (f) $[Co(L)\cdot H_2O]-Y$. Reproduction with permission from Reference [162]. Copyright (2017) Elsevier B.V.

Table 5. Commercial/hierarchical zeolites and related materials applications as catalytic supports for the oxidation of aromatics.

Support	Catalyst	Reaction Type	Observations	Reference
FAU	$[Fe(bpy)_3]^{2+}$ (bpy = bipyridine)	oxidation of benzene with H_2O_2	Fe-bipyridine complex was encapsulated into cation-exchanged Y-type zeolites (M-Na-Y: M = K^+ , Cs^+ , Mg^{2+} , Ca^{2+} , NH_4^+ , tetramethylammonium (TMA^+), or tetrabutylammonium (TBA^+). The catalytic activity towards phenol production in different solvents is dependent on the accessibility of benzene to the iron site in $[Fe(bpy)_3]@M-Na-Y$, controlled by the hydrated ionic radius of the cation (M) introduced.	[18]
			Efficient selective formation of phenol in acetonitrile–water mixed solvents over $[Fe(bpy)_3]^{2+}$ encapsulated in Y zeolite. The catalytic activity improved by increasing the amount of water added to acetonitrile.	[168]
FAU	Cu(II) and Co(II) complexes of phthalocyanine	oxidation of benzene with H_2O_2	Metal complexes encapsulated into the supercages of Y zeolite by the flexible ligand method. The prepared catalysts were reused three times with almost no change in catalytic activity. Cobalt encapsulated metal complex afforded the best catalytic activity.	[169]

Table 5. Cont.

Support	Catalyst	Reaction Type	Observations	Reference
SBA-15	<i>N,N</i> -dihydroxypyromellitimide (NDHPI) and Co	oxidation of toluene with O ₂	Composite catalyst prepared by immobilizing NDHPI on Co-doped mesoporous sieve SBA-15 doped with Co, using 3-glycidoxypropyltrimethoxysilane (GPTMS) the silylation agent. The presence of N–OH active sites was confirmed, as well as the preservation of the mesoporous structure of the catalyst. The catalyst kept the activity, and no Co was lost from SBA-15 after 3 reaction runs.	[170]
Hierarchical MFI	Fe	oxidation of benzene with N ₂ O	Hierarchical Fe-HZSM-5 prepared through different synthetic routes: carbon black as hard template, organosilane as soft template, and postsynthesis desilication. The best catalytic performance was achieved by organosilane templated zeolites.	[29]
			Hierarchical Fe-ZSM-5 catalyst directly synthesized in the presence of the silane coupling agent (GPTMS). Internal mass transfer limitations of the hierarchical Fe-ZSM-5 significantly improved.	[57]
			Crystallization of hierarchical ZSM-5 in the presence of the organosilane octadecyl-dimethyl-(3-trimethoxysilyl-propyl)-ammonium chloride as the mesoporogen. Iron precursor introduced during synthesis. Fe-containing zeolites are excellent catalysts since hierarchical pore structure leads to higher reaction rates due to increased mass transfer and increased catalyst longevity despite more substantial coke formation.	[55]
Hierarchical MFI	Fe	oxidation of benzene with N ₂ O	Parent zeolites containing small amount of iron as impurities (~0.04 wt.%) modified by post synthesis treatments of commercial ZSM-5: alkali, acid or steam treatment, combination of acid-alkali treatments, and combination of steam-acid-alkali treatments. Such modifications led to remarkable catalytic performance in the oxidation of benzene to phenol.	[67]
			Hierarchical Fe/ZSM-5 zeolites synthesized with a diquatery ammonium surfactant containing a hydrophobic tail. The sheet-like zeolites deactivate much slower than bulk Fe/ZSM-5, which was attributed to the much lower probability of secondary reactions of phenol in the short straight channels of the sheets.	[58]
Hierarchical MFI	ceria–zirconia	oxidation of ethyl benzene with <i>t</i> -BuOOH	Hierarchical MFI supported ceria–zirconia solid solution was synthesized by deposition–precipitation method. The catalyst was resistant to leaching and retained its activity even after the fifth run.	[171]

Table 5. Cont.

Support	Catalyst	Reaction Type	Observations	Reference
FAU	δ -MnO ₂	oxidation of toluene with O ₃	δ -MnO ₂ /USY with different contents of δ -MnO ₂ was synthesized using hydrothermal method. 3.0 wt.% δ -MnO ₂ /USY displayed the best performance.	[172]
Hollow structured MFI	MnO _x	oxidation of toluene with O ₂	HZSM-5 zeolites with micro-/nano-crystallites and hollow structure were, respectively, synthesized for the preparation of supported MnO _x catalysts. The active MnO _x nanoparticles on MnO _x /H-ZSM-5 surface significantly accelerated the oxidative destruction of toluene and other organics, reducing the coke formation.	[173]
MFI	native active sites of zeolite	oxidation of toluene with <i>t</i> -BuOOH	The smaller crystallite size, higher surface area, and total pore volume of the sample synthesized in the presence of a surfactant as mesopore template produced an effective catalyst that could be reused for a minimum of four runs without significant loss of in conversion and selectivity.	[56]

The proposed reaction mechanism (Figure 21) involves the formation of a peroxide intermediate (path *a*) that undergoes decomposition to formaldehyde and benzaldehyde (the major product) within Co₃O₄@-HZSM-5, promoting styrene conversion. Formaldehyde is oxidized by H₂O₂ to form a peroxyacid able to react with styrene (path *b*) to afford styrene oxide, which partially hydrolyses into 1-phenyl-1, 2-ethanediol as the reaction proceeds.

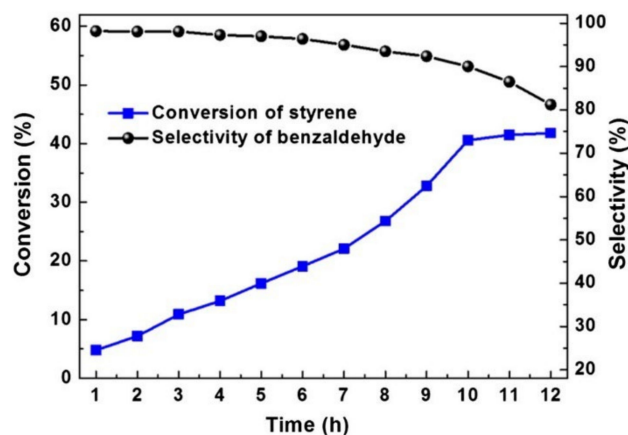


Figure 20. Selective oxidation of styrene to benzaldehyde by hydrogen peroxide, catalyzed by Co₃O₄@-HZSM-5. Adapted with permission from Reference [144]. Copyright (2018) Elsevier Inc. (Amsterdam, The Netherlands).

The use of hierarchical zeolites as catalytic supports has also been reported with proved benefits on the immobilization of bulky catalysts as well as increased diffusion of both reactants and products. The supported catalysis state of the art reports the use of hierarchical structures prepared through the synthetic or postsynthetic procedures previously discussed (Section 3.1). An example of a modified support during the synthesis was provided by Hoang et al. [50], who introduced mesoporosity at ZSM-5 during the zeolite synthesis by using CTAB surfactant. Later, chromium and tungsten were immobilized by the conventional incipient wetness impregnation method. Metal-loaded hierarchical ZSM-5 zeolites (Cr-ZSM-5 and W-Cr-ZSM-5) were used for the oxidation of styrene by

H_2O_2 at 70 °C for 6 h and displayed high catalytic performance. Remarkable styrene conversion (>85%) and selectivity for benzaldehyde (>74%) were attained in the presence of mesoporous Cr/ZSM-5. The tungsten-loaded Cr-ZSM-5 (W-Cr-ZSM-5) exhibited superior catalytic performance than Cr-ZSM-5 for the oxidation of fatty acids, although with reduced selectivity to aldehydes.

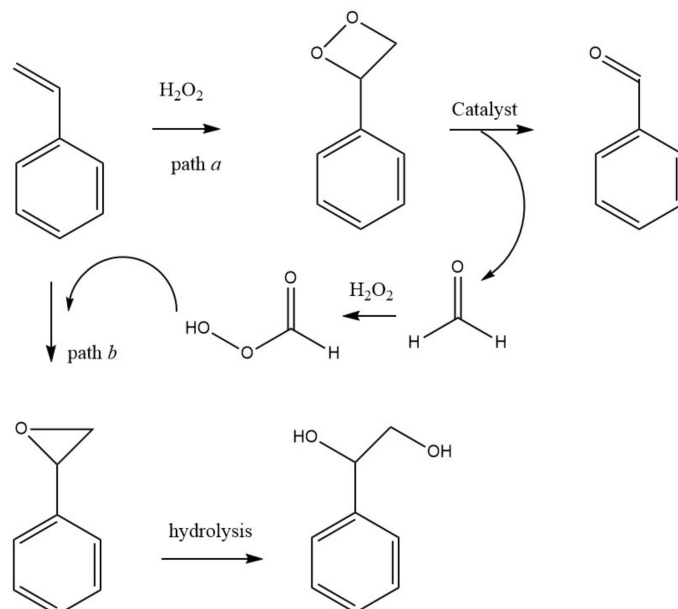


Figure 21. Proposed mechanism for the oxidation of styrene catalyzed by Co_3O_4 @-HZSM-5 [144].

To effectively immobilize a voluminous molybdenum complex at ZSM-5, Li and co-workers [48] developed a method to create large intercrystalline mesopores and OH rich surface by adding asymmetrical gemini surfactants [anionic-nonionic gemini surfactants (polyoxymethylene laurinol ether sodium sulfoitaconate: Gemini- n , $n = 3, 6, 9, 15$)] during the zeolite synthesis (Figure 8, Section 3.1.1). To immobilize $[\text{MoO}_2(\text{acac})_2]$ (acac = acetylacetonate) over the pore surface of hierarchical ZSM-5 (HZSM-5), the authors first grafted it with 3-aminopropyltrimethoxysilane (APTS), leading to A-HZSM-5 (Figure 22), to achieve an effective immobilization of the molybdenum complex through the formation of a stable Mo-O bond: Mo-A-HZSM-5. Then, the catalytic ability of Mo-A-HZSM-5 toward the epoxidation of alkenes (e.g., styrene, cyclooctene, cyclohexene, norbornene) by *tert*-butylhydroperoxide (TBHP) at 80 °C for 5 h was investigated and compared with the activity of $[\text{MoO}_2(\text{acac})_2]$ immobilized onto the purely microporous support, i.e., Mo-A-ZSM-5 (Figure 23). The superior catalytic performance of Mo-A-HZSM-5 for bulky cyclic olefins such as cyclohexene or cyclooctene was not surprising since HZSM-5 zeolites exhibit larger mesoporous surface area and larger pore diameter, which contribute to enhancing higher metal complex loading and improve diffusion.

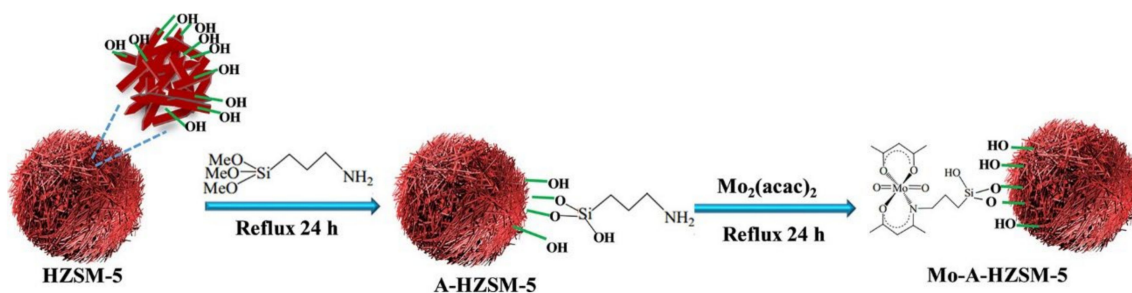


Figure 22. Schematic representation of Mo-A-HZSM-5 synthesis. Reproduced with permission from Reference [48]. Copyright (2021), Wiley-VCH GmbH.

Post-synthesis modifications performed over purely microporous zeolites also originated effective supports. You et al. [66] modified BEA zeolite through dealumination treatment performed on a steel autoclave with a Teflon liner at 80 °C for 12 h, followed by titanation by adding tetrabutyl titanate (TBOT) followed by heating at 140 °C for 1 h, originating a hierarchical three-dimensional ordered mesoporous BEA zeolite (3DOM-I Ti-beta). The synthesis method achieved the effective heteroatomic substitution through the removal of framework aluminium and subsequent reinsertion of the extra-framework positions. The catalytic behavior of this highly interconnected intracrystalline meso/microporous material was investigated for the epoxidation of bulky cyclic olefins, cyclohexene, and cyclooctene, at 60 °C, by H₂O₂. When compared to other catalytic systems, 3DOM-I Ti-beta zeolite exhibited significantly improved catalytic performance, far beyond that of conventional solely microporous Ti-beta either in micro- or nano-sizes (M-Ti-beta and N-Ti-beta) and TS-1 (Figure 24).

3DOM-I Ti-beta catalyst showed a considerable recyclability upon each catalytic run, up to the fourth cycle. Between cycles, the catalyst was simply washed with acetonitrile. It was found that 80–85% of the initial conversion of the fresh catalyst could be recovered (Figure 25). After the fourth cycle, the spent catalyst was submitted to calcination in air at 550 °C for 6 h to burn adsorbed species and subjected to a fifth run where it was found that the catalytic conversion reached 97.6% of the initial conversion, demonstrating the superior recyclability of 3DOM-i Ti-beta as a heterogeneous catalyst.

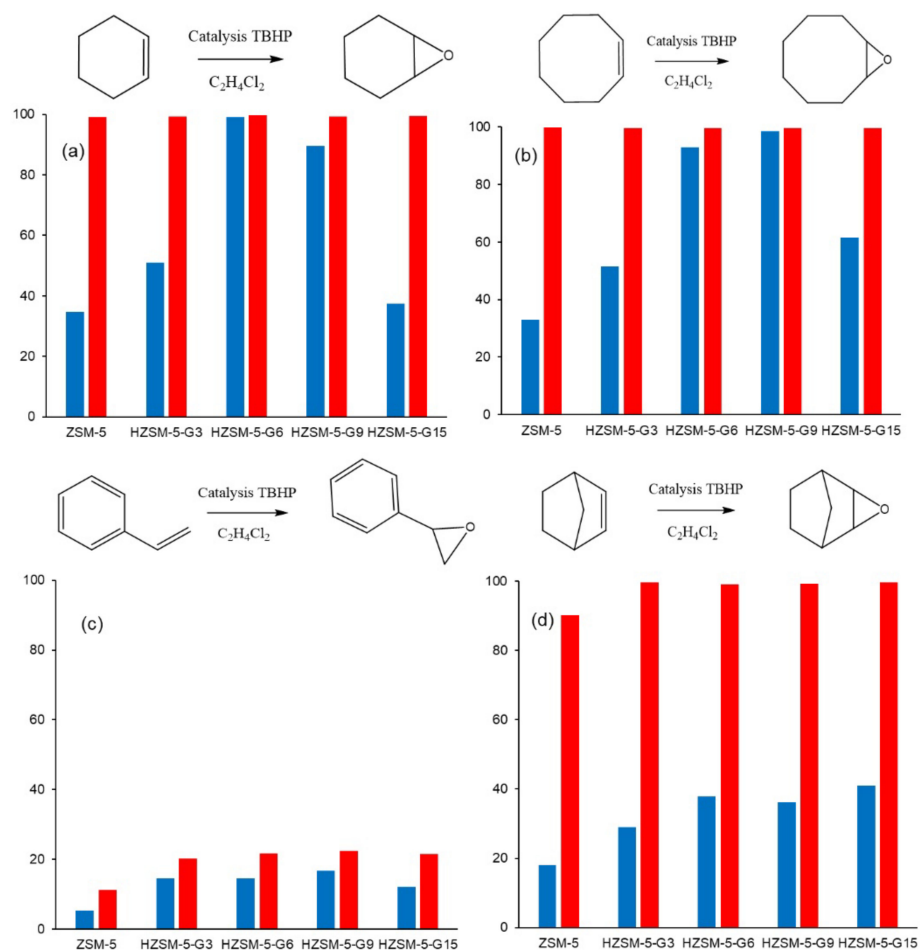


Figure 23. Conversion (%; blue bars) and selectivity (%; red bars) for the epoxidation of cyclohexene (a), cyclooctene (b), styrene (c), and norbornene (d), catalyzed by Mo-A-HZSM-5 (Gemini 9 as template) and Mo-A-ZSM-5. Adapted with permission Reference [48]. Copyright (2021) Wiley-VCH GmbH.Inc.

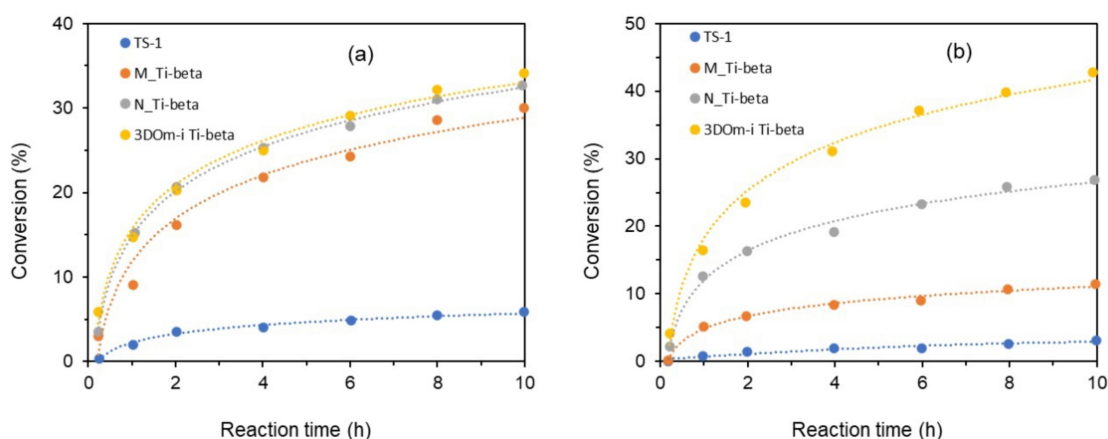


Figure 24. Conversion of cyclohexene (a) and cyclooctene (b) over 3DOM-I Ti-beta and other comparison catalysts, as a function of reaction time. [66].

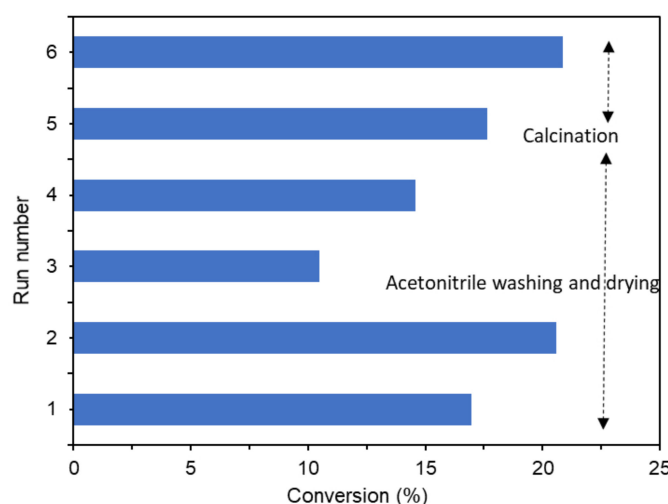


Figure 25. Recycling 3DOM-I Ti-beta catalyst for the epoxidation of cyclooctane [66].

5.3. Oxidation of Aromatics

For oxidation reactions involving aromatic substrates, the large size of those molecules, as well as, the bulky reaction intermediates and correspondent reaction products, demands for supports with wider pores. Thus, it is not surprising that the number of publications involving hierarchical zeolitic structures and mesoporous materials is more significant. Table 5 shows representative examples of aromatic substrates oxidation taking place on supported metal or metal complexes. Selected examples are discussed in deep ahead.

Due to the presence of supercages, several examples in the literature still report the use of Y zeolite as support for the immobilization of catalysts for the oxidation of aromatic molecules. Briefly mentioning a few, Yamaguchi et al. [18] encapsulated cationic bipyridine iron(II) complexes $[\text{Fe}(\text{bpy})_3]^{2+}$ (bpy = bipyridine) into cation-exchanged Y-type zeolites (M-Na-Y: M = K^+ , Cs^+ , Mg^{2+} , Ca^{2+} , NH_4^+ , TMA^+ , and TBA^+) and applied them as catalysts for the oxidation of benzene to phenol by hydrogen peroxide in different solvents (CH_3CN , H_2O , and 1:1 $\text{CH}_3\text{CN}:\text{H}_2\text{O}$). No considerable difference in the catalytic performance of $[\text{Fe}(\text{bpy})_3]@\text{M-Na-Y}$ was detected in 1:1 $\text{CH}_3\text{CN}:\text{H}_2\text{O}$ solvent. By contrast, different catalytic activities were exhibited in CH_3CN and H_2O . The authors suggested that the catalytic performance of the studied materials is dependent on the accessibility of benzene to the iron site in $[\text{Fe}(\text{bpy})_3]@\text{M-Na-Y}$, controlled by the hydrated ionic radius of the counter cation (M). By contrast, the catalytic activity of iron complex-encapsulated zeolite catalyst ($[\text{Fe}(\text{bpy})_3]@\text{Y}$) for oxidation of benzene [168] increased with the increase

in the amount of water added to acetonitrile. The maximum value was obtained for the 1:1 volume ratio of solvents. Moreover, after a reaction at 24 h, the turnover number of $[\text{Fe}(\text{bpy})_3]@\text{Y}$ was higher than that of $[\text{Fe}(\text{bpy})_3](\text{ClO}_4)_2$ as a homogeneous catalyst.

The role of hierarchical supports in oxidation of benzene to phenol was explored by Koekkoek and coworkers [29]. These researchers synthesized hierarchical Fe/ZSM-5 zeolites using different methodologies: carbon black as hard template and organosilane as soft template. Postsynthesis desilications were also performed on the same zeolite structure. The catalytic behavior was compared with the reference Fe/ZSM-5. The characterization results showed that the average pore size distribution changes substantially for the supports prepared according to the used methodologies. When carbon black was used, a large mesopore volume was obtained with a uniform pore size of ca. 20 nm, in accordance with the particle size of the carbon black of ca. 18 nm. On the other hand, desilication and organosilane templating originated materials with a much broader pore size distribution and smaller mesopore size. The number of active Fe(II) species present on the supported catalysts was determined by titration with nitrous oxide at 250 °C. The materials prepared by organosilane templating and desilication have shown an identical load of Fe(II) (79 and 61 $\mu\text{mol g}^{-1}_{\text{cat}}$, respectively), closer to the value obtained for the reference Fe/ZSM-5 (77 $\mu\text{mol g}^{-1}_{\text{cat}}$) and significantly higher than the one determined for the carbon templated sample (32 $\mu\text{mol g}^{-1}_{\text{cat}}$ for the best case). Catalytic tests for the oxidation of benzene with N_2O were performed at 350 °C. The catalytic activity is correlated with the textural properties of the supports as well as the amount of Fe(II) active sites. Accordingly, the best catalytic performance was obtained for the organosilane templated catalysts, with a conversion of 45 and 24%, higher than 36 and 10% obtained for the reference Fe/ZSM-5 (5 min and 5 h reaction time, respectively). Considering that the active site density is similar in the two catalysts, the improved catalytic performance is assigned to the textural properties, namely the much larger mesopore volume that enhanced the mass transport of reactants and products.

Following the same research line, Koekkoer et al. [58] also synthesized a hierarchical Fe/ZSM-5 zeolite using a diquatery ammonium surfactant containing a hydrophobic tail as a structure directing agent and studied the catalytic behavior for the oxidation of benzene by N_2O . Thin Fe/ZSM-5 nanosheets with limited dimensions in the directions of the straight channels with a high proportion of isolated Fe centers were obtained, which resulted in a superior catalytic performance in the selective oxidation of benzene to phenol, compared to the conventional Fe/ZSM-5. The authors pointed out that the sheet-like zeolites deactivate much more slowly than Fe supported on the microporous zeolite due to the much lower probability of secondary reactions of phenol on the short straight channels of the sheets. On the other hand, the deposition of carbonaceous deposits is limited on the nanosheet catalyst because of the short molecular pathways, limiting its deposition at the external surface of the nanosheets, in contrast to the conventional Fe/ZSM-5 where a rapid deactivation occurs due to the rapid clogging of the continuous micropore network.

A different approach was taken by Shahid and colleagues [67], who performed several postsynthesis treatments on a commercial ZSM-5 zeolite ($\text{SiO}_2/\text{Al}_2\text{O}_3 = 27$), named HM27, with small amounts of iron as impurities (ca. 0.04 wt.%): alkali treatment (AT), acid treatment (acT), steam treatment (St), combination of acid-alkali treatment, and combination of steam-acid-alkali treatment. The characterization techniques applied showed that the combination of steam-acid-alkali treatments led to a significant high level of mesoporosity with considerable preserved microporosity, which was not possible to attain by the other treatment methods. The direct oxidation of benzene to phenol in the presence of nitrous oxide was performed at 440 °C. Benzene conversion and phenol yield with time on stream is shown in Figure 26.

As can be observed, the parent sample (HM27) shows the highest deactivation rate whereas the steam-acid-alkali sample (HM27_St_AcT_AT) displays the lowest deactivation rate (ranging from 40% to 24% in 3 h time on stream) as well as the highest phenol yield. This behavior shows that the sequence of steam-acid-alkali treatments promotes modifications

that are not attained with only one isolated treatment. Accordingly, the modifications of the iron species, as impurities on the commercial zeolite, occurred during the steam treatment of the parent zeolite. In addition, when the steamed sample was subjected to subsequent acid and alkali treatment, modification on the pore structure occurred. In fact, according to the authors, the alkali treatment heals the destructive part of the zeolite that was caused by the steam and acid treatment. These modifications in the pore structure and iron species led to excellent catalytic performance in the oxidation of benzene to phenol.

More reactive aromatic compounds, namely toluene, were also subject of great interest as oxidation substrates due to their huge industrial importance.

An interesting example concerning the use of mesoporous silica SBA-15 was reported by Li and coworkers [170], who developed a composite resulting from the immobilization of *N,N*-dihydroxypyromellitimide (NDHPI) on Co-doped mesoporous sieve SBA-15 using the silylation agent 3-(glycidoxypropyl) trimethoxysilane (Figure 27). The characterization of the composite catalyst NDHPI-epoxy/Co-SBA-15 confirmed the presence of N–OH active sites, as well as the preservation of its mesoporous structure. A high efficiency toward toluene aerobic oxidation at 90 °C, in acetonitrile or under solvent-free conditions, was demonstrated by the composite catalyst, resulting from the joint action of N–OH active sites and Co immobilized in the framework of mesoporous SBA-15. In fact, 22% toluene conversion and 30% selectivity for benzaldehyde and benzyl alcohol were attained. Moreover, toluene conversion increased up to 30% in solvent-free conditions, although with a selectivity decrease. NDHPI-epoxy/Co-SBA-15 catalyst kept its catalytic activity after being reused for three times towards toluene aerobic oxidation, without Co leaching from SBA-15 and preserving its structure.

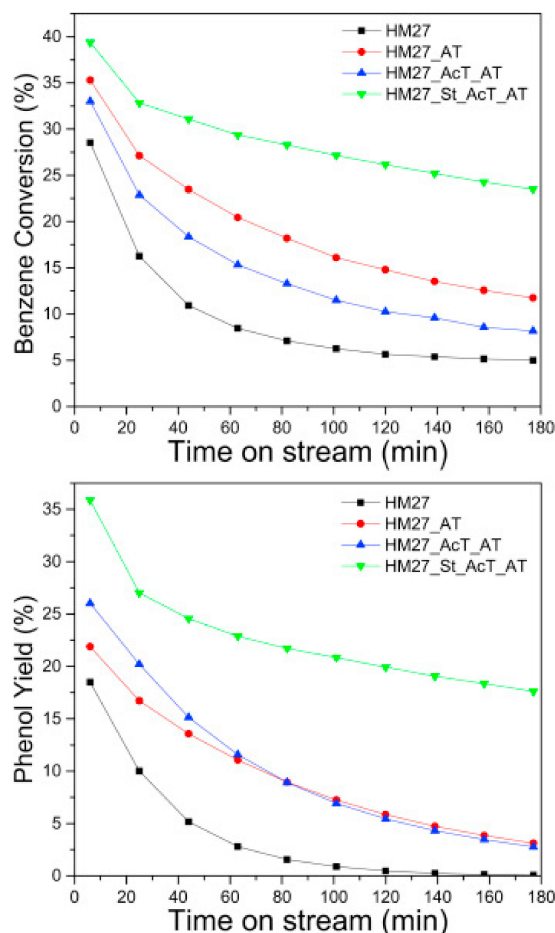


Figure 26. Benzene conversion and phenol yield with time on stream. Reproduced with permission from Reference [67]. Copyright (2016) Elsevier B. V.

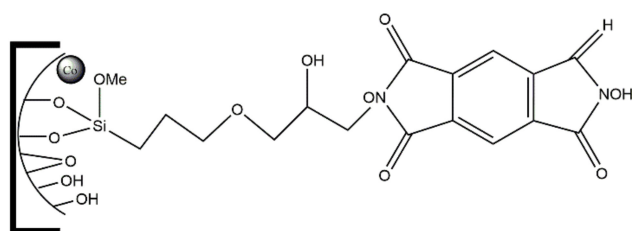


Figure 27. Structure of NDHPI-epoxy/Co-SBA-15 [170].

The role of the size and structure of a zeolitic support was explored by Zhang et al. [173] by comparing the catalytic behavior of MnO_x immobilized on microsolid (M-Z5), nanosolid (N-Z5) and nanohollow HZSM-5 zeolite (H-Z5) for the aerobic oxidation of toluene. The micro- and nano-scale ZSM-5 supports were prepared according to procedures described in the literature [174,175], while the hollow zeolite was obtained upon an alkali treatment of the nanoscale NaZSM-5, followed by ion exchange and calcination. An incipient impregnation method was applied to prepare HZSM-5 supported MnO_x catalysts with 10 wt.% of manganese contents. Figure 28 displays SEM and TEM images of MnO_x immobilized on the three zeolitic supports, where the overall morphologies were essentially retained after the loading of MnO_x on the zeolitic supports. Indeed, a homogeneous dispersion of MnO_x was observed on the surface of N-Z5 and H-Z5, but later, there were MnO_x nanograins with average particle size of 10–15 nm distributed both on the external surface and interior of the hollow structure.

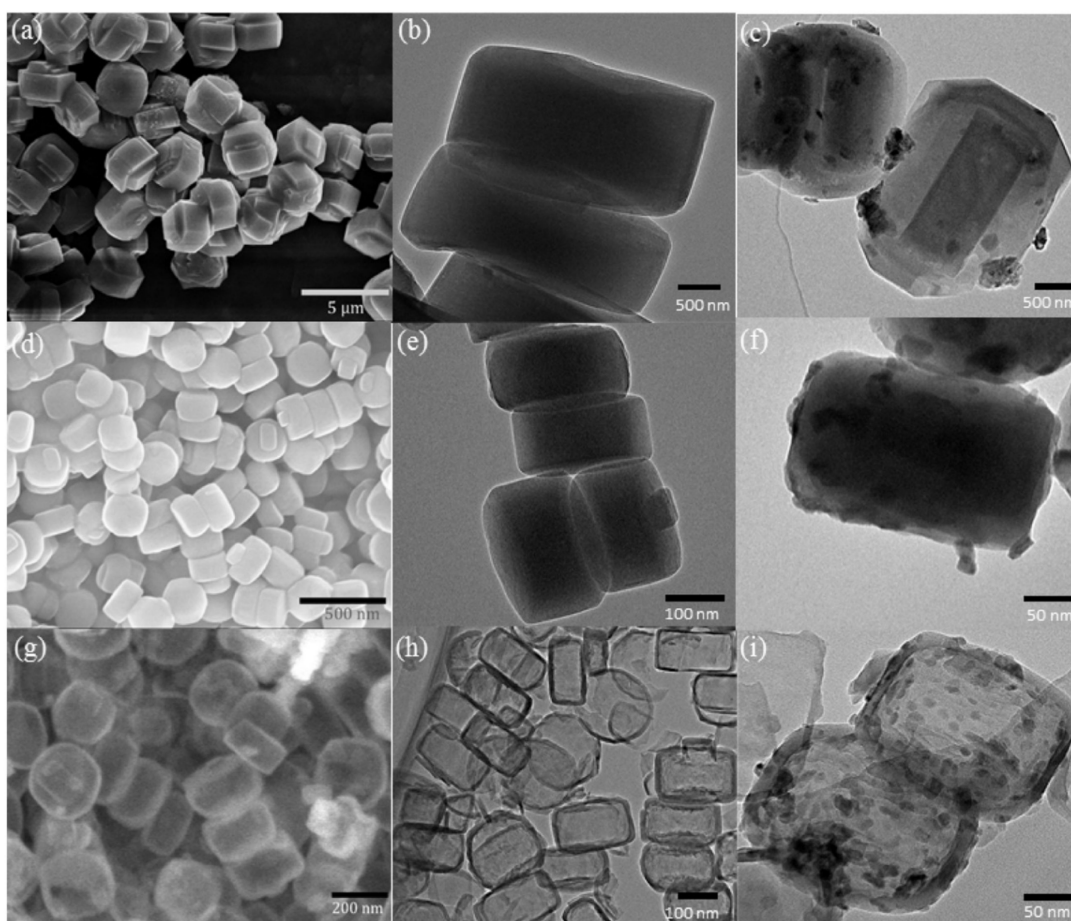


Figure 28. SEM images of zeolitic supports (a) M-Z5, (d) N-Z5, and (g) H-Z5, TEM images of the supports and supported catalysts: (b) M-Z5 (c) MnO_x /M-Z5, (e) N-Z5, (f) MnO_x /N-Z5, (h) H-Z5, and (i) MnO_x /HZ-5. Reproduced with permission from Reference [173]. Copyright (2019) Elsevier B. V.

The catalytic behavior of MnO_x immobilized on the three zeolitic supports clearly evidences the role of the support porosity (Figure 29). Both catalytic conversion and TOF values vs. reaction temperature show a deviation to low temperature in the case of $\text{MnO}_x/\text{H-Z5}$, indicating a notable catalytic efficiency for this supported catalyst, showing that the hollow structure and micro-/meso-porous porosity of HZSM-5 facilitates the reactant adsorption and diffusion.

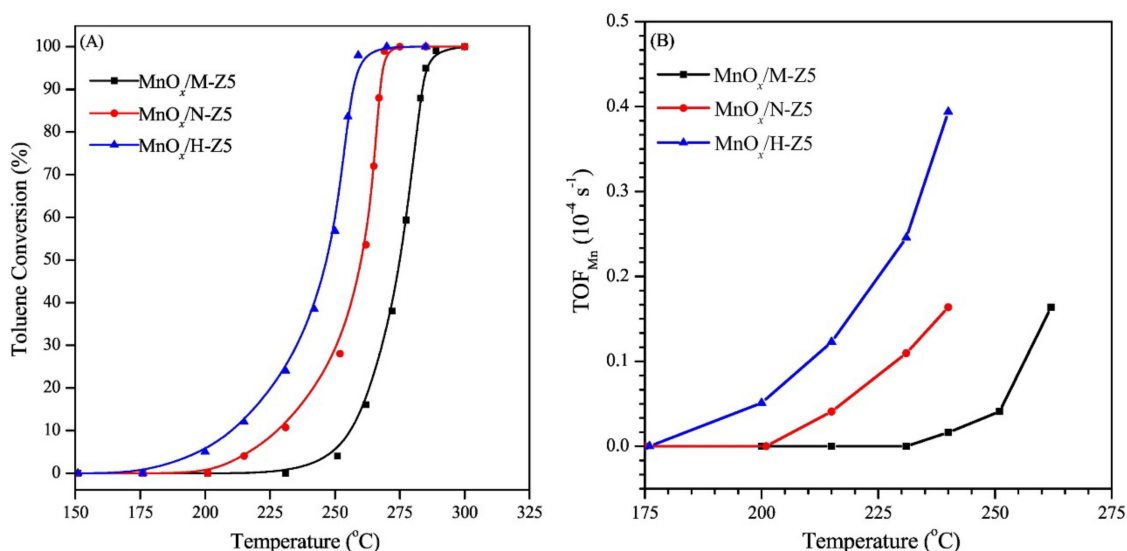


Figure 29. Catalytic conversion (A) and TOF (B) as a function of the reaction temperature. Adapted with permission from Reference [173]. Copyright (2019) Elsevier B. V.

The present review deals mainly with supported catalysts where the role of the zeolite or other related materials is to anchor the active species, allowing its heterogenization. However, there are a few literature examples reporting the catalytic activity of zeolites, without the immobilization of further metals or metal complexes, toward the oxidation of hydrocarbons. Some examples are briefly mentioned. The oxidation of styrene to benzaldehyde using hierarchical ZSM-5, synthesized in the presence of TPAOH, with different Si/Al ratios (20, 60 and 100) was reported by Narayanan et al. [163]. The authors explored the catalytic performance of MFI zeolite structure by studying the effect of several operation conditions in the selective oxidation of styrene to benzaldehyde, namely the Si/Al ratio, type of oxidant (TBHP, H_2O_2 or NaOCl), catalyst load, reaction temperature (45–85 °C), TBHP/styrene ratio (0.75–1.75), and reusability of the catalyst. The authors demonstrated that the reaction parameters strongly influence the catalytic behavior. Thus, the highest conversion of styrene as well as selectivity and yield of benzaldehyde were obtained at styrene/TBHP ratio of 1.5 over ZSM-5 with Si/Al = 60, ZSM-5(60), in acetonitrile at 65 °C for 6 h. The superior catalytic performance of ZSM-5(60) was attributed to the achieved optimal balance between the acidity and texture. Catalyst ZSM-5(60) was recovered and recycled three times without a significant loss of selectivity. The authors believe that this catalytic system should be further explored to assess a clean catalytic process for perfumery grade benzaldehyde, avoiding the presence of benzoic acid. Another example of catalytic activity of zeolites toward the oxidation of hydrocarbons was also presented by Narayanan and coworkers [56] and deals with the selective oxidation of toluene using hierarchical ZSM-5 hexagonal cubes, synthesized in the presence of TPAOH as mesopore template. The textural analysis of the surfactant-assisted zeolite showed an increase in mesoporosity without destroying the native microporosity, attributed to its smaller crystallite size. The selective oxidation of toluene is strongly influenced by the catalysts amount, reaction temperature, oxidant/substrate ratio, and the choice of oxidant. Hence, under the optimal reaction conditions, it was possible to reuse hierarchical ZSM-5 up to four runs without a significant loss in conversion and selectivity. On the other hand,

zeolite or silicalite materials with framework incorporated metals, such as Sn-Beta [176] or Ti-TS-1 [177,178], has been reported as catalysts with remarkable performance in oxidation reactions using H_2O_2 as oxidant agent. For example, nanosize hierarchical Ti-rich TS-1, synthesized via TritonX-100, was recently investigated in the hydroxylation of benzene to phenol with H_2O_2 as oxidizing agent and deionized water as solvent, showing high catalytic activity [178].

6. Concluding Remarks

The present work overviews the studies from the last 10 years concerning hydrocarbon oxidation reactions using zeolites and other related porous materials as supports for organometallic or metallic active species.

The catalytic oxidation of hydrocarbons is a key industrial process that allows the production of important chemicals from petroleum-based feedstocks, with application in all areas of chemical industries. In response to current environmental challenges, most traditional processes, involving homogeneous catalysts that operate in harsh conditions and originating large amounts of toxic effluents, are being transformed into modern processes that use heterogeneous catalysts which can operate in milder conditions. In addition, these catalysts can be recovered and reused in many catalytic cycles. This work reviews the published works concerning the use of immobilized catalysts on zeolites, hierarchical zeolites, and related porous materials as supports. In fact, these materials are the most studied supports due to their combined properties of mechanical and thermal stability that allows it an easy regeneration and recycling. Additionally, the porosity of these materials is a key factor that allows the effective immobilization of the active species preventing leaching during the catalytic cycles. It ranges from solely microporous in the case of commercial zeolites to purely mesoporous materials in the case of mesoporous silicas. Hierarchical zeolites, comprising micro- and meso-porosity that can be produced through synthesis or postsynthesis methods, are comprehensively presented in this review with selected examples.

The immobilization methods of organometallic or metallic catalyst on the porous supports are described, highlighting the advantages of each method.

The catalytic applications were classified according to the family of hydrocarbons: alkanes, alkenes, and aromatics. In all cases, when organometallic complexes are the active species, the use medium or small pore zeolites generally limits the anchorage to the external surface of the zeolites, which may lead to significant leaching phenomena. On the other hand, when metal particles are the active sites, medium pore zeolite structures, are preferred, especially when those metals are introduced during the zeolite synthesis, although other postsynthesis methods are also cited. As the substrates, intermediates, and reaction products become more voluminous, the use of hierarchical zeolites and mesoporous silicas becomes more important. The presented case studies showed improved adsorption/desorption as well as faster molecular diffusion, which is attributed to the presence of mesopores. In addition, an increase in reuse and number of catalytic cycles is mentioned due to the less expressive blockage of the support porosity.

Author Contributions: Conceptualization, writing—original draft preparation, and supervision, A.M.; writing—review and editing, A.M., N.N., A.P.C. and L.M.D.R.S.M. All authors have read and agreed to the published version of the manuscript.

Funding: This research was funded by Fundação para a Ciência e a Tecnologia (FCT) through UIDB/00100/2020. UIDP/00100/2020 and LA/P/0056/2020.

Institutional Review Board Statement: Not applicable.

Informed Consent Statement: Not applicable.

Data Availability Statement: Not applicable.

Conflicts of Interest: The authors declare no conflict of interest.

References

1. Rios, J.; Lebeau, J.; Yang, T.; Li, S.; Lynch, M.D. A critical review on the progress and challenges to a more sustainable, cost competitive synthesis of adipic acid. *Green Chem.* **2021**, *23*, 3172–3190. [CrossRef]
2. Hodnett, B.K. *Heterogeneous Catalytic Oxidation. Fundamental and Technological Aspects of the Selective Oxidation of Organic Compounds*; Wiley: New York, NY, USA, 2000; ISBN 978-0-471-48994-8.
3. *Ullmann's Encyclopedia of Industrial Chemistry*; Wiley, VCH: Weinheim, Germany, 2002. [CrossRef]
4. Clerici, M.G.; Ricci, M.S.G. Formation of C-O bonds by oxidation. In *Metal-Catalysis in Industrial Organic Processes*; Gian Paolo Chiusoli, P.M.M., Ed.; Royal Society of Chemistry: London, UK, 2006; pp. 23–78. [CrossRef]
5. Martins, L.M.D.R.S. Catalytic oxidation of alkanes to high-added value products: The role of C-Scorpionate metal complexes. In *Alkanes, Properties, Production and Applications*; Martins, L.M.D.R.S., Ed.; Nova Science Publishers: New York, NY, USA, 2019; pp. 69–92.
6. Li, Y.; Yu, J. New stories of zeolite structures: Their descriptions, determinations, predictions, and evaluations. *Chem. Rev.* **2014**, *114*, 7268–7316. [CrossRef]
7. Barrer, R.M. Zeolites and their synthesis. *Zeolites* **1981**, *1*, 130–140. [CrossRef]
8. Ribeiro, F.R.; Guisnet, M. *Les Zeolithes: Un Nanomonde au Service de la Catalyse*; EDP Science: Les Ullis, France, 2006.
9. International Zeolite Association International Zeolite Association Structure Commission, (n.d.). Available online: <http://iza-online.org/> (accessed on 29 December 2021).
10. Liang, J.; Liang, Z.; Zou, R.; Zhao, Y. Heterogeneous Catalysis in Zeolites, Mesoporous Silica, and Metal–Organic Frameworks. *Adv. Mater.* **2017**, *29*, 1–21. [CrossRef] [PubMed]
11. Costa, C.; Marques, J.C. Feasibility of Eco-friendly binary and ternary blended binders made of a fly-ash and oil-refinery spent catalyst in ready-mixed concrete production. *Sustainability* **2018**, *10*, 3136. [CrossRef]
12. Abubakar, A.; Waba, I.E.; Yunusa, S.; Gano, Z.S. Use of Reactivated Spent FCC Catalyst as Adsorbent for Lead (II) Ions from Refinery-based Simulated Wastewater. *Aech Int. J. Sci. Technol.* **2021**, *10*, 100–116. [CrossRef]
13. Li, D.; Chen, Y.; Hu, J.; Deng, B.; Cheng, X.; Zhang, Y. Synthesis of Hierarchical Chabazite Zeolite via Interzeolite Transformation of Coke-containing Spent MFI. *Appl. Catal. B Environ.* **2020**, *270*, 118881. [CrossRef]
14. Kumar Kundu, B.; Chhabra, V.; Malviya, N.; Ganguly, R.; Mishra, G.S.; Mukhopadhyay, S. Zeolite encapsulated host-guest Cu(II) Schiff base complexes: Superior activity towards oxidation reactions over homogenous catalytic systems. *Microporous Mesoporous Mater.* **2018**, *271*, 100–117. [CrossRef]
15. Parmar, D.K.; Butani, P.M.; Thumar, N.J.; Jasani, P.M.; Padaliya, R.V.; Sandhiya, P.R.; Nakum, H.D.; Khan, M.N.; Makwana, D. Oxy-functionalization of olefins with neat and heterogenized binuclear V(IV)O and Fe(II) complexes: Effect of steric hindrance on product selectivity and output in homogeneous and heterogeneous phase. *Mol. Catal.* **2019**, *474*, 110424. [CrossRef]
16. Desai, N.C.; Chudasama, J.A.; Karkar, T.J.; Patel, B.Y.; Jadeja, K.A.; Godhani, D.R.; Mehta, J.P. Studies of styrene oxidation by catalyst based on zeolite-Y nanohybrid materials. *J. Mol. Catal. A Chem.* **2016**, *424*, 203–219. [CrossRef]
17. Godhani, D.R.; Nakum, H.D.; Parmar, D.K.; Mehta, J.P.; Desai, N.C. Zeolite-Y immobilized Metallo-ligand complexes: A novel heterogeneous catalysts for selective oxidation. *Inorg. Chem. Commun.* **2016**, *72*, 105–116. [CrossRef]
18. Yamaguchi, S.; Miyake, Y.; Takiguchi, K.; Ihara, D.; Yahiro, H. Oxidation of cyclic hydrocarbons with hydrogen peroxide over iron complexes encapsulated in cation-exchanged zeolite. *Catal. Today* **2018**, *303*, 249–255. [CrossRef]
19. Xu, D.; Lv, H.; Liu, B. Encapsulation of metal nanoparticle catalysts within mesoporous zeolites and their enhanced catalytic performances: A review. *Front. Chem.* **2018**, *6*, 550. [CrossRef]
20. Farrusseng, D.; Tuel, A. Perspectives on zeolite-encapsulated metal nanoparticles and their applications in catalysis. *New J. Chem.* **2016**, *40*, 3933–3949. [CrossRef]
21. Wang, L.; Xu, S.; He, S.; Xiao, F.S. Rational construction of metal nanoparticles fixed in zeolite crystals as highly efficient heterogeneous catalysts. *Nano Today* **2018**, *20*, 74–83. [CrossRef]
22. Jampana, S.R.; Jia, L.; Ramarao, B.V.; Kumar, D. Experimental investigation of the adsorption and desorption of cellulase enzymes on zeolite- β for enzyme recycling applications. *Bioprocess Biosyst. Eng.* **2021**, *44*, 495–505. [CrossRef] [PubMed]
23. Zhang, H.; Jiang, Z.; Xia, Q.; Zhou, D. Progress and perspective of enzyme immobilization on zeolite crystal materials. *Biochem. Eng. J.* **2021**, *172*, 108033. [CrossRef]
24. Chen, N.Y.; Garwood, W.E.; Dwyer, F.G. *Shape Selective Catalysis in Industrial Applications*, 2nd ed.; Dekker, M., Ed.; CRC Press: New York, NY, USA, 1996.
25. Schwieger, W.; Machoke, A.G.; Weissenberger, T.; Inayat, A.; Selvam, T.; Klumpp, M.; Inayat, A. Hierarchy concepts: Classification and preparation strategies for zeolite containing materials with hierarchical porosity. *Chem. Soc. Rev.* **2016**, *45*, 3353–3376. [CrossRef]
26. Madsen, C.; Jacobsen, C.J.H. Nanosized zeolite crystals—Convenient control of crystal size distribution by confined space synthesis. *Chem. Commun.* **1999**, 673–674. [CrossRef]
27. Jacobsen, C.J.H.; Madsen, C.; Houzvicka, J.; Schmidt, I.; Carlsson, A. Mesoporous zeolite single crystals. *J. Am. Chem. Soc.* **2000**, *122*, 7116–7117. [CrossRef]
28. Kustova, M.Y.; Hasselriis, P.; Christensen, C.H. Mesoporous MEL—Type zeolite single crystal catalysts. *Catal. Lett.* **2004**, *96*, 205–211. [CrossRef]

29. Koekkoek, A.J.J.; Xin, H.; Yang, Q.; Li, C.; Hensen, E.J.M. Microporous and Mesoporous Materials Hierarchically structured Fe/ZSM-5 as catalysts for the oxidation of benzene to phenol. *Microporous Mesoporous Mater.* **2011**, *145*, 172–181. [[CrossRef](#)]
30. Bértolo, R.; Silva, J.M.; Ribeiro, F.; Maldonado-Hódar, F.J.; Fernandes, A.; Martins, A. Effects of oxidant acid treatments on carbon-templated hierarchical SAPO-11 materials: Synthesis, characterization and catalytic evaluation in n-decane hydroisomerization. *Appl. Catal. A Gen.* **2014**, *485*, 230–237. [[CrossRef](#)]
31. García-Martínez, J.; Cazorla-Amorós, D.; Linares-Solano, A.; Lin, Y.S. Synthesis and characterisation of MFI-type zeolites supported on carbon materials. *Microporous Mesoporous Mater.* **2001**, *42*, 255–268. [[CrossRef](#)]
32. Sakthivel, A.; Huang, S.J.; Chen, W.H.; Lan, Z.H.; Chen, K.H.; Kim, T.W.; Ryoo, R.; Chiang, A.S.T.; Liu, S. Bin Replication of mesoporous aluminosilicate molecular sieves (RMMs) with zeolite framework from mesoporous carbons (CMKs). *Chem. Mater.* **2004**, *16*, 3168–3175. [[CrossRef](#)]
33. Tao, Y.; Kanoh, H.; Kaneko, K. ZSM-5 monolith of uniform mesoporous channels. *J. Am. Chem. Soc.* **2003**, *125*, 6044–6045. [[CrossRef](#)]
34. Khoshbin, R.; Oruji, S.; Karimzadeh, R. Catalytic cracking of light naphtha over hierarchical ZSM-5 using rice husk ash as silica source in presence of ultrasound energy: Effect of carbon nanotube content. *Adv. Powder Technol.* **2018**, *29*, 2176–2187. [[CrossRef](#)]
35. Zhang, L.; Sun, X.; Pan, M.; Yang, X.; Liu, Y.; Sun, J.; Wang, Q.; Zheng, J.; Wang, Y.; Ma, J.; et al. Interfacial effects between carbon nanotube templates and precursors on fabricating a wall-crystallized hierarchical pore system in zeolite crystals. *J. Mater. Sci.* **2020**, *55*, 10412–10426. [[CrossRef](#)]
36. Tao, Y.; Kanoh, H.; Kaneko, K. Uniform mesopore-donated zeolite Y using carbon aerogel templating. *J. Phys. Chem. B* **2003**, *107*, 10974–10976. [[CrossRef](#)]
37. Naydenov, V.; Tosheva, L.; Antzutkin, O.N.; Sterte, J. Meso/macroporous AlPO-5 spherical macrostructures tailored by resin templating. *Microporous Mesoporous Mater.* **2005**, *78*, 181–188. [[CrossRef](#)]
38. Holland, B.T.; Abrams, L.; Stein, A. Dual templating of macroporous silicates with zeolitic microporous frameworks. *J. Am. Chem. Soc.* **1999**, *121*, 4308–4309. [[CrossRef](#)]
39. Zhu, H.; Liu, Z.; Wang, Y.; Kong, D.; Yuan, X.; Xie, Z. Nanosized CaCO₃ as hard template for creation of intracrystal pores within silicalite-1 crystal. *Chem. Mater.* **2008**, *20*, 1134–1139. [[CrossRef](#)]
40. Zhang, B.; Davis, S.A.; Mann, S. Starch gel templating of spongelike macroporous silicalite monoliths and mesoporous films. *Chem. Mater.* **2002**, *14*, 1369–1375. [[CrossRef](#)]
41. Dong, A.; Wang, Y.; Tang, Y.; Ren, N.; Zhang, Y.; Yue, Y.; Gao, Z. Zeolitic tissue through wood cell templating. *Adv. Mater.* **2002**, *14*, 926–929. [[CrossRef](#)]
42. Valtchev, V.P.; Smaïhi, M.; Faust, A.C.; Vidal, L. Equisetum arvense Templating of Zeolite Beta Macrostructures with Hierarchical Porosity. *Chem. Mater.* **2004**, *16*, 1350–1355. [[CrossRef](#)]
43. Wang, H.; Pinnavaia, T.J. MFI zeolite with small and uniform intracrystal mesopores. *Angew. Chem.-Int. Ed.* **2006**, *45*, 7603–7606. [[CrossRef](#)]
44. Tao, Y.; Kanoh, H.; Kaneko, K. Synthesis of Mesoporous Zeolite A by Resorcinol—Formaldehyde Aerogel Templating. *Langmuir* **2005**, *21*, 504–507. [[CrossRef](#)] [[PubMed](#)]
45. Groen, J.C.; Zhu, W.; Brouwer, S.; Huynink, S.J.; Kapteijn, F.; Moulijn, J.A.; Pérez-Ramírez, J. Direct demonstration of enhanced diffusion in mesoporous ZSM-5 zeolite obtained via controlled desilication. *J. Am. Chem. Soc.* **2007**, *129*, 355–360. [[CrossRef](#)]
46. Choi, M.; Srivastava, R.; Ryoo, R. Organosilane surfactant-directed synthesis of mesoporous aluminophosphates constructed with crystalline microporous frameworks. *Chem. Commun.* **2006**, 4380–4382. [[CrossRef](#)]
47. Wang, B.; Guo, T.; Peng, X.; Chen, F.; Lin, M.; Xia, C.; Zhu, B.; Liao, W.; Luo, Y.; Shu, X. Molybdenum-Confined Hierarchical Titanium Silicalite-1: The Synthesis, Characterization, and Catalytic Activity in Alkene Oxidation. *Ind. Eng. Chem. Res.* **2020**, *59*, 1093–1100. [[CrossRef](#)]
48. Li, P.; Li, A.; Ruan, R.; Guo, Y.; He, Q.; Zou, W.; Hou, L. Asymmetrical Gemini Surfactants Directed Synthesis Of Hierarchical ZSM-5 Zeolites and Their Immobilization of Molybdenum Complex for the Catalytic Epoxidation of Alkenes. *ChemCatChem* **2021**, *13*, 4442–4452. [[CrossRef](#)]
49. Wang, Q.; Xu, S.; Chen, J.; Wei, Y.; Li, J.; Fan, D.; Yu, Z.; Qi, Y.; He, Y.; Xu, S.; et al. Synthesis of mesoporous ZSM-5 catalysts using different mesogenous templates and the application in methanol conversion for enhanced catalyst lifespan. *RSC Adv.* **2014**, *41*, 21479. [[CrossRef](#)]
50. Hoang, P.H.; Van Don, B.; Chung, N.H. Cleavage of double bond using metal-loaded ZSM-5 zeolite catalysts for renewable biochemical application. *Can. J. Chem. Eng.* **2019**, *97*, 1086–1091. [[CrossRef](#)]
51. Inayat, A.; Knoke, I.; Spiecker, E.; Schwieger, W. Assemblies of mesoporous FAU-type zeolite nanosheets. *Angew. Chem.-Int. Ed.* **2012**, *51*, 1962–1965. [[CrossRef](#)] [[PubMed](#)]
52. Zhu, Y.; Hua, Z.; Zhou, J.; Wang, L.; Zhao, J.; Gong, Y.; Wu, W.; Ruan, M.; Shi, J. Hierarchical mesoporous zeolites: Direct self-assembly synthesis in a conventional surfactant solution by kinetic control over the zeolite seed formation. *Chem.-A Eur. J.* **2011**, *17*, 14618–14627. [[CrossRef](#)]
53. Lin, J.C.; Yates, M.Z. Altering the crystal morphology of silicalite-1 through microemulsion-based synthesis. *Langmuir* **2005**, *21*, 2117–2120. [[CrossRef](#)] [[PubMed](#)]
54. Lee, S.; Shantz, D.F. Zeolite growth in nonionic microemulsions: Synthesis of hierarchically structured zeolite particles. *Chem. Mater.* **2005**, *17*, 409–417. [[CrossRef](#)]

55. Koekkoek, A.J.J.; Tempelman, C.H.L.; Degirmenci, V.; Guo, M.; Feng, Z.; Li, C.; Hensen, E.J.M. Hierarchical zeolites prepared by organosilane templating: A study of the synthesis mechanism and catalytic activity. *Catal. Today* **2011**, *168*, 96–111. [[CrossRef](#)]
56. Narayanan, S.; Vijaya, J.J.; Sivasanker, S.; Kennedy, L.J.; Kathirgamanathan, P.; Azhagu Raj, R. Synthesis of hierarchical ZSM-5 hexagonal cubes and their catalytic activity in the solvent-free selective oxidation of toluene. *J. Porous Mater.* **2015**, *22*, 907–918. [[CrossRef](#)]
57. Li, L.; Meng, Q.; Wen, J.; Wang, J.; Tu, G.; Xu, C.; Zhang, F.; Zhong, Y.; Zhu, W.; Xiao, Q. Improved performance of hierarchical Fe-ZSM-5 in the direct oxidation of benzene to phenol by N₂O. *Microporous Mesoporous Mater.* **2016**, *227*, 252–257. [[CrossRef](#)]
58. Koekkoek, A.J.J.; Kim, W.; Degirmenci, V.; Xin, H.; Ryoo, R.; Hensen, E.J.M. Catalytic performance of sheet-like Fe/ZSM-5 zeolites for the selective oxidation of benzene with nitrous oxide. *J. Catal.* **2013**, *299*, 81–89. [[CrossRef](#)]
59. Serrano, D.P.; Aguado, J.; Escola, J.M.; Rodríguez, J.M.; Peral, A. Hierarchical zeolites with enhanced textural and catalytic properties synthesized from organofunctionalized seeds. *Chem. Mater.* **2006**, *18*, 2462–2464. [[CrossRef](#)]
60. Tompsett, G.A.; Conner, C.; Yngvesson, K.S. Microwave Synthesis of Nanoporous Materials. *ChemPhysChem* **2006**, *7*, 296–319. [[CrossRef](#)] [[PubMed](#)]
61. Kawai, T. Adsorption characteristics of polyvinyl alcohols on modified zeolites. *Colloid Polym. Sci.* **2014**, *292*, 533–538. [[CrossRef](#)]
62. Janssen, A.H.; Koster, A.J.; De Jong, K.P.; De Jong, K.P. On the shape of the mesopores in zeolite Y: A three-dimensional transmission electron microscopy study combined with texture analysis. *J. Phys. Chem. B* **2002**, *106*, 11905–11909. [[CrossRef](#)]
63. Xue, H.; Huang, X.; Zhan, E.; Ma, M.; Shen, W. Selective dealumination of mordenite for enhancing its stability in dimethyl ether carbonylation. *Catal. Commun.* **2013**, *37*, 75–79. [[CrossRef](#)]
64. De Baerdemaeker, T.; Yilmaz, B.; Müller, U.; Feyen, M.; Xiao, F.S.; Zhang, W.; Tatsumi, T.; Gies, H.; Bao, X.; De Vos, D. Catalytic applications of OSDA-free Beta zeolite. *J. Catal.* **2013**, *308*, 73–81. [[CrossRef](#)]
65. Mériaudeau, P.; Tuan, V.A.; Nghiem, V.T.; Lefevbre, F.; Ha, V.T. Characterization and catalytic properties of hydrothermally dealuminated MCM-22. *J. Catal.* **1999**, *185*, 378–385. [[CrossRef](#)]
66. You, Q.; Wang, X.; Wu, Y.; Bi, C.; Yang, X.; Sun, M.; Zhang, J.; Hao, Q.; Chen, H.; Ma, X. Hierarchical Ti-beta with a three-dimensional ordered mesoporosity for catalytic epoxidation of bulky cyclic olefins. *New J. Chem.* **2021**, *45*, 10303–10314. [[CrossRef](#)]
67. Shahid, A.; Reddy, V.; Hartmann, M.; Schwieger, W. Direct oxidation of benzene to phenol over hierarchical ZSM-5 zeolites prepared by sequential post synthesis modification. *Microporous Mesoporous Mater.* **2017**, *237*, 151–159. [[CrossRef](#)]
68. Groen, J.C.; Hamminga, G.M.; Moulijn, A.; Pe, J. In situ monitoring of desilication of MFI-type zeolites in alkaline medium. *Phys. Chem. Chem. Phys.* **2007**, *9*, 4822–4830. [[CrossRef](#)] [[PubMed](#)]
69. Verboekend, D.; Mitchell, S.; Milina, M.; Groen, J.C.; Javier, P. Full Compositional Flexibility in the Preparation of Mesoporous MFI Zeolites by Desilication. *J. Phys. Chem* **2011**, *115*, 14193–14203. [[CrossRef](#)]
70. Paixão, V.; Carvalho, A.P.; Rocha, J.; Fernandes, A.; Martins, A. Modification of MOR by desilication treatments: Structural, textural and acidic characterization. *Microporous Mesoporous Mater.* **2010**, *131*, 350–357. [[CrossRef](#)]
71. Holm, M.S.; Hansen, K.; Hviid, C. “One-Pot” Ion-Exchange and Mesopore Formation During Desilication. *Eur. J. Inorg. Chem.* **2009**, *9*, 1194–1198. [[CrossRef](#)]
72. Machado, V.; Rocha, J.; Carvalho, A.P.; Martins, A. Modification of MCM-22 zeolite through sequential post-synthesis treatments. Implications on the acidic and catalytic behaviour. *Appl. Catal. A Gen.* **2012**, *445–446*, 329–338. [[CrossRef](#)]
73. Aleixo, R.; Elvas-leitão, R.; Martins, F.; Carvalho, A.P.A.P.; Brigas, A.; Nunes, R.; Fernandes, A.; Rocha, J.; Martins, A.; Nunes, N. Zooming in with QSPR on Friedel-Crafts acylation reactions over modified BEA zeolites. *Mol. Catal.* **2019**, *476*, 110495. [[CrossRef](#)]
74. Andrade, M.A.; Ansari, L.M.S.; Pombeiro, A.J.L.; Carvalho, A.P.; Martins, A.; Martins, L.M.D.R.S. Fe@hierarchical bea zeolite catalyst for mw-assisted alcohol oxidation reaction: A greener approach. *Catalysts* **2020**, *10*, 1029. [[CrossRef](#)]
75. Paixão, V.; Monteiro, R.; Andrade, M.; Fernandes, A.; Rocha, J.; Carvalho, A.P.P.; Martins, A. Desilication of MOR zeolite: Conventional versus microwave assisted heating. *Appl. Catal. A Gen.* **2011**, *402*, 59–68. [[CrossRef](#)]
76. Barrer, R.M.; Makki, M.B. Molecular Sieve Sorbents From Clinoptilolite. *Can. J. Chem.* **1964**, *42*, 1481–1487. [[CrossRef](#)]
77. Carvalho, A.P.; Nunes, N.; Martins, A. Hierarchical Zeolites: Preparation, Properties and Catalytic Applications. In *Comprehensive Guide for Mesoporous Materials, Vol. 3: Properties and Development*; Aliofkhaezrai, M., Ed.; Nova Science Publishers: Hauppauge, NY, USA, 2015; pp. 147–211, ISBN 978-1-63463-318-5.
78. Serrano, D.P.; Escola, J.M.; Pizarro, P. Synthesis strategies in the search for hierarchical zeolites. *Chem. Soc. Rev.* **2013**, *42*, 4004–4035. [[CrossRef](#)]
79. Bai, R.; Song, Y.; Li, Y.; Yu, J. Creating Hierarchical Pores in Zeolite Catalysts. *Trends Chem.* **2019**, *1*, 601–611. [[CrossRef](#)]
80. Kerstens, D.; Smeyers, B.; Van Waeyenberg, J.; Zhang, Q.; Yu, J.; Sels, B.F. State of the Art and Perspectives of Hierarchical Zeolites: Practical Overview of Synthesis Methods and Use in Catalysis. *Adv. Mater.* **2020**, *32*, 1–47. [[CrossRef](#)] [[PubMed](#)]
81. Triantafyllidis, C.S.; Vlessidis, A.G.; Evmiridis, N.P. Dealuminated H-Y zeolites: Influence of the degree and the type of dealumination method on the structural and acidic characteristics of H-Y zeolites. *Ind. Eng. Chem. Res.* **2000**, *39*, 307–319. [[CrossRef](#)]
82. Valtchev, V.; Majano, G.; Mintova, S.; Pérez-Ramírez, J. Tailored crystalline microporous materials by post-synthesis modification. *Chem. Soc. Rev.* **2013**, *42*, 263–290. [[CrossRef](#)]
83. Dessau, R.M.; Valyocsik, E.W.; Goeke, N.H. Aluminum zoning in ZSM-5 as revealed by selective silica removal. *Zeolites* **1992**, *12*, 776–779. [[CrossRef](#)]
84. Lietz, G.; Schnabel, K.H.; Peuker, C.; Gross, T.; Storek, W.; Völter, J. Modifications of H-ZSM-5 catalysts by NaOH treatment. *J. Catal.* **1994**, *148*, 562–568. [[CrossRef](#)]

85. Ogura, M.; Shinomiya, S.Y.; Tateno, J.; Nara, Y.; Kikuchi, E.; Matsukata, M. Formation of uniform mesopores in ZSM-5 zeolite through treatment in alkaline solution. *Chem. Lett.* **2000**, *8*, 882–883. [[CrossRef](#)]
86. Christensen, C.H.; Egeblad, K.; Christensen, C.H.; Groen, J.C. Hierarchical zeolites: Enhanced utilisation of microporous crystals in catalysis by advances in materials design. *Chem. Soc. Rev.* **2008**, *37*, 2530–2542. [[CrossRef](#)]
87. Groen, J.C.; Moulijn, J.A.; Pe, J.; Pérez-Ramírez, J. Alkaline posttreatment of MFI zeolites. From accelerated screening to scale-up. *Ind. Eng. Chem. Res.* **2007**, *46*, 4193–4201. [[CrossRef](#)]
88. Groen, J.C.; Peffer, L.A.A.; Moulijn, J.A. Mesoporosity development in ZSM-5 zeolite upon optimized desilication conditions in alkaline medium. *Colloids Surf. A Physicochem. Eng. Asp.* **2004**, *241*, 53–58. [[CrossRef](#)]
89. Groen, J.C.; Jansen, J.C.; Moulijn, J.A.; Pe, J. Optimal Aluminum-Assisted Mesoporosity Development in MFI Zeolites by Desilication. *J. Phys. Chem. B* **2004**, *108*, 13062–13065. [[CrossRef](#)]
90. Martins, L.M.D.R.S.; Martins, A.; Alegria, E.C.B.A.; Carvalho, A.P.; Pombeiro, A.J.L. Efficient cyclohexane oxidation with hydrogen peroxide catalysed by a C-scorpionate iron(II) complex immobilized on desilicated MOR zeolite. *Appl. Catal. A Gen.* **2013**, *464–465*, 43–50. [[CrossRef](#)]
91. Verboekend, D.; Vilé, G.; Pérez-Ramírez, J. Mesopore Formation in USY and Beta Zeolites by Base Leaching: Selection Criteria and Optimization of Pore-Directing Agents. *Cryst. Growth Des.* **2012**, *12*, 3123–3132. [[CrossRef](#)]
92. Verboekend, D.; Pérez-Ramírez, J. Desilication mechanism revisited: Highly mesoporous all-silica zeolites enabled through pore-directing agents. *Chem.-A Eur. J.* **2011**, *17*, 1137–1147. [[CrossRef](#)] [[PubMed](#)]
93. Abelló, S.; Pérez-Ramírez, J. Accelerated generation of intracrystalline mesoporosity in zeolites by microwave-mediated desilication. *PCCP* **2009**, *11*, 2959–2963. [[CrossRef](#)]
94. García-Martínez, J.; Johnson, M.; Valla, J.; Li, K.; Ying, J.Y. Mesostructured zeolite y—High hydrothermal stability and superior FCC catalytic performance. *Catal. Sci. Technol.* **2012**, *2*, 987–994. [[CrossRef](#)]
95. Garcia-Martinez, J. Mesostructured Zeolitic Materials, and Methods of Making and Using the Same. U.S. Patent 8524624 B2, 14 November 2013.
96. García-Martínez, J.; Li, K. Surfactant-templated mesostructuring of zeolites: From discovery to commercialization. In *Mesoporous Zeolites: Preparation, Characterization and Applications*; García-Martínez, J., Li, K., Eds.; Wiley, VCH: Weinheim, Germany, 2015; pp. 321–345, ISBN 9783527673957.
97. Mendoza-castro, M.J.; Serrano, E.; Linares, N.; García-Martínez, J. Surfactant-Templated Zeolites: From Thermodynamics to Direct Observation. *Adv. Mater. Interfaces* **2020**, *8*, 1–23. [[CrossRef](#)]
98. Ivanova, I.I.; Kuznetsov, A.S.; Yuschenko, V.V.; Knyazeva, E.E. Design of composite micro/mesoporous molecular sieve catalysts. *Pure Appl. Chem.* **2004**, *76*, 1647–1658. [[CrossRef](#)]
99. Wang, S.; Dou, T.; Li, Y.; Zhang, Y.; Li, X.; Yan, Z. A novel method for the preparation of MOR/MCM-41 composite molecular sieve. *Catal. Commun.* **2005**, *6*, 87–91. [[CrossRef](#)]
100. Van-Dúnem, V.; Carvalho, A.P.; Martins, L.M.D.R.S.; Martins, A. Improved Cyclohexane Oxidation Catalyzed by a Heterogenized Iron (II) Complex on Hierarchical Y Zeolite through Surfactant Mediated Technology. *ChemCatChem* **2018**, *10*, 4058–4066. [[CrossRef](#)]
101. Al-Ani, A.; Haslam, J.J.C.; Mordvinova, N.E.; Lebedev, O.I.; Vicente, A.; Fernandez, C.; Zholobenko, V. Synthesis of nanostructured catalysts by surfactant templating of large-pore zeolites. *Nanoscale Adv.* **2019**, *1*, 2029–2039. [[CrossRef](#)]
102. Martins, A.; Neves, V.; Moutinho, J.; Nunes, N.; Carvalho, A.P. Friedel-Crafts acylation reaction over hierarchical Y zeo-lite modified through surfactant mediated technology. *Microporous Mesoporous Mater.* **2021**, *323*, 111167. [[CrossRef](#)]
103. Ottaviani, D.; Van-Dúnem, V.; Carvalho, A.P.; Martins, A.; Martins, L. Eco-friendly cyclohexane oxidation by a V-scorpionate complex immobilized at hierarchical MOR zeolite. *Catal. Today* **2020**, *348*, 37–44. [[CrossRef](#)]
104. Li, K.; Valla, J.; Garcia-Martinez, J. Realizing the commercial potential of hierarchical zeolites: New opportunities in catalytic cracking. *ChemCatChem* **2014**, *6*, 46–66. [[CrossRef](#)]
105. Linares, N.; Cirujano, F.G.; De Vos, D.E.; Garcia-Martinez, J. Surfactant-templated zeolites for the production of active pharmaceutical intermediates. *Chem. Commun.* **2019**, *55*, 12869–12872. [[CrossRef](#)]
106. Majano, G.; Borchardt, L.; Mitchell, S.; Valtchev, V.; Pérez-Ramírez, J. Rediscovering zeolite mechanochemistry—A pathway beyond current synthesis and modification boundaries. *Microporous Mesoporous Mater.* **2014**, *194*, 106–114. [[CrossRef](#)]
107. Akcay, K.; Sirkecioğlu, A.; Tatlier, M.; Savaşçı, Ö.T.; Erdem-Şenatalar, A. Wet ball milling of zeolite HY. *Powder Technol.* **2004**, *142*, 121–128. [[CrossRef](#)]
108. Hernandez-Ramírez, O.; Al-nasri, S.K.; Holmes, S.M. Hierarchical structures based on natural carbons and zeolites. *J. Mater. Chem.* **2011**, *21*, 16529–16534. [[CrossRef](#)]
109. Ferreira, L.; Ribeiro, F.; Fernandes, A.; Martins, A. Ball Milling Modified SAPO-11 Based Catalysts for n-Decane Hydroisomerization. *ChemistrySelect* **2019**, *4*, 6713–6718. [[CrossRef](#)]
110. Carvalho, A.P.; Castanheira, C.; Cardoso, B.; Pires, J.; Silva, A.R.; Freire, C.; De Castro, B.; De Carvalho, M.B. Simultaneous aluminium oxide pillaring and copper(ii) Schiff base complexes encapsulation in a montmorillonite. *J. Mater. Chem.* **2004**, *14*, 374–379. [[CrossRef](#)]
111. Figueiredo, H.; Silva, B.; Kuźniarska-Biernacka, I.; Fonseca, A.M.; Medina, R.; Rasmussen, S.; Bañares, M.A.; Neves, I.C.; Tavares, T. Oxidation of cyclohexanol and cyclohexene with triazenido complexes of chromium immobilized in biosorption FAU supports. *Chem. Eng. J.* **2014**, *247*, 134–141. [[CrossRef](#)]

112. Kresge, C.T.; Roth, W.J.; Simmons, K.G.; Vartuli, J.C. Acid Oxide with Micro and Mesoporous Characteristics: MCM-36. World Patent WO92/11934, 23 July 1992.
113. Roth, W.J.; Kresge, C.T.; Vartuli, J.C.; Leonowicz, M.E.; Fung, A.S.; McCullen, S.B. MCM-36: The first pillared molecular sieve with zeolite properties. *Stud. Surf. Sci. Catal.* **1995**, *94*, 301–308. [[CrossRef](#)]
114. Liu, G.; Jiang, J.G.; Yang, B.; Fang, X.; Xu, H.; Peng, H.; Xu, L.; Liu, Y.; Wu, P. Hydrothermal synthesis of MWW-type stannosilicate and its post-structural transformation to MCM-56 analogue. *Microporous Mesoporous Mater.* **2013**, *165*, 210–218. [[CrossRef](#)]
115. Na, K.; Chol, M.; Park, W.; Sakamoto, Y.; Terasaki, O.; Ryoo, R. Pillared MFI zeolite nanosheets of a single-unit-cell thickness. *J. Am. Chem. Soc.* **2010**, *132*, 4169–4177. [[CrossRef](#)] [[PubMed](#)]
116. Xiaoling, L.I.U.; Yan, W.; Xujin, W.; Yafei, Z.; Yanjun, G.; Qinghu, X.U.; Jun, X.U. Characterization and Catalytic Performance in n-Hexane Cracking of HEU-1 Zeolites Dealuminated Using Hydrochloric Acid and Hydrothermal Treatments. *Chin. J. Catal.* **2012**, *33*, 1889–1900. [[CrossRef](#)]
117. Corma, A.; Fornés, V.; Pergher, S.B.C. Zeolite ITQ-2. World Patent WO9717290A1, 5 May 1997.
118. Corma, A.; Diaz, U.; Domine, M.E.; Fornés, V. AIITQ-6 and TiITQ-6: Synthesis, characterization, and catalytic activity. *Angew. Chem.-Int. Ed.* **2000**, *39*, 1499–1501. [[CrossRef](#)]
119. Corma, A.; Fornés, V.; Díaz, U. ITQ-18 a new delaminated stable zeolite. *Chem. Commun.* **2001**, *1*, 2642–2643. [[CrossRef](#)]
120. Beck, J.S.; Vartuli, J.C.; Roth, W.J.; Leonowicz, M.E.; Kresge, C.T.; Schmitt, K.D.; Chu, C.T.W.; Olson, D.H.; Sheppard, E.W.; McCullen, S.B.; et al. A New Family of Mesoporous Molecular Sieves Prepared with Liquid Crystal Templates. *J. Am. Chem. Soc.* **1992**, *114*, 10834–10843. [[CrossRef](#)]
121. Trong On, D.; Desplandier-Giscard, D.; Danumah, C.; Kaliaguine, S. Perspectives in catalytic applications of mesostructured materials. *Appl. Catal. A Gen.* **2001**, *222*, 299–357. [[CrossRef](#)]
122. Mandal, S.; Sinhamahapatra, A.; Rakesh, B.; Kumar, R.; Panda, A.; Chowdhury, B. Synthesis, characterization of Ga-TUD-1 catalyst and its activity towards styrene epoxidation reaction. *Catal. Commun.* **2011**, *12*, 734–738. [[CrossRef](#)]
123. Meoto, S.; Kent, N.; Nigra, M.M.; Coppens, M.O. Effect of stirring rate on the morphology of FDU-12 mesoporous silica particles. *Microporous Mesoporous Mater.* **2017**, *249*, 61–66. [[CrossRef](#)]
124. Kishor, R.; Ghoshal, A.K. Understanding the hydrothermal, thermal, mechanical and hydrolytic stability of mesoporous KIT-6: A comprehensive study. *Microporous Mesoporous Mater.* **2017**, *242*, 127–135. [[CrossRef](#)]
125. Patcas, F.C. The methanol-to-olefins conversion over zeolite-coated ceramic foams. *J. Catal.* **2005**, *231*, 194–200. [[CrossRef](#)]
126. Mitra, B.; Kunzru, D. Washcoating of different zeolites on cordierite monoliths. *J. Am. Ceram. Soc.* **2008**, *91*, 64–70. [[CrossRef](#)]
127. Ivanova, S.; Louis, B.; Madani, B.; Tessonnier, J.P.; Ledoux, M.J.; Pham-Huu, C. ZSM-5 coatings on β -SiC monoliths: Possible new structured catalyst for the methanol-to-olefins process. *J. Phys. Chem. C* **2007**, *111*, 4368–4374. [[CrossRef](#)]
128. Louis, B.; Ocampo, F.; Yun, H.S.; Tessonnier, J.P.; Pereira, M.M. Hierarchical pore ZSM-5 zeolite structures: From micro- to macro-engineering of structured catalysts. *Chem. Eng. J.* **2010**, *161*, 397–402. [[CrossRef](#)]
129. Barg, S.; Soltmann, C.; Schwab, A.; Koch, D.; Schwiager, W.; Grathwohl, G. Novel open cell aluminum foams and their use as reactive support for zeolite crystallization. *J. Porous Mater.* **2011**, *18*, 89–98. [[CrossRef](#)]
130. Qian, X.; Du, J.; Li, B.; Si, M.; Yang, Y.; Hu, Y.; Niu, G.; Zhang, Y.; Xu, H.; Tu, B.; et al. Controllable fabrication of uniform core-shell structured zeolite@SBA-15 composites. *Chem. Sci.* **2011**, *2*, 2006–2016. [[CrossRef](#)]
131. Qian, X.; Che, R.; Asiri, A.M. Exploring Meso-/Microporous Composite Molecular Sieves with Core-Shell Exploring Meso-/Microporous Composite Molecular Sieves with Core-Shell. *Chem. Eur. J.* **2012**, *18*, 931–939. [[CrossRef](#)]
132. Lv, Y.; Qian, X.; Tu, B.; Zhao, D. Generalized synthesis of core-shell structured nano-zeolite@ordered mesoporous silica composites. *Catal. Today* **2013**, *204*, 2–7. [[CrossRef](#)]
133. Xu, L.; Peng, H.G.; Zhang, K.; Wu, H.; Chen, L.; Liu, Y.; Wu, P. Core-shell-structured titanosilicate as a robust catalyst for cyclohexanone ammoxidation. *ACS Catal.* **2013**, *3*, 103–110. [[CrossRef](#)]
134. Jarrais, B.; Pereira, C.; Silva, A.R.; Carvalho, A.P.; Pires, J.; Freire, C. Grafting of vanadyl acetylacetonate onto organo-hexagonal mesoporous silica and catalytic activity in the allylic epoxidation of geraniol. *Polyhedron* **2009**, *28*, 994–1000. [[CrossRef](#)]
135. Pinto, V.H.A.; Rebouças, J.S.; Ucoski, G.M.; de Faria, E.H.; Ferreira, B.F.; Silva San Gil, R.A.; Nakagaki, S. Mn porphyrins immobilized on non-modified and chloropropyl-functionalized mesoporous silica SBA-15 as catalysts for cyclohexane oxidation. *Appl. Catal. A Gen.* **2016**, *526*, 9–20. [[CrossRef](#)]
136. Machado, K.; Tavares, P.B.; Mishra, G.S. Synthesis and application of FeIII, NiII and Mn II complexes anchored to HMS as efficient catalysts for cycloalkane oxyfunctionalization. *J. Mol. Catal. A Chem.* **2014**, *383–384*, 159–166. [[CrossRef](#)]
137. Dorbes, S.; Pereira, C.; Andrade, M.; Barros, D.; Pereira, A.M.; Rebelo, S.L.H.; Araújo, J.P.; Pires, J.; Carvalho, A.P.; Freire, C. Oxidovanadium(IV) acetylacetonate immobilized onto CMK-3 for heterogeneous epoxidation of geraniol. *Microporous Mesoporous Mater.* **2012**, *160*, 67–74. [[CrossRef](#)]
138. Gaspar, H.; Andrade, M.; Pereira, C.; Pereira, A.M.; Rebelo, S.L.H.; Araújo, J.P.; Pires, J.; Carvalho, A.P.; Freire, C. Alkene epoxidation by manganese(III) complexes immobilized onto nanostructured carbon CMK-3. *Catal. Today* **2013**, *203*, 103–110. [[CrossRef](#)]
139. Kuźniarska-Biernacka, I.; Pereira, C.; Carvalho, A.P.; Pires, J.; Freire, C. Epoxidation of olefins catalyzed by manganese(III) salen complexes grafted to porous heterostructured clays. *Appl. Clay Sci.* **2011**, *53*, 195–203. [[CrossRef](#)]
140. Kuźniarska-Biernacka, I.; Silva, A.R.; Carvalho, A.P.; Pires, J.; Freire, C. Anchoring of chiral manganese(III) salen complex onto organo clay and porous clay heterostructure and catalytic activity in alkene epoxidation. *Catal. Lett.* **2010**, *134*, 63–71. [[CrossRef](#)]

141. Martins, A.; Silva, J.M.M.; Ribeiro, F.R.R.; Guisnet, M.; Ribeiro, M.F.F. n-Hexane hydroisomerisation over bifunctional Pt/MCM-22 catalysts. Influence of the mode of Pt introduction. *Stud. Surf. Sci. Catal.* **2008**, *174*, 1135–1138. [[CrossRef](#)]
142. Azzolina Jury, F.; Polaert, I.; Pierella, L.B.; Estel, L. Optimized benzaldehyde production over a new Co-ZSM-11 catalyst: Reaction parameters effects and kinetics. *Catal. Commun.* **2014**, *46*, 6–10. [[CrossRef](#)]
143. Martins, A.; Silva, J.M.M.; Ribeiro, F.R.R.; Ribeiro, M.F.F. Hydroisomerization of n-hexane over Pt-Ni/HBEA using catalysts prepared by different methods. *Catal. Lett.* **2006**, *109*, 83–87. [[CrossRef](#)]
144. Liu, J.; Wang, Z.; Jian, P.; Jian, R. Highly selective oxidation of styrene to benzaldehyde over a tailor-made cobalt oxide encapsulated zeolite catalyst. *J. Colloid Interface Sci.* **2018**, *517*, 144–154. [[CrossRef](#)] [[PubMed](#)]
145. Bértolo, R.; Fernandes, A.; Ribeiro, F.; Silva, J.M.; Martins, A.; Ribeiro, F.R. Hydroisomerization of n-decane over SAPO-11 catalysts synthesized with methylamine as co-template. *React. Kinet. Mech. Catal.* **2010**, *99*, 183–191. [[CrossRef](#)]
146. Bértolo, R.; Silva, J.M.; Ribeiro, M.F.; Martins, A.; Fernandes, A. Microwave synthesis of SAPO-11 materials for long chain n-alkanes hydroisomerization: Effect of physical parameters and chemical gel composition. *Appl. Catal. A Gen.* **2017**, *542*, 28–37. [[CrossRef](#)]
147. Wang, H.; Wang, L.; Xiao, F.S. Metal@zeolite hybrid materials for catalysis. *ACS Cent. Sci.* **2020**, *6*, 1685–1697. [[CrossRef](#)]
148. Wang, G.; Xu, S.; Wang, L.; Liu, Z.; Dong, X.; Wang, L.; Zheng, A.; Meng, X.; Xiao, F. Traps of zeolite crystals for sinter-resistant catalysts. *Chem. Commun.* **2018**, *54*, 3274–3277. [[CrossRef](#)]
149. Zhang, J.; Rao, C.; Peng, H.; Peng, C.; Zhang, L.; Xu, X.; Liu, W.; Wang, Z.; Zhang, N.; Wang, X. Enhanced toluene combustion performance over Pt loaded hierarchical porous MOR zeolite. *Chem. Eng. J.* **2018**, *334*, 10–18. [[CrossRef](#)]
150. Salavati-Niasari, M.; Shakouri-Arani, M.; Davar, F. Flexible ligand synthesis, characterization and catalytic oxidation of cyclohexane with host (nanocavity of zeolite-Y)/guest (Mn(II), Co(II), Ni(II) and Cu(II) complexes of tetrahydro-salophen) nanocomposite materials. *Microporous Mesoporous Mater.* **2008**, *116*, 77–85. [[CrossRef](#)]
151. Modi, C.K.; Trivedi, P.M.; Chudasama, J.A.; Nakum, H.D.; Parmar, D.K.; Gupta, S.K.; Jha, P.K. Zeolite-Y entrapped bivalent transition metal complexes as hybrid nanocatalysts: Density functional theory investigation and catalytic aspects. *Green Chem. Lett. Rev.* **2014**, *7*, 278–287. [[CrossRef](#)]
152. Zhou, X.; Chen, H.; Cui, X.; Hua, Z.; Chen, Y.; Zhu, Y.; Song, Y.; Gong, Y.; Shi, J. A facile one-pot synthesis of hierarchically porous Cu(I)-ZSM-5 for radicals-involved oxidation of cyclohexane. *Appl. Catal. A Gen.* **2013**, *451*, 112–119. [[CrossRef](#)]
153. Alavi, S.; Hosseini-Monfared, H.; Siczek, M. A new manganese(III) complex anchored onto SBA-15 as efficient catalyst for selective oxidation of cycloalkanes and cyclohexene with hydrogen peroxide. *J. Mol. Catal. A Chem.* **2013**, *377*, 16–28. [[CrossRef](#)]
154. Niu, X.R.; Li, J.; Zhang, L.; Lei, Z.T.; Zhao, X.L.; Yang, C.H. ZSM-5 functionalized in situ with manganese ions for the catalytic oxidation of cyclohexane. *RSC Adv.* **2017**, *7*, 50619–50625. [[CrossRef](#)]
155. Fu, Y.; Zhan, W.; Guo, Y.; Wang, Y.; Liu, X.; Guo, Y.; Wang, Y.; Lu, G. Effect of surface functionalization of cerium-doped MCM-48 on its catalytic performance for liquid-phase free-solvent oxidation of cyclohexane with molecular oxygen. *Microporous Mesoporous Mater.* **2015**, *214*, 101–107. [[CrossRef](#)]
156. Rezaei, M.; Chermahini, A.N.; Dabbagh, H.A. Green and selective oxidation of cyclohexane over vanadium pyrophosphate supported on mesoporous KIT-6. *Chem. Eng. J.* **2017**, *314*, 515–525. [[CrossRef](#)]
157. Unnarkat, A.P.; Sridhar, T.; Wang, H.; Mahajani, S.M. Study of cobalt molybdenum oxide supported on mesoporous silica for liquid phase cyclohexane oxidation. *Catal. Today* **2018**, *310*, 116–129. [[CrossRef](#)]
158. Alshehri, A.A.; Alhanash, A.M.; Eissa, M.; Hamdy, M.S. New catalysts with dual-functionality for cyclohexane selective oxidation. *Appl. Catal. A Gen.* **2018**, *554*, 71–79. [[CrossRef](#)]
159. Ghorbanloo, M.; Rahmani, S.; Yahiro, H. Encapsulation of a binuclear manganese(II) complex with an amino acid-based ligand in zeolite Y and its catalytic epoxidation of cyclohexene. *Transit. Met. Chem.* **2013**, *38*, 725–732. [[CrossRef](#)]
160. Von Willingh, G.; Abbo, H.S.; Titinchi, S.J.J. Selective oxidation reactions over tri- and tetradentate oxovanadium(IV) complexes encapsulated in zeolite-Y. *Catal. Today* **2014**, *227*, 96–104. [[CrossRef](#)]
161. Rayati, S.; Rafiee, N.; Nejabat, F. CHEMISTRY Oxidation of Alkenes with tert-Butyl Hydroperoxide Catalyzed by Mn (II), Cu (II) and VO (IV) Schiff Base Complexes Encapsulated in the Zeolite-Y: A Comparative Study. *Inorg. Chem. Res.* **2020**, *4*, 86–93. [[CrossRef](#)]
162. Modi, C.K.; Vithalani, R.S.; Patel, D.S.; Som, N.N.; Jha, P.K. Zeolite-Y entrapped metallo-pyrazolone complexes as heterogeneous catalysts: Synthesis, catalytic aptitude and computational investigation. *Microporous Mesoporous Mater.* **2018**, *261*, 275–285. [[CrossRef](#)]
163. Narayanan, S.; Vijaya, J.J.; Sivasanker, S.; Ragupathi, C.; Sankaranarayanan, T.M.; Kennedy, L.J. Hierarchical ZSM-5 catalytic performance evaluated in the selective oxidation of styrene to benzaldehyde using TBHP. *J. Porous Mater.* **2016**, *23*, 741–752. [[CrossRef](#)]
164. Thao, N.T.; Thi, L.; Huyen, K. Catalytic oxidation of styrene over Cu-doped hydrotalcites. *Chem. Eng. J.* **2015**, *279*, 840–850. [[CrossRef](#)]
165. Wang, X.; Wu, S.; Li, Z.; Yang, X.; Su, H.; Hu, J.; Huo, Q.; Guan, J.; Kan, Q. Cu (II), Co (II), Fe (III) or VO (II) Schiff base complexes immobilized onto CMK-3 for styrene epoxidation. *Microporous Mesoporous Mater.* **2016**, *221*, 58–66. [[CrossRef](#)]
166. Yang, Y.; Zhang, T.; Zhou, D.; Liu, X.; Yang, S.; Lu, X.; Xia, Q. Hierarchical Ti-containing hollownest-structured zeolite synthesized by seed-assisted method for catalytic epoxidation of alkenes efficiently. *Mater. Chem. Phys.* **2019**, *236*, 121754. [[CrossRef](#)]

167. Azzolina Jury, F.; Polaert, I.; Estel, L.; Pierella, L.B. Synthesis and characterization of MEL and FAU zeolites doped with transition metals for their application to the fine chemistry under microwave irradiation. *Appl. Catal. A Gen.* **2013**, *453*, 92–101. [[CrossRef](#)]
168. Yamaguchi, S.; Ohnishi, T.; Miyake, Y.; Hidenori, Y. Effect of Water Added into Acetonitrile Solvent on Oxidation of Benzene with Hydrogen Peroxide over Iron Complexes Encapsulated in Zeolite. *Chem. Lett.* **2015**, *44*, 1287–1288. [[CrossRef](#)]
169. Akinlolu, K.; Omolara, B.; Kehinde, O.; Shailendra, T.; Kumar, M. Synthesis and characterization of Cu(II) and Co(II) encapsulated metal complexes in zeolite-Y for the oxidation of phenol and benzene. In Proceedings of the IOP Conference Series: Materials Science and Engineering, Semarang, Indonesia, 7–8 September 2018; IOP Publishing: Bristol, UK, 2019; Volume 509.
170. Li, X.; Guo, L.; He, P.; Yuan, X.; Jiao, F. Co-SBA-15-Immobilized NDHPI as a New Composite Catalyst for Toluene Aerobic Oxidation. *Catal. Lett.* **2017**, *147*, 856–864. [[CrossRef](#)]
171. Nandi, M.; Talukdar, A.K. Ceria—Zirconia solid solution loaded hierarchical MFI zeolite: An efficient catalyst for solvent free oxidation of ethyl benzene. *Arab. J. Chem.* **2019**, *12*, 3753–3763. [[CrossRef](#)]
172. Yang, R.; Han, P.; Fan, Y.; Guo, Z.; Zhao, Q. The performance and reaction pathway of d-MnO₂/USY for catalytic oxidation of toluene in the presence of ozone at room temperature. *Chemosphere* **2020**, *247*, 125864. [[CrossRef](#)]
173. Zhang, C.; Wang, C.; Huang, H.; Zeng, K.; Wang, Z.; Jia, H. Insights into the size and structural effects of zeolitic supports on gaseous toluene oxidation over MnO_x/HZSM-5 catalysts. *Appl. Surf. Sci.* **2019**, *486*, 108–120. [[CrossRef](#)]
174. Zhang, C.; Huang, H.; Li, G.; Wang, L.; Song, L.; Li, X. Zeolitic acidity as a promoter for the catalytic oxidation of toluene over MnO_x/HZSM-5 catalysts. *Catal. Today* **2019**, *327*, 374–381. [[CrossRef](#)]
175. Mochizuki, H.; Yokoi, T.; Imai, H.; Watanabe, R.; Namba, S.; Kondo, J.N.; Tatsumi, T. Facile control of crystallite size of ZSM-5 catalyst for cracking of hexane. *Microporous Mesoporous Mater.* **2011**, *145*, 165–171. [[CrossRef](#)]
176. Nemeth, L.; Moscoso, J.; Erdman, N.; Bare, S.R.; Oroskar, A.; Kelly, S.D.; Corma, A.; Valencia, S.; Renz, M. Synthesis and characterization of Sn-Beta as a selective oxidation catalyst. In *Studies in Surface Science and Catalysis*; van Steen, L.H.E., Callanan, M.C., Eds.; Elsevier B.V.: Amsterdam, The Netherlands, 2004; Volume 154, pp. 2626–2631.
177. Wilde, N.; Přeč, J.; Pelz, M.; Kubů, M.; Čejka, J.; Gläser, R. Accessibility enhancement of TS-1-based catalysts for improving the epoxidation of plant oil-derived substrates. *Catal. Sci. Technol.* **2016**, *6*, 7280–7288. [[CrossRef](#)]
178. Shen, X.; Wang, J.; Liu, M.; Li, M.; Lu, J. Preparation of the Hierarchical Ti-Rich TS-1 via TritonX-100-Assisted Synthetic Strategy for the Direct Oxidation of Benzene. *Catal. Lett.* **2019**, *149*, 2586–2596. [[CrossRef](#)]